UNIVERSITÀ DEGLI STUDI DI TORINO

P53 in Myelodysplastic Syndromes and Iron chelation with Deferasirox effects on p53 and its family members.

XXXII Cycle **PhD Programme in Experimental Medicine and Therapy**

PhD student: **Chiara Calabrese**

Tutor: Prof.ssa Daniela Cilloni

Department of Clinical and Molecular Sciences

Ringraziamenti

Ringrazio tutti coloro che in questi anni di studio universitario mi hanno aiutato a coltivare la passione che nutro per la biologia.

……Voglio spiegarvi perché per me questo lavoro è tanto importante……

Quando ero piccola la mia insegnante di danza ci fece una domanda: chi volevamo diventare da grandi. Risposi che volevo morire e diventare un "Angelo" per poter aiutare le persone. Preoccupata, lo disse alla mamma, ma lei sorrise serena. È così che ho passato gran parte della vita, cercando di aiutare le persone in difficoltà.

Per me questo lavoro è un tassello importantissimo per poter proseguire il mio progetto di vita.

Credo fortemente nella biologia e, spero un giorno di poter essere fiera di me stessa, aiutando, almeno in piccola parte, la medicina a proseguire nelle sue innovazioni per il benessere pubblico.

In particolare ***ringrazio la Prof.ssa Daniela Cilloni****, la quale mi ha accolta e ha creduto in me fin dall'inizio. In questi anni mi ha sostenuto e aiutato molto facendomi crescere professionalmente.*

Ringrazio i miei genitori *perché mi hanno reso la persona che sono. Spero che questo traguardo sia per loro motivo di orgoglio e fonte di soddisfazione. Mi hanno insegnato la bontà di cuore e vorrei poter trasmettere questo dono a mio figlio Francesco, che presto nascerà.*

Non sarai un ostacolo, ma la spinta a far sempre di più, sempre meglio, e a realizzare il mio sogno.

Infine ringrazio tutte le persone che mi sono sempre state accanto e non mi hanno mai giudicato per il mio modo bizzarro di essere.

Grazie a tutti per avermi indirizzata e guidata in questo cammino, che non terminerà qui perchè son sicura che ad ogni traguardo sussegue un nuovo inizio.

1. ABSTRACT

Mitochondria are dynamic organelles whose morphology continuously changes via fusion and fission. A precise balance in their dynamics is crucial for the maintenance of mitochondrial function and the responses to external stress. Previous studies have shown that mitochondrial alteration is closely related to changes in mitochondrial function as well as cell fate. Moreover, mitochondria are a known site of iron accumulation as well as the main source for reactive oxygen species (ROS) production, but first of all, they are the main energetic source for the cell. In this regard, cancer energetic metabolism is an emerging issue that could represent an attractive therapeutic target.

Finally, they are the key regulators of intrinsic apoptosis, which is the main feature of ineffective hematopoiesis, typical of Myelodysplastic Syndrome (MDS). For all these reasons, the present study attempted to order this "mitochondrial" puzzle in the MDS field, trying to connect mitochondria, oxidative stress, and iron overload, being the latter one responsible for increased ROS production and damaged hematopoiesis.

To do this, we compared total ATP production, glycolysis, mitochondrial efficiency, and lipid peroxidation of cells derived from patients with myelodysplastic features with those of cells derived from healthy controls. Moreover, we analyzed the same parameters after incubation of the cells with different iron chelators. Our study clearly demonstrated that mitochondrial function is altered in MDS, leading to a strong energetic deficit and an increase in oxidative stress and that iron chelation was partially able to restore this impairment. Interestingly, these results didn't correlate with any clinical parameter. All together, these findings led us to hypothesize a new pathogenetic model where, in presence of ineffective hematopoiesis, iron overload occurs specifically at the mitochondrion level, damaging mitochondrial energetic function. Therefore, we confirm that iron deprivation condition, via mitochondrial impairment, leads to apoptosis and impairs cell growth of leukemia cell lines and MDS patient cells.

Finally, to identify a key player in the regulation of mitochondrial activity and apoptosis, we investigated p53, an oncosuppressor crucial to these processes. Indeed, p53 can move to mitochondria and induce caspase activation during the apoptosis process and it plays a role in mitochondrial dynamics by regulating genes such as *DRP1*. Furthermore, it is known that iron depletion increases p53 protein amount by preventing its proteasomal degradation. Through a remarkable reduction of MDM2, known to regulate the stability of p53 and p73 proteins, we observed an enhancement of p53

transcriptional activity after DFX. Interestingly, this iron depletion-triggered signaling is enabled by p73, in the absence of p53, or the presence of a p53 mutant form.

In conclusion, we propose a mechanism by which the p53 transcriptional activity enhancement could explain the potential benefits of iron chelation therapy in improving OS and delaying leukemic transformation in MDS patients.

2. INTRODUCTION

2.1 Myelodysplastic Syndromes

2.1.1 General

Myelodysplastic syndromes (MDS) are a heterogeneous group of diseases characterized by the clonal expansion of an altered myeloid stem cell. This altered myeloid stem cell gives rise to defective myeloid progenitors with a selective advantage, which are unable to produce well-differentiated and functional myeloid cells capable of acting at the peripheral level. The result is an ineffective clonal myeloid hematopoiesis, characterized by an increase in bone marrow turnover (due to apoptosis or necrosis of myeloid progenitors) and one or more peripheral cytopenias [1].

From an epidemiological point of view, MDSs mainly affects the older population: at the time of diagnosis, about 86% of patients with MDS have an age greater than or equal to 60 years (the average age is 75 years) and only 6% are under 50 years (**Table 1**). The incidence increases dramatically with increasing age and is greater in sex male and white [2,3].

From a clinical point of view, cytopenia is common, it is related to one of the three myeloid lines (erythrocytes, granulocytes and platelets) or more, often causing asthenia, recurrent infections, and bleeding; thus, patients frequently are constrained to different degrees of transfusion-dependence.

SITE	BOTH SEXE		MALE		FEMALES	
Myelodysplastic Syndromes (MDS) by age	RATE	COUNT	RATE	COUNT	RATE	COUNT
Age <40	0.1	441	0.1	229	0.1	212
Ages 40-49	0.7	507	0.7	259	0.6	248
Ages 50-59	2.0	1,694	2.4	971	1.7	723
Ages 60-69	8.1	4,899	10.2	2,932	6.1	1,967
Ages 70-79	26.3	8,693	35.7	5,262	18.7	3,431
Ages 80+	54.2	11,798	81.1	6,585	38.1	5,213
By race						
All races	4.3	28,032	6.0	16,238	3.2	11,794
White	4.6	28,032	6.3	13,954	3.3	9,781
Black	3.5	23,735	4.5	1,123	2.9	1,102
Asian/Pacific Islander	2.9	2,225	3.9	932	2.2	731
American Indian/Alaska Native	2.4	1,663	3.5	47	1.5	24
Hispanic	3.1	2,204	3.8	1,139	2.6	1,065

Table 1: Incidence rate of myelodysplastic syndromes (MDS) in different age groups in the United States (2013 to 2017). Adapted from NCI SEER*Stat Database.

2.1.2 Classification of MDS and prognostic factors

Initially the WHO (World Health Organization) classification of MDS was based on pathological features found in the bone marrow and in peripheral blood, and paid particular attention to the quantity of blasts identified [4].

Other important parameters influenced the prognosis of MDS, and for this reason several internationally validated scores (such as IPSS, R-IPSS, WPSS) were used. They allowed myelodysplasias to be divided into further classes and were often used to predict survival and the risk of evolution to acute myeloid leukemia (AML). These scores took into account the number of bone marrow blasts, the number and severity of cytopenias and cytogenetic abnormalities [5-7].

Thanks to the IPSS (International Prognostic Scoring System), the MDS were divided into 4 categories: low risk, intermediate risk I, intermediate risk II, high risk; the R-IPSS (Revised International Prognostic Scoring System) is a system that, compared to the previous one, is more precise (in particular it emphasizes the prognostic value of chromosomal anomalies recognized in MDS) (**Table 2-A, 2-B**) [5].

Cytogenetic prognostic subgroups	Cytogenetic abnormalities
Very good	-Y, del(11q)
Good	Normal, del(5q), del(12p), del(20q), double including del(5q)
Intermediate	del(7q), +8, +19, i(17q), any other single or double independent clones

Poor	-7, inv(3)/t(3q)/del(3q), double including -7/del(7q), Complex: 3 abnormalities
Very poor	Complex: >3 abnormalities

Tabella 2-A: R-IPSS Cytogenetic risk groups. Adapted from Shazan et al., Journal of Clinical Ontology, 2012. [5].

RISK CATEGORY	**RISK SCORE**
Very low	<=1.5
Low	>1.5 – 3
Intermediate	>3 - 4.5
High	>4.5 – 6
Very high	>

Table 2-B: R-IPSS Prognostic Risk Categories/Scores. Adapted from Shazanet al., Journal of Clinical Ontology, 2012 [5].

In 2016, the WHO classification (World Health Organization) was revised [6] and is currently used. It is based on the morphology of cells in the blood and bone marrow as well as on the analysis of chromosomes (cytogenetics). MDS is diagnosed to a patient in the presence of significant cytopenia (hemoglobin <10 g / dl, absolute neutrophil count <1.8 x 109 / l or platelet count <100 x 109 / l), associated with at least one of the following:

- morphological evidence of significant dysplasia in at least 10% of the cells of one or more cell lines (erythroid precursors, granulocytes or megakaryocytes) in the bone marrow aspirate;
- presence of medullary myeloid blasts from 5 to 19% of the medullary cellularity;
- presence of at least 15% of ring sideroblasts (or> 5% in the presence of a mutation of the SF3B1 gene);
- cytogenetic abnormalities in the bone marrow specimen (such as deletion of chromosome 5 or deletion of chromosome 7) in conjunction with a picture of persistent cytopenia, even in the absence of the minimum morphological criteria. Some frequent acquired chromosomal abnormalities such as the Y deletion, deletion (20q) and trisomy of 8 [6,7] are not included among these.

Furthermore, similar dysplastic cells can also be found in the peripheral blood or bone marrow of healthy people over the age of 50 [8]. Therefore, further laboratory tests are needed to complete the evaluation of the patient with MDS. The most important among these is the bone marrow cytogenetic analysis, useful for the prognostic stratification of patients and for selecting the most

effective type of therapy. Further investigations that can be used are flow cytometry, fluorescent in situ hybridization (FISH) and genomic sequencing techniques.

Flow cytometry can help in the identification of abnormal phenotypic patterns and cases with minimal dysplasia. In addition, since somatic mutations have frequently been found in genes involved in DNA methylation and repair, chromatin regulation, RNA splicing, and signal translation in myelodysplastic patients, genomic sequencing techniques can be useful to define or confirm the diagnosis of MDS. Although none of these mutations meet the diagnostic criteria of MDS, except for the SF3B1 mutation (which defines MDS with ring sideroblasts in the presence of at least 5% ring sideroblasts), specific mutational aspects closely correlate with particular subtypes of MDS and could define its diagnosis in the future [9].

The following **table 2-C** summarizes the main categories present:

MDS	**CELLS AFFECTED**	**BLAST**	**COMMENTS**
MDS with unilinear dysplasia (MSD-SLD)	Peripheral cytopenia affecting one or two cell lines. Abnormalities of a single cell line in the bone marrow.	None or rare (<1%) in circulation, no increase in bone marrow (<5%)	Good prognosis; generally long life expectancy
MDS with multilineage dysplasia (MDS-MLD).	Peripheral cytopenia affecting one or two cell lines. Abnormalities of two or more cell lines in the bone marrow.	None or rare (<1%) in circulation, no increase in bone marrow (<5%).	In about 10% of cases there is an evolution towards acute leukemia. About half of patients die within two years of diagnosis.
MDS with ring sideroblasts (MDS-RS)	Immature red blood cells in the bone marrow (≥15%) with a ring of iron deposits around the nucleus. In the event that only one cell line in the marrow appears significantly altered, we speak of MDS-RS-SLD. In the event that the anomalies involve two or more cell lines, we speak of MDS-RS-MLD.	None or rare (<1%) in circulation, no increase in bone marrow (<5%)	Generally good prognosis. If the SF3B1 mutation is present, the number of sideroblasts required is>5%.
MDS associated with isolated 5q- alteration	Low red blood cells, normal white blood cells, increased platelets	None or rare (<1%) in circulation, no increase in bone marrow (<5%), absence of Auer's bodies.	Affected cells present a deletion (loss) of one arm of chromosome 5 (del (5q)) alone or in association with a chromosome 7 abnormality. Usually the prognosis is good. Less than 10% of people develop acute leukemia. Responds to Lenalidomide treatment.

MDS with excess type I blasts (MDS-EB-1)	Peripheral cytopenia affecting one or more cell lines with or without significant abnormalities among bone marrow cells.	Increased number of blasts but less than 10% in the marrow (5-9%) and less than 5% of circulating leukocytes (2-4%). Absence of Auer's bodies.	Approximately 25% of cases progress to acute myeloid leukemia (AML) and most die within two years of diagnosis.
SMD with excess type II blasts (MDS-EB-2)	Like the MDS-EB-1	Greater amount of blasts in the bone marrow (10-19%) and / or in the circulation (5-19%) or number of blasts similar to MDS-EB-1 but with Auer's bodies.	More than 50% of people progress to AML; the remainder die of bone marrow failure.
Unclassifiable MDS (MDS-U)	Peripheral cytopenia of one or more cell lines with or without significant abnormalities in bone marrow cells.	None or rare (<1% or exactly 1%) in circulation, no increase in bone marrow (<5%)	It is a rare form. People are classified as MDS-U when the characteristics of the disease do not reflect any of the previous categories (e.g. blasts = 1%, anomalies in a single cell line but cytopenia covering all three lines or the presence of anomalies but in the absence of reduction the number of cells in circulation).

Table 2-C: WHO classification (World Health Organization) 2016. Adapted from Aberet al., Blood, 2016 [6].

Cut-off values for MDS: hemoglobin<10 g/dL, neutrophils < 1800/microliter, and platelets < 100,000/microliter.

2.1.3 Pathogenetic molecular mechanisms

Several molecular mechanisms are implicated in the genesis of MDS, confirming their extreme clinical heterogeneity. In recent years, several altered pathways emerged:

- ✓ Genes involved in RNA splicing, including SF3B1, SRSF2, U2AF1, ZRSR2
- ✓ Genes involved in epigenetic modifications (both DNA methylation and histone modifications), including TET2, ASXL1, DNMT3A
- ✓ Signal transducers such as JAK2 and NRAS transcription factors such as *RUNX1* and *Tp53*
- ✓ Cohesin complex and SETBP1
- ✓ RPS14 (a ribosomal protein involved in the pathogenesis of Syndrome from 5q- in conditions of haploinsufficiency)

Numerous studies have found frequent associations between genes belonging to different classes. In particular, it has been seen that often in myelodysplasias mutations at the spliceosome level tend to associate with mutations in genes involved in epigenetic modifications; thus the phenotype of MDS

could derive from the cooperation of these anomalies. Spliceosome mutations associated with epigenetic modifications seem to occur early, unlike mutations in the genes responsible for modification of chromatin and cellular signaling, which appear later during the disease [10].
As regards cytogenetic anomalies, the most frequent ones are represented by deletions, while translocations are rare. A characteristic example is given by a particular sub-type of MDS: the 5q- Syndrome, characterized by a defect in erythroid differentiation. The haploinsufficiency of the gene coding for the protein ribosomal RPS14 plays a key role in the development of anemia in this syndrome [11]. Subsequent studies have highlighted the main pathological mechanism responsible for phenotype 5q-, which involves the indirect activation of p53 and apoptosis. RPS14 impairment induces altered biogenesis of the ribosomes; this on the one hand implies an altered translation of different mRNAs and the persistence of free ribosomal proteins, which may bind and inhibit several proteins, including MDM2, the main negative p53 regulator. These events cause an increase in the transcriptional activity of p53 with subsequent cell cycle inhibition and apoptosis induction.
Therefore, new systems of classification and prognostic evaluation for MDSs are needed. Integrating clinical data with those genomic and transcriptional will be crucial to improve the therapeutic performance [10]. The prognostic relevance of recurrent molecular mutations in MDS is summarized in **table 2-D** [12].

Cytogenetics		
Abnormal Karyotype (45*-51%)		
Sole abnormalities n≥ 10%	Complex ≥ 3 abnormalities (9*-11%)	*- Schanz et al., JCO 2012 #- Gangat et al., Mayo Clinic Proceedings 2015 na- not available
Del 5q (6*/26)	3 Abnormalities (2*/NA)	
+8 (5*/15#)	>3 Abnormalities (7*/NA)	
-y (2*/12#)		
Del 20q (2*/14#)		
-7 (2*/4#)		
del(11q) (1*/3#)		
del(12p) (1*/na#)		
del(7q) (1*/na#)		
i17(q10) (0.4*/na#)		
inv3/t(3q)/del(3q)(0.4*/na#)		
+19 (0.4*/na#)		

Molecular genetics			
Mutated gene	Function	Mutational Frequency	Prognostic relevance
Chromatin Modification			
Addition of sex combs-like 1 (ASXL1)	Polycomb repressive complex 2 (PRC2)-mediated transcriptional repression	14-29%	- Shortened survival (Bejar et al., NEJM 2011, JCO 2012, Thol, et al., JCO 2011)
Enhancer of zeste homolog 2 (EZH2)	Catalytic subunit of PRC2 involved in repressing gene expression through methylation of histone H3 on lysine 27 (H3K27)	6-8%	- Shortened survival (Bejar et al., NEJM 2011, JCO 2012)
DNA methylation			
Ten-eleven translocation 2 (TET2)	Cytosine demethylation and chromatin modification	12-23%	- No impact on survival (Smith et al., Blood 2010, Bejar et al., NEJM 2011, JCO 2012) - Shortened survival after transplant (Bejar et al., JCO 2014)
DNA methyltransferase 3A (DNMT3A)	Catalyze addition of methyl group to the cytosine residue of CpG dinucleotides	13-18%	- Shortened survival after transplant (Bejar et al., JCO 2014) - Shortened survival (Walter et al., Leukemia 2011)
Isocitrate dehydrogenase 2 (IDH2)	Catalyze oxidative decarboxylation of isocitrate to α-KG in the mitochondria	2-9%	- No impact on survival (Patnaik et al., Leukemia 2012) - Shortened survival (Bejar et al., NEJM 2011)
Isocitrate dehydrogenase 1 (IDH1)	Catalyze oxidative decarboxylation of isocitrate to α-KG in the cytosol	2-4%	- Shortened survival (Patnaik et al., Leukemia 2012) - No impact on survival (Bejar et al., JCO 2014)
RNA splicing			
Splicing factor 3B1 (SF3B1)	Involved in binding of the spliceosomal U2 snRNP to the branch point close to the 3′ splicing sites	9-75%	- Longer survival (Papaemmanui et al., NEJM 2011) - No impact on survival (Patnaik et al., Blood 2011, Bejar et al., 2012)
U2 snRNP auxiliary factor 1(U2AF1/U2AF35)	regulatory subunit of the U2AF splicing factor that binds the 3′ AG splice acceptor dinucleotide of the pre-mRNA target intron, and forms a heterodimer with U2AF2, which binds the adjacent polypyrimidine tract	12-16%	- No impact on survival (Bejar et al., JCO 2012) - Shortened survival (Makishima et al., Blood 2012)

Serine/arginine-rich splicing factor 2 (SRSF2)	Involved in splice-site selection, spliceosome assembly and both constitutive and alternative splicing.	12-15%	- Shortened survival (Wu et al., Blood 2012, Thol et al., Blood 2012, Damm et al., Blood 2013) - No impact on survival (Bejar et al., JCO 2012)
U2 small nuclear ribonucleoprotein auxiliary factor 35 kDa subunit-related protein 2 (ZRSR2)	Involved in splice-site selection, spliceosome assembly and both constitutive and alternative splicing	3-11%	- No impact on survival (Thol et al., Blood 2012) - *Shortened survival in* $ZRSR2^{mut}/TET2^{wt,}$ (Damm et al., Blood 2013)
DNA repair			
Tumor protein p53(TP53)	Role in apoptosis, G1 arrest, and DNA repair. p53 functions as a transcription factor and upregulates a number of genes involved in these processes	2-21%	- Shortened survival (Bejar et al., NEJM 2011, JCO 2012) after transplant (Bejar et al., JCO 2014)
Transcription regulation			
Runt-related transcription factor 1 (RUNX1) also known as acute myeloid leukemia 1 protein (AML1) or core-binding factor subunit alpha-2 (CBFA2)	Runx1/CBF beta functions as a transcriptional activator of target gene expression	9-16%	- Shortened survival (Bejar et al., NEJM 2011, JCO 2012)
BCL-6 corepressor, (BcoR)	BCL-6 repression. Specific class I and II histone deacetylases (HDACs) interact in vivo with BCoR	4%	- Shortened survival (Damm et al., Blood 2013)
E-26 transforming specific ETS variant 6 (ETV6)	Transcriptional repressor	1.3-3%	- Shortened survival (Bejar et al., NEJM 2011)
Signal transduction			
Neuroblastoma RAS viral (v-ras) oncogene (NRAS)	Enzyme with GTP/GDP binding and GTPase activity involved in the normal control of cell growth	3-4%	- Shortened survival (Bejar et al., NEJM 2011)
Janus kinase 2 (Jak2)	Association with cytokine receptors and involved signal transduction by mediating tyrosine phosphorylation	3%	- No impact on survival (Bejar et al., NEJM 2011, JCO 2012)
Casitas B-lineage lymphoma (CBL)	E3 ubiquitin ligase that such functions as a negative regulator of signal transduction pathways	2%	- Shortened survival (Bejar et al., NEJM 2011)
Cohesin complex			

Stromal antigen 2 (STAG2)	Part of the cohesion complex required for the cohesion of sister chromatids after DNA replication	6-8%	- Shortened survival (Thota et al., Blood 2014)

Table 2-D: **cytogenetic and molecular aberrations in MDS. Adapted from *Gangat et al., American Journal of hematology,2016* [12].**

2.1.4 Mutation in myelodysplastic syndromes

Thanks to next-generation sequencing, recurrent somatic mutations with an independent prognostic impact have been observed in more than 90% of myelodysplastic patients [13]. There are mutations involved in epigenetic regulation (TET2, ASXL1, EZH2, DNMT3A, IDH1, IDH2), RNAsplicing (SF3B1, SRSF2, U2AF35, ZRSR2), DNA repair (TP53), transcriptional regulation (RUNX1, BCOR, ETV6), signal transduction (CBL, NRAS, JAK2) and the cohesin complex (STAG2). However, these mutations can occur in about 10% of healthy individuals with 10-20% lower allelic loads.

In **Table 3** the summary of the main mutations involved in myelodysplasia are illustrated. Mutations in epigenetic modifiers (DNMT3A, TET2, IDH1 / 2, ASXL1, EZH2) are relevant in MDS [14-16]. DNMT3A mutations occur in 10% of MDS patients, and the most common mutation (40% –60%) involving R882 represents the most inactivating event, leading to hypermethylation, in MDS. Furthermore, *DNMT3A*-mutated cells are still present in patients with long-lasting complete remission, and this is consistent with the idea that epigenetic mutations, as *DNMT3A* mutations, could be preleukemic events. This could also support the idea that additional mutations arising as a second hit in a preleukemic *DNMT3A*-mutated clone could be in some cases responsible for relapse [17].

The TET family of enzymes (TET1, TET2, TET3) oxidizes 5-methylcytosine to 5-hydroxymethylcytosine in an α-ketoglutarate-dependent enzymatic reaction. The loss of TET2 function alters its catalytic activity leading to the accumulation of 5-methylcytosine. TET2 mutations have been shown to predict response to DNMT inhibitor therapy in MDS [18,19].

Finally, the IDH mutations are found in exon 4 and affect three specific arginine residues: R132 (IDH1), R172 (IDH2) and R140 (IDH2) [20]. The presence of IDH 1/2 mutations determines the production of 2-hydroxyglutarate which is structurally similar to α-ketoglutarate, and provides competitive inhibition to the enzymatic processes dependent on α-ketoglutarate. Recently, the Food

and Drug Administration (FDA) approved IDH1 and IDH2 inhibitors ivosidenib and enasidenib for the treatment of adult relapsed or refractory AML with IDH1 and IDH2 mutations.

The homo-sapiens tumor protein p53 (TP53) dysregulation plays a crucial role in MDS phenotype, in response to treatment and in AML risk transformation [21,22].

TP53 is a 19,144 bp tumor suppressor gene containing 11 exons, located on chromosome 17p13.1. The protein has five functional domains: the transactivation domain and a proline-rich domain, located in the N-terminal region; the oligomerization domain and a regulatory domain, located in the C-terminus region; the DNA binding domain (DBD) in the central core [23,24].

The p53 transcription factor responds to various cellular stresses to regulate target genes that induce cell cycle arrest, apoptosis, senescence, DNA repair, or changes in metabolism. Furthermore, p53 appears to induce apoptosis through non-transcriptional cytoplasmic processes. In unstressed cells, p53 is essentially kept inactive through the action of the ubiquitin ligase MDM2, which inhibits the transcriptional activity of p53 through ubiquitination. Numerous post-translational modifications modulate p53 activity, in particular phosphorylation and acetylation. Moreover, several p53 isoforms may also modulate p53 activity. P53 activity is ubiquitously lost in human cancer either by mutation of the p53 gene itself or by loss of cell signal upstream or downstream of p53 [25-27].

Its dysregulation is generally associated with a negative prognostic impact in oncological diseases [28]. TP53 is the most studied gene in cancer and its own role is widely documented in several hematological malignancies, including myeloid diseases such as AML [29]. In de novo MDS the frequency of mutations is about 5-10% [30] while in therapy-related neoplasms may reach 30%.

In general, this mutation is mainly observed in high-risk MDS [31], but it is particularly frequent both in patients with isolated del(5q) and those with complex karyotype associated with -5/5q- [30,32]. For this reason, the majority of studies have explored the association of p53 to del(5q) MDS. Its presence is linked with an unfavorable prognosis and with a reduced OS, regardless of prognostic or cytogenetic category. It has been shown that the cases of complex karyotype without TP53 mutations have better survival compared to those with mutations, at least in the transplant setting [33]. In addition, the presence of TP53 mutations also increases the risk of progression to leukemia in MDS patients with isolated del(5q) and leads to poor survival in patients with normal karyotype **[15,34,35].**

Mutations	Frequency (%)	Typical clinical phenotype	Prognostic impact	Prognostic Impactb after alloSCT
RNA splicing machinery				
SF3B1	15-30	RARS	Good overall survival,low-risk of leucemic evolution.	No data
SRSF2	10-20	RCMD. RAEB	Poor overall survival, high-risk of lekaemic evolution	Not shorter OS after alloSCT
U2AF1	5-10	RCMD, RAEB	High-risk of leukaemic evolution	Not shorter OS after alloSCT
ZRSR2	5-10	Subtypes without ring sideroblasts	Shorter OS in co-existing with TET2 mutation	No data
DNA methylation				
TET2	19-26	All MDS subtypes	No impact in OS, predict response to hypomethylating agents	Shorter OS after alloSCT No prognostic impact
DNMT3A	5-18	All MDS subtypes	Adverse outcome in RCMD and RAEB , but not in RARS	Shorter OS after alloSCT No prognostic impact
IDH1/IDH2	2-9	RCMD, RAEB	Adverse outcome	No prognostic impact
Chromatin modification				
ASXL1	15-20	RCMD, RAEB	Adverse outcome	No prognostic impact
EZH2	5-6	RCMD, RAEB	Adverse outcome	No data
Transcription factors				
RUNX1	5-15	RCMD, RAEB	Adverse outcome	No prognostic impact
BCOR	2-4	RCMD, RAEB	Adverse outcome	No prognostic impact
Dna repair control				
TP53	5-10	Advanced stage of disease, complex karyotype, often in MDS with deletion of the q arm of chromosome 5	Poor OS, high-risk of leukaemic evolution, predicts poor response to lenalidomide in MDS with deletion of the q arm of chromosome 5	Shorter OS after alloSCT

Table 3: main mutations involved in myelodysplasia. Adapted from Blau et al., Oncology, 2016.

Although the altered regulation of several biological processes characterizes MDS, increased apoptosis induced by several factors including reactive oxygen species (ROS) and iron excess, seems to be the main cause. Moreover, mitochondrial changes in MDS patients are closely related to the apoptotic activity of their bone marrow cells.

2.2 Apoptosis

Apoptosis is a process of programmed cell death, strictly regulated and once started unstoppable. Although many stimuli and pathways can lead to apoptosis, they all eventually converge in the activation of caspases, which are the final perpetrators of apoptosis: these cysteine proteases act through the cleavage of the protein substrate, as structural proteins, apoptosis regulatory proteins, DNA repair, and cell cycle-related proteins. Among the first, we can distinguish the caspases 8, 10, 2, and 9, which activate the executioner caspases 3 and 7 through their cleavage at the N-terminal pro-domain. Caspases are constitutively expressed as an inactive zymogen and are activated by apoptotic signals through internal proteolysis [36]. This cleavage, and hence activation, is prevented by specific inhibitors of the IAP family such as XIAP, c-IAP1, c-IAP2 and survivin [37].

During apoptotic signaling, IAPs are antagonized by mitochondrial-derived Smac / Diablo and Omi/ HtrA2 proteins, allowing for caspase-mediated execution [38,39].

The two best known activation mechanisms are the intrinsic pathway (also called the mitochondrial pathway) and the extrinsic pathway (**Figure 1**) [40]. The extrinsic pathway, or death receptor pathway, is mediated by death receptors in which ligand-receptor binding initiates protein-protein interactions at cell membranes and activates caspases cascade. Among the most important we included Fas, TNF receptor 1 (TNFR1), TNF-related apoptosis-inducing ligand (TRAIL) receptor 1 (TRAIL-R1), and TRAIL receptor 2 (TRAIL-R2). Ligands that activate death receptors belong to the TNF superfamily of cytokines; these include TNFα, Fas ligand (FasL), and TRAIL.

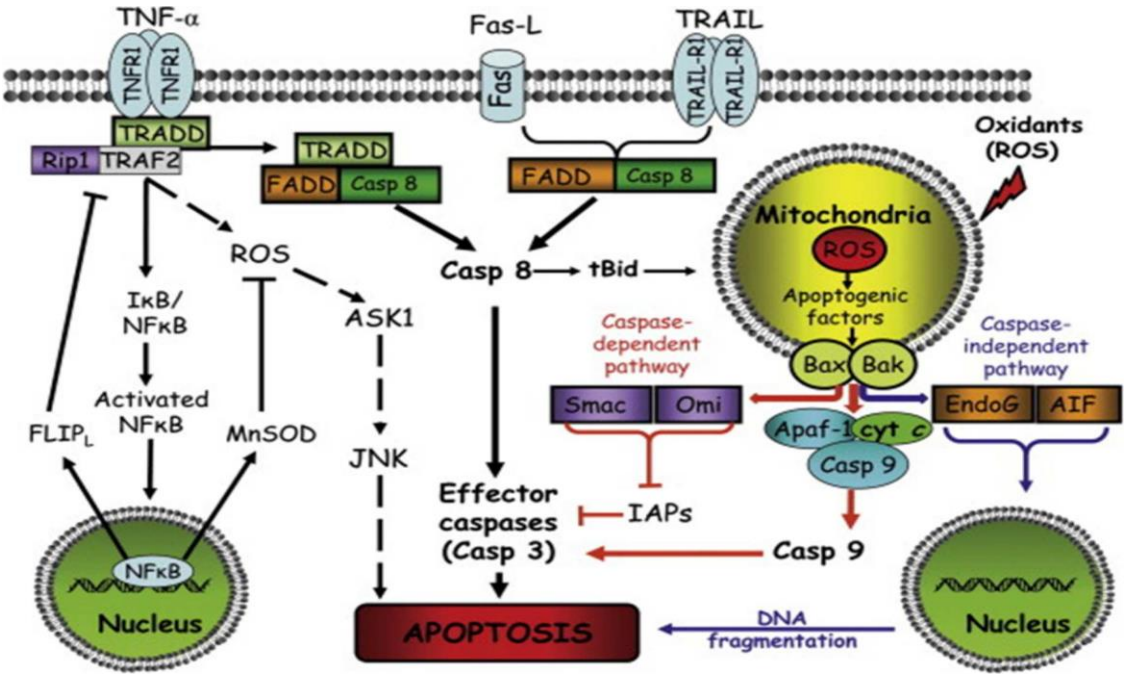

FIGURE 1: Schematic view of intrinsic and extrinsic apoptosis. Adapted from Circu, free radical biology & medicine, 2010 [40].

The binding of ligands to respective receptors induces lipid raft formation, which favors receptor trimerization and crosslinking, a step that is necessary for receptor stabilization and activity; at this point, downstream signaling is activated, Fas associated death domain (FADD) and pro-caspase-8 are recruited, and the resultant death-inducing signaling complex (DISC) is formed. The extent of activated caspase-8 at the DISC determines Type 1 or Type 2 mechanisms; significant caspase-8 activation directly activate caspase-3 (Type 1), while low caspase-8 activation mediates caspase-3 activation through an amplification loop involving the mitochondria (Type 2). In Type 2 apoptosis, activated caspase-8 cleaves pro-apoptotic Bid that induces outer mitochondrial membrane permeabilization through the interactions of truncated tBid with Bax/Bak.
As we can see in **Figure 1**, there are multiple feedbacks; in particular, activation of the NF-κB survival pathway enhances transcription of the anti-apoptotic proteins like FLIPL or MnSOD and apoptosis blockade. NF-kB is activated by several different stimuli, among which ROS and TNF pathways themselves. In the intrinsic or mitochondrial pathway, various apoptotic stimuli mediate permeabilization of the mitochondrial outer membrane and the release of pro-apoptotic proteins. Within the cytosol, cytochrome c together with Apaf-1 and dATP form the apoptosome complex to which the initiator procaspase-9 is recruited and activated. Caspase-9-catalyzed activation of the effector caspase-3 executes the final steps of apoptosis. Caspase activation is further enhanced through the neutralization of caspase inhibitors by apoptogenic proteins like Smac/Diablo and Omi/HtrA2 that are released from the mitochondria. In addition, mitochondrial proteins such as AIF and endoG promote caspase-independent apoptosis through nuclear translocation and mediating genomic DNA fragmentation. Central to mitochondrial permeabilization and mitochondrial release of apoptogenic factors is the permeability transition pore (PTP), a megapore spanning the inner and outer mitochondrial membrane.
There are three PTP component proteins: cyclophilin D (cypD), voltage dependent anion channel (VDAC), and the adenine nucleotide translocase (ANT). The BcL-2 superfamily of proteins includes anti-apoptotic (Bcl-2, Bcl-XL, and Bcl-w) and pro-apoptotic (Bax, Bak, Bad, Bim, and Bid) proteins, which are major players in mitochondrial outer membrane permeabilization and apoptotic susceptibility. In the presence of an apoptotic stimulus, tBid promotes Bax/Bak oligomerization and membrane insertion that results in megapore formation. Conversely, anti-apoptotic Bcl2 proteins inhibit megapores formation. The pivotal contribution of tBid to apoptotic signaling in both the mitochondrial and death receptor pathways is consistent with cross-talk between intrinsic and extrinsic apoptotic signaling [40]. As we have already mentioned, several

factors influence apoptosis, and its activation is tightly regulated. ROS play a major role in both the extrinsic and intrinsic apoptosis pathways.

First of all, ROS are known triggers of the intrinsic apoptotic cascade via interactions with proteins of the mitochondrial permeability transition complex: VDAC, ANT and cypD are targets of ROS, and oxidative modifications of PTP proteins will significantly impact mitochondrial anion fluxes. Moreover, significant mitochondrial loss of cytochrome c will lead to further ROS increase due to a disrupted electron transport chain, causing a vicious cycle. Furthermore, ROS are a major cause of mitochondrial DNA (mtDNA) oxidation and damage. mtDNA damage-induced decreased respiratory function enhances ROS generation, thus eliciting a vicious cycle of ROS-mtDNA damage that ultimately triggers apoptosis [41,42]. Hence, it becomes clear that the protection of mtDNA integrity is critical not only to bioenergetic homeostasis, but to cell survival as well. Mitochondrial GSh (mtGSH) is a critical determinant of the extent of oxidant-induced DNA damage. An inverse relationship between GSH and basal oxidative DNA damage [43], and an association between ROS-induced DNA mutations with GSH depletion/oxidation have been documented [44]. Moreover, age-derived ROS-induced mtDNA damage was linked to mtGSH oxidation [45]. It remains to be established as to whether GSH functions in attenuating mtDNA damage or in stimulating mtDNA repair.

2.3 Mitochondrial activity

2.3.1 Oxidative Phosphorylation

Oxidative phosphorylation is a metabolic process that allows cells to produce ATP under aerobic conditions. Many catabolic biochemical processes (glycolysis, cycle citric acid, and indirectly beta-oxidation) produce the reduced coenzyme NAD (i.e. NADH), which contains electrons with a high transfer potential. The electrons removed by NADH are transferred to molecular oxygen passing through the so-called "electron transport chain"; the energy released is used for produce ATP from ADP and Pi [46] (**Figure 2**).

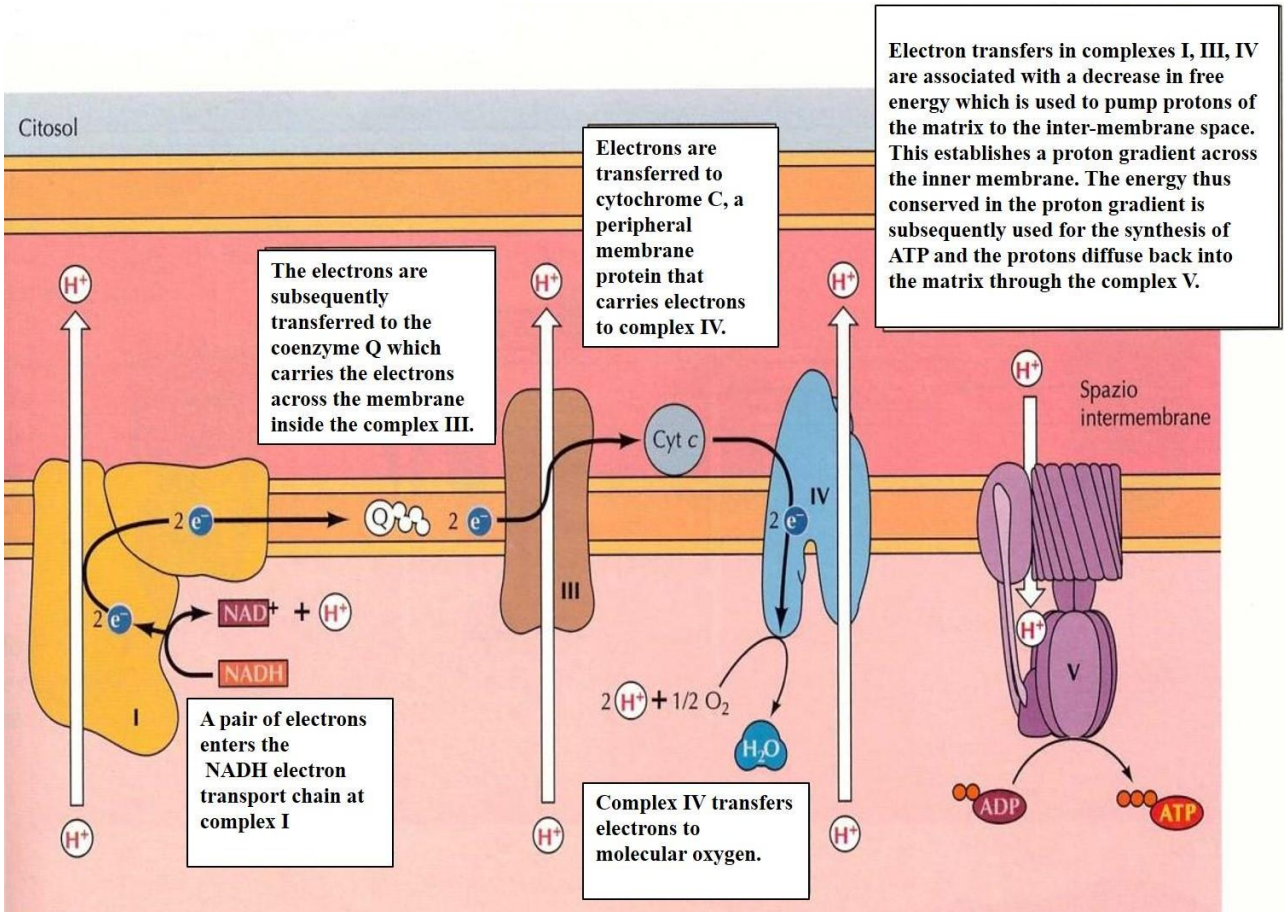

Figure 2: Passage of electrons from NADH along the transport chain, Adapted from Cooper et al., 2009 [46].

2.3.2 The electronic transport chain

The electron transport chain consists of four localized complexes on the inner mitochondrial membrane. They are made up of internal protein membranes, except for cytochrome c, located on the outer face of the membrane and able to move between complexes III and IV. These complexes have the characteristic of containing prosthetic groups (heme, iron-sulfur, flavins, copper), which are acceptors/donors of electrons (being a substrate of redox reactions); CoQ (coenzyme Q or ubiquinone) carries electrons and protons, but is not bound as a prosthetic group to either protein, but to a hydrophobic chain that anchors it to the lipid bilayer. Their arrangement of electron carriers starting from complex I to IV is not random: they have increasing reduction potentials and therefore form a chain that allows a flow of spontaneous electrons up to the last acceptor, oxygen, with the most reduction potential high. Electron transfers in complexes I, III and IV are associated with proton transport (resulting from the reoxidation of NADH into NAD +) from the matrix to the intermembrane space (**Figure 2-3** passage of electrons from NADH along the transport chain); the translocation of

protons in the intermembrane space has two effects: thanks to the accumulation of charges positive on the external surface, it helps to generate an electrical gradient of the membrane and causes the formation of a chemical gradient of protons.

The energy released by electrons flowing through this electron transport chain is used to 7 pump protons across the inner mitochondrial membrane. This generates a potential energy in the form of a pH gradient and an electrical potential across this membrane. This store of energy is tapped by allowing protons to flow back across the membrane and down this gradient, through a large enzyme called ATP synthase, that uses this energy to generate ATP from adenosine diphosphate (ADP), in a phosphorylation reaction. Going into details, there exist four different complexes plus the ATP synthase. The first complex is called NADH coenzyme Q oxidoreductase, or NADH dehydrogenase. It catalyzes the two electron oxidation of NADH by coenzyme Q10 (or ubiquinone), a lipid-soluble quinone that is found in the mitochondrial membrane. It allows 4 H+ to pass into the intermembrane space.

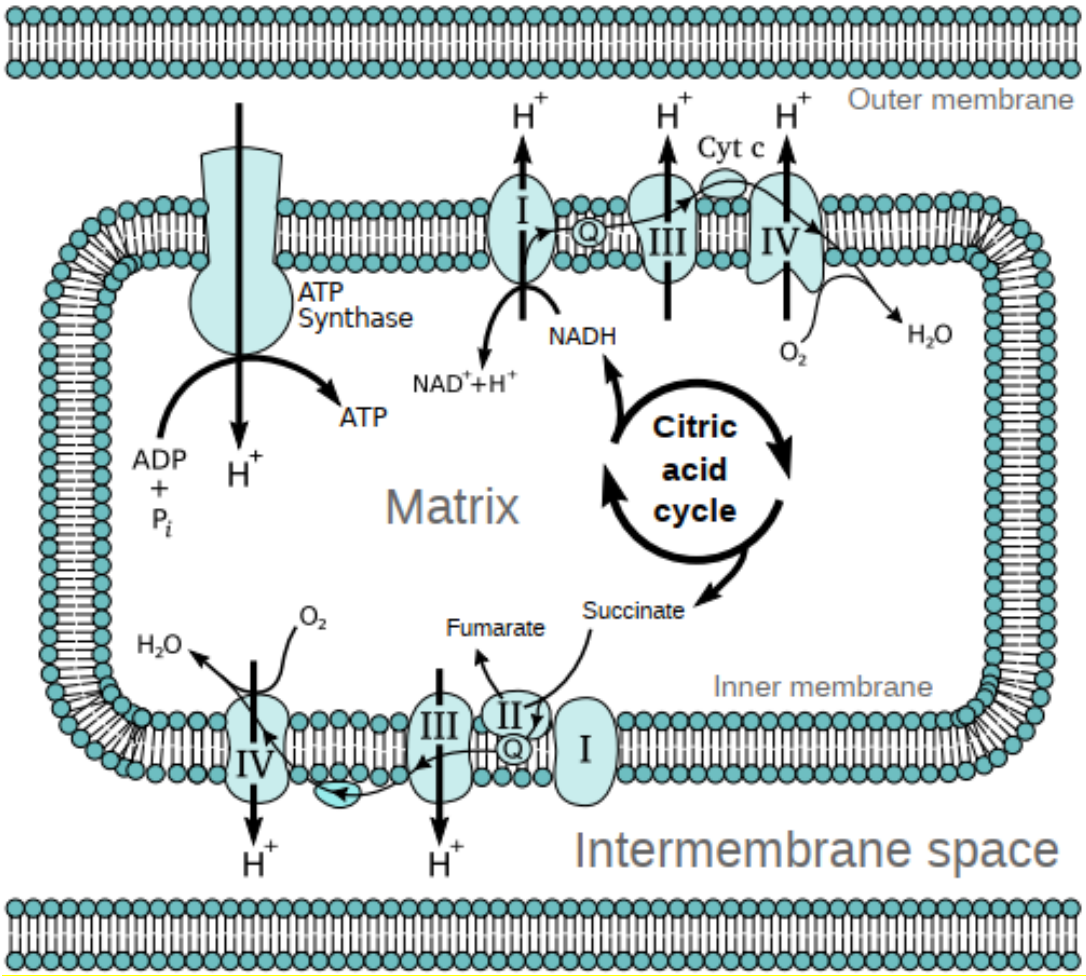

Figure 3: The electron transport chain, schematic view [47,48].

$NADH + Q + 5H+_{matrix} \rightarrow NAD+ + QH2 + 4H+_{intermembrane}$

The second complex is called Succinate-Q oxidoreductase, or succinate dehydrogenase, and is a second entry point to the electron transport chain. In fact, it catalyzes the oxidation of succinate to fumarate and reduces ubiquinone, as follows:

$Succinate + Q \rightarrow Fumarate + QH2$

The third complex is called cytochrome c oxidoreductase. A cytochrome is a kind of electron-transferring protein that contains at least one heme group. The iron atoms inside complex III's heme groups alternate between a reduced ferrous (+2) and oxidized ferric (+3) state as the electrons are transferred through the protein. Complex III catalyzes the oxidation of one molecule of ubiquinol and the reduction of two molecules of cytochrome c, which is loosely associated with the mitochondrion. It allows 4 H+ to pass into the intermembrane space.

$QH2 + 2Cytcox + 2H+ matrix \rightarrow Q + 2Cytcred + 4H+ intermembrane$

The fourth complex is called Cytochrome c oxidase and is the final protein complex in the electron transport chain. This enzyme transfers electrons to oxygen, which is then reduced to water while pumping protons across the membrane:

$4Cytcred + O2 + 8H+ matrix \rightarrow 4Cytcox + 2H2O + 4H+ intermembrane$

Both the direct pumping of protons and the consumption of matrix protons in the reduction of oxygen contribute to the proton gradient. Oxidative phosphorylation ends with the ATP synthase, also known as complex V. This enzyme uses the energy stored in a proton gradient across a membrane to drive the synthesis of ATP from ADP and phosphate, as shown below:

$ADP + Pi + 4H+ intermembrane \rightleftharpoons AT P + H2O + 4H+ matrix$

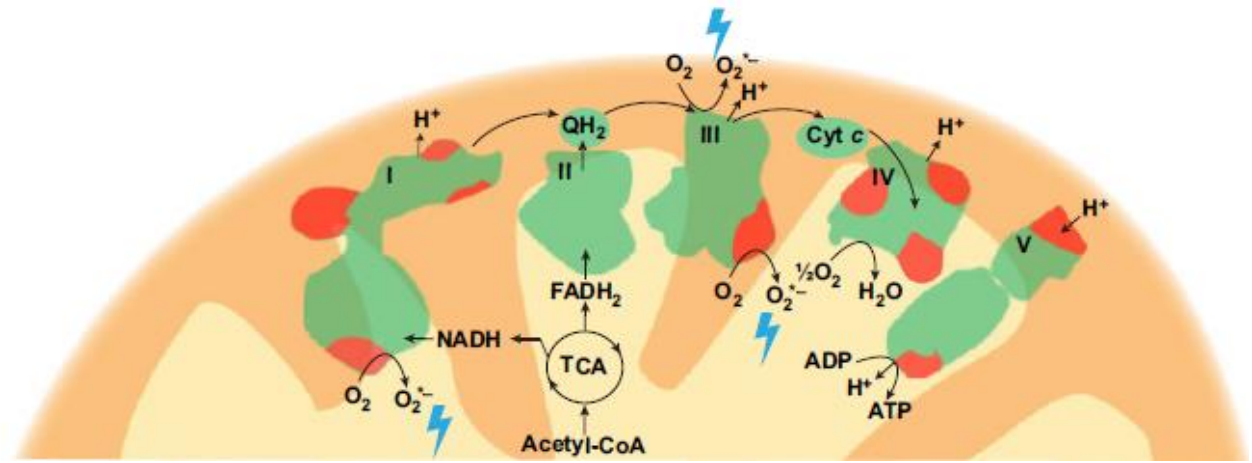

Figure 4: The electron transport chain [49].

2.3.3 Synthesis of ATP

The inner mitochondrial membrane is impermeable to protons and they fall back into the matrix through the ion channels of ATP synthase (**Figure 5**). ATP synthase is a membrane protein composed of 2 components, F_1 and F_0. F_0 crosses the membrane and acts as a protein channel for the passage of H^+. F_1 protrudes into the matrix and contains the extension catalytic site for the synthesis of ATP. When the protons re-enter the matrix, the flow of H^+ determines a conformational change of the ATP synthase which makes the enzyme active, capable of phosphorylating ADP to ATP. Hence, the electrochemical energy of the gradient proton provides the energy for the synthesis of ATP from ADP and P_i (this is the chemiosmotic theory that associates the flow proton to ATP synthesis).

$$ADP + P_i + 4H^+ intermembrane \rightleftharpoons ATP + H2O + 4H^+ matrix$$

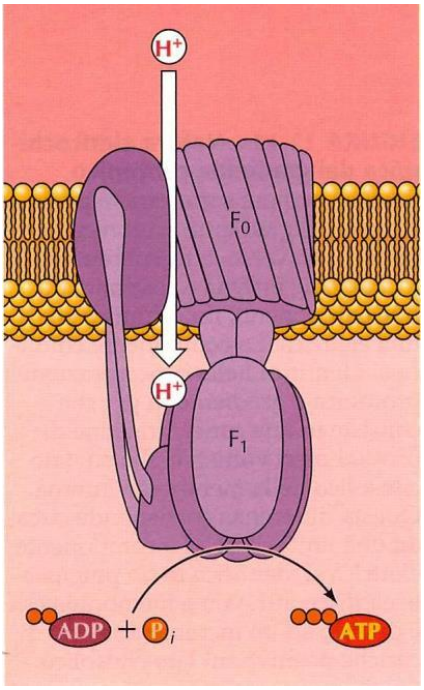

Figure 5: Structure of ATP synthase [46].

The number of ATP molecules produced depends on the protons that emerge from the matrix towards the intermembrane space: 4 from complex I, 4 from complex III, 2 from complex IV. For each pair of electrons transferred from NADH to the electron transport chain (complexes I, III, IV) 10 H^+ come out. For each pair of electrons transferred by the FADH2 6 H + emerge from the electron transport chain (complexes III, IV). 4 protons that fall through the ATP synthase produce the energy for the synthesis of 1 molecule of ATP.

If the electron donor is NADH, 2.5 molecules of ATP are produced. If the electron donor is FADH2, 1.5 molecules of ATP are produced.

2.3.4 The regulation of oxidative phosphorylation

Oxidative phosphorylation is regulated to produce many ATP molecules adapted to the needs of the cell. The main regulator is the charge cellular energy: the concentration of ADP and the ratio [ATP]/([ADP] [Pi]) are measurements of the energy state of the cell.

If the ADP concentration increases (and the proton-motive force is high) → the velocities of electron transport and oxidative phosphorylation increase (the balance shown above proceeds from left to right).

If the ADP concentration decreases (and the proton-motive force is absent) → the velocities of electron transport and oxidative phosphorylation decrease.

This phosphorylation reaction is an equilibrium, which can be shifted by altering the proton-motive force. In the absence of a proton-motive force, the ATP synthase reaction will run from right to left, hydrolyzing ATP and pumping protons out of the matrix across the membrane. However, when the proton-motive force is high, the reaction is forced to run in the opposite direction; it proceeds from left to right, allowing protons to flow down their concentration gradient and turning ADP into ATP.

Even though the cytochrome-c oxidase complex is highly efficient at reducing oxygen to water, and it releases very few partly reduced intermediates, small amounts of superoxide anion and peroxide are produced by the electron transport chain. Particularly important is the reduction of coenzyme Q in complex III, as a highly reactive ubisemiquinone free radical is formed as an intermediate during this redox reaction. This unstable species can lead to electron "leakage" when electrons transfer directly to oxygen, forming superoxide. It is conceivable, therefore, that alterations of the respiratory chain proteins could potentially lead to an increase of reactive oxygen species (ROS) generation. As the production of ROS by these proton-pumping complexes is greatest at high membrane potentials, it has been proposed that mitochondria regulate their activity to maintain the membrane potential within a narrow range that balances ATP production against oxidant generation. For instance, oxidants can activate uncoupling proteins that reduce membrane potential [50]. It has been calculated that 1-2% of total mitochondrial O2 consumed is diverted to the formation of ROS, mainly at the level of complex I and complex III of the respiratory chain, and is believed to be tissue and species dependent [51]. As we will see in the next chapter, however, free radicals have important physiological roles; they become toxic when the cell is not able to control their amount and disposal.

2.3.5 Free radicals and alternative roles for mitochondria

The main function of mitochondria is the supply of energy for all cellular compartments. Besides this important function, these organelles exhibit many other fundamental activities for cellular life [52,53] for example they are involved in the production of heat, regulation of apoptosis vs cell proliferation, detoxification from dangerous compounds, biosynthesis of heme and iron-sulfur groups, regulation of the cellular redox state and regulation of different levels of the second messenger (**Figure 6**).

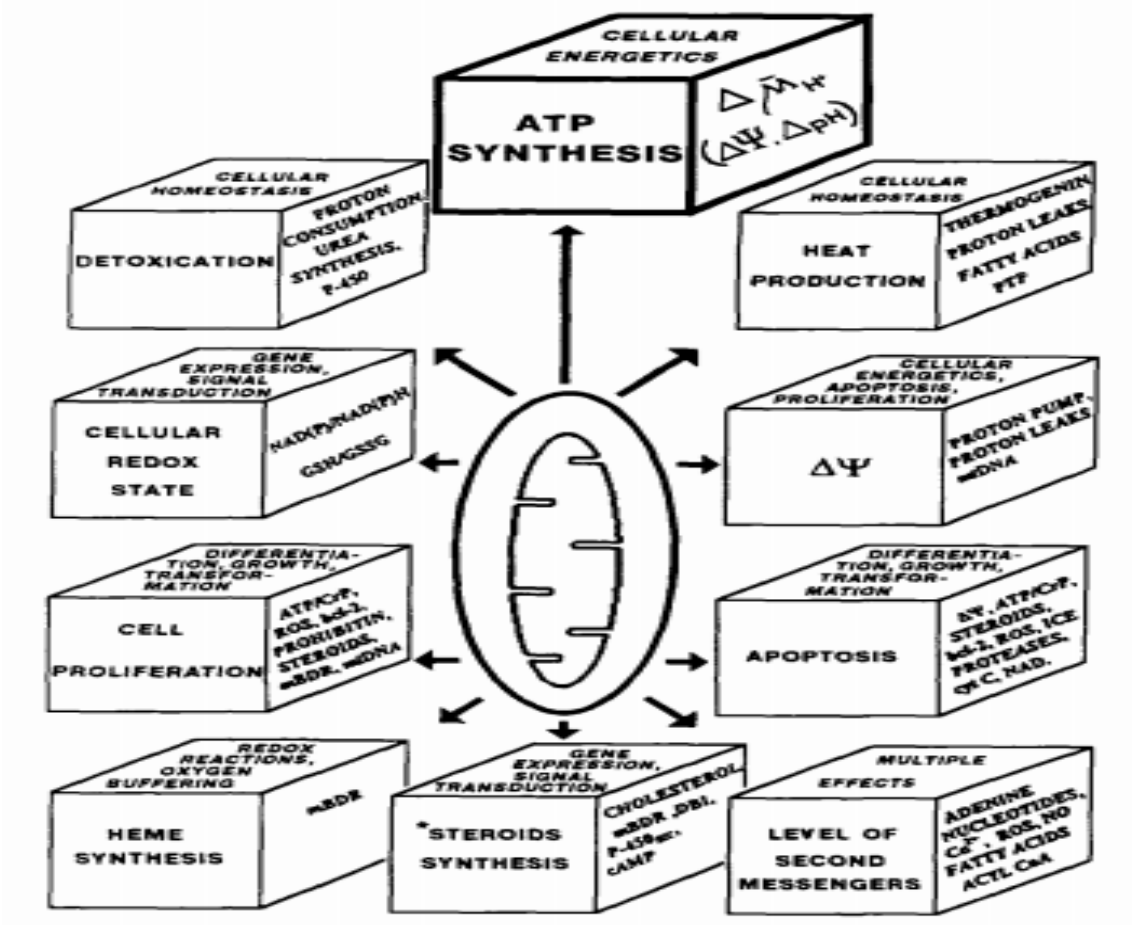

Figure 6: The most important mitochondrial functions. Front panel of each box, macro-effects of mitochondria on the cellular activity. Right side of a box, microenvironment (some of the significant factors involved in a function). Upper sides of a box, the resulting effect(s). Note factors overlapping on all sides of the box as a lack of understanding the causality. * For steroidogenic tissues only. Figure adapted from Zorovet al., Bioscience Reports, Vol. 17, No. 6, 1997 [53].

Many of these functions involve free radicals, which are molecules with 1 or more unpaired electrons. Electron acceptors such as molecular oxygen (O2) react with free radicals to become radicals themselves. The first single electron reduction molecular oxygen produces the superoxide radical (O2-), which has low reactivity and toxicity but can function as an important second messenger in the cell. O2- is then reduced to hydrogen peroxide (H2O2). Hydrogen peroxide is

highly reactive and reacts with partially reduced metal ions such as Fe3 + and Cu2 + to produce an extremely powerful oxidant, the hydroxyl radical (OH ·), through the Fenton reaction [54]

$$Fe_2^{+} + H_2O_2 \rightarrow Fe3^{+} + \cdot OH + OH\cdot$$

Since oxygen and iron are found abundantly in the mitochondria, these organelles are the main ROS production sites (superoxide radicals, hydrogen peroxide and hydroxyl radical), and also of RNS (Reactive Nitrogen Species - in particular nitric oxide, NO • and peroxynitrite, ONOO−). These compounds, at physiological levels, have different roles in the normal cellular metabolome [55] (**Figure 7**). For example, many studies have shown the role of ROS, and RNS as messengers secondary. One of the most important pathways in which ROS are involved is the regulation of NF-kB (nuclear factor kappa-light-chain-enhancer of activated B cells); NF-kB is a factor of transcription that plays a primary role in regulating the immune response to infections, inflammation, cell proliferation and inhibition of apoptosis. The ROS interact with the NF-kB pathway in different ways: in some cases, they activate this pathway, in other cases inhibit the NF-kB signal. The relationships between ROS and the NF-kB pathway are therefore complex, due to the ability of ROS to act simultaneously in points different of the pathway and in a different way, activating or inhibiting [56]. At high concentrations, ROS are harmful to the body as they attack the major constituents of the cell (proteins, nucleic acids, lipids). DNA damage is due to mutations or breaks of the double strand; free radicals can alter the structure chemistry of nitrogenous bases, forming new ones. At the protein level, ROS oxidize I lateral groups of amino acids, impairing their function. Finally, ROS can damage cell membranes through lipid peroxidation [57].

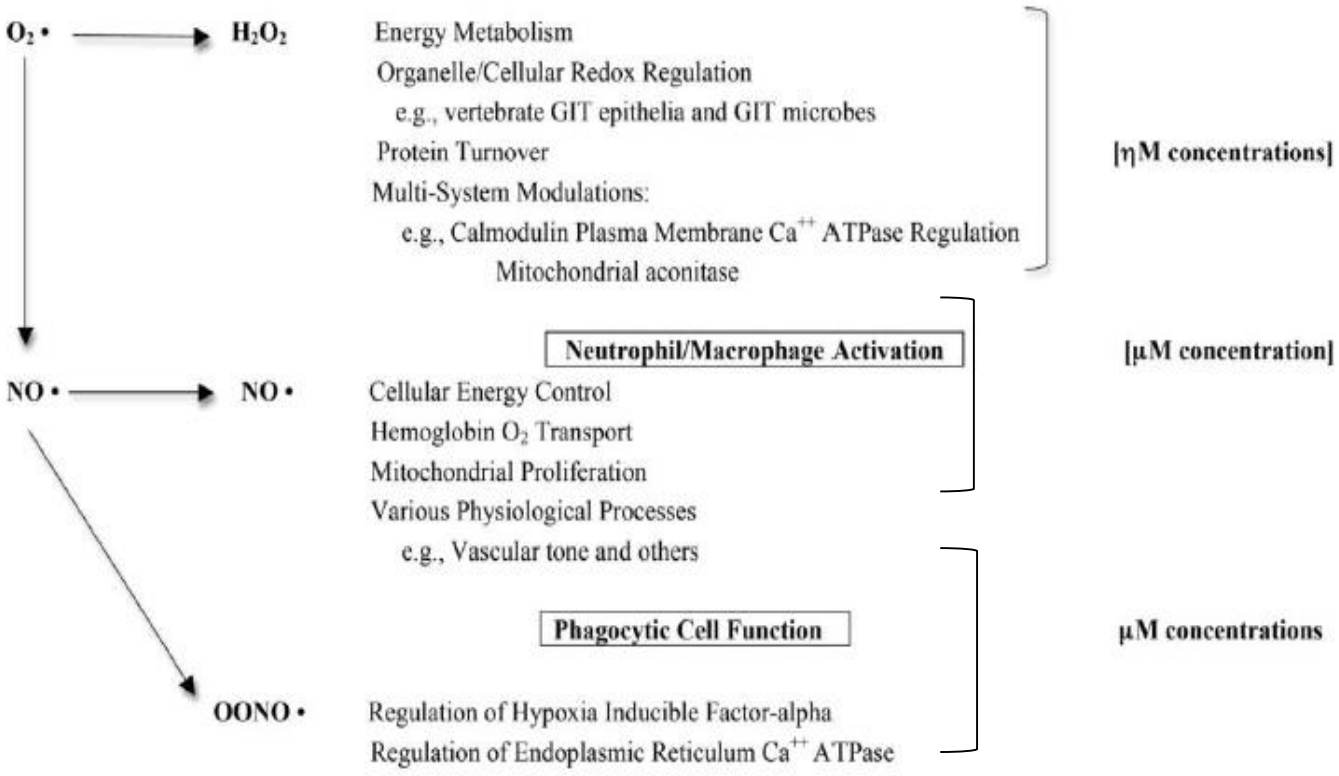

Figure 7: Physiological roles of ROS and RNS. Figure adapted from Linnane et al., 2007 [55].

2.3.6 Mitochondrial dysfunction in MDS

As we have already mentioned above, the pathogenesis and phenotype of MDS are likely to be the results of many different alterations: karyotype abnormalities, point mutations, copy number changes, loss of heterozygosity, haploinsufficiency, epigenetic changes, alterations of the immune system, bone marrow stroma and cytokine milieu have all been described to play a role in this heterogeneous group of diseases. Several lines of evidence suggest that mitochondrial defects may be another factor involved in the pathogenesis of MDS. First of all, mitochondria are key regulators of apoptosis, one of the hallmarks of MDS.

Second, mitochondria are important site of iron accumulation, a process which is known to occur in MDS and that favors ROS production. Moreover, different factors influencing mitochondrial functions are known to cause dyserythropoiesis: for example, chloramphenicol and linezolid alter mitochondrial protein synthesis and can induce myelosuppression with dyserythropoiesis [58]. Another example is Person syndrome, a congenital disorder caused by large scale deletions of mtDNA and characterized by profound sideroblastic anemia. Moreover, at the experimental level, animals with specific mitochondrial DNA instability develop an age-dependent macrocytic anemia with abnormal erythroid maturation [59]. Finally, there is increasing evidence that the mitochondrial genome is altered in MDS [60]. Indeed, the mitochondrial genome is quite prone to mutations. Human

mtDNA is a double stranded ring molecule which contains only 13 protein genes, all of them coding for subunits of the respiratory chain and ATP synthase. In contrast to chromosomal DNA, the mitochondrial genome has no introns, making it very likely that mutations will strike a coding DNA sequence. mtDNA has no protective histones and lacks an effective DNA repair system. Because it is located near the inner mitochondrial membrane, mtDNA is highly exposed to oxygen free radicals generated by the respiratory chain. Altogether, this results in a mutation rate more than 10 times that of chromosomal DNA. Furthermore, also mitochondrial proteins encoded by nuclear DNA can be altered. In 2001, an ortholog of the ferritin gene was discovered [61]; it coded for the mitochondrial ferritin (MtF), a new form of ferritin which efficiently oxidized and stores iron, with a higher affinity for iron compared to cytosolic ferritin, and whose transcription is apparently not directly controlled by iron levels (i.e., it doesn't have an iron response element in the promoter). MtF was found to dramatically increase in iron loaded sideroblasts of RARS (refractory anemia with ringed sideroblasts), but not in classical erythroid precursors in refractory anemia [62]. MtF in vitro overexpression was associated with reduced cytosolic ferritin levels, increased surface transferrin receptor, reduced cell proliferation and increased apoptosis that is consistent with RARS phenotype. MtF overexpression was present also in RARS with wild type SF3B1 [63]. Moreover, in a recent paper, Visconte et al showed that SF3B1 mutation was associated with an SCL25A37 splice variant. This protein is a crucial importer of ferrous iron into the mitochondria, and could be one of the responsible for the sideroblastic phenotype frequently associated with SF3B1 mutation [64]. Predictably, the transcription of the respiratory chain proteins was also found to be altered in MDS. Schildgen at al [65] evaluated the transcription of four pivotal subunits of the mitochondrial respiratory chain in CD34+ cells from MDS patients. The transcription rate was clearly reduced, much more than expected compared to the known age-associated decline of mitochondrial transcripts. Moreover, the stoichiometry of mitochondrial mRNA was altered, while a balanced stoichiometry of subunits has been shown to be important for the correct functioning of mitochondrial respiratory chain [66,67]. In Shildgen's study, results did not differ significantly in different MDS subtypes. The authors did not find a correlation between these alterations and the presence of acquired mtDNA mutations. One possible speculation of the authors was that the reduced transcription could be secondary to a switch toward more glycolytic metabolism, which occurs in many solid tumors, and is known as the Warburg effect.

2.3.7 The Warburg effect

In tumors or in proliferating or developing cells the rate of glucose consumption and lactate production increases markedly, even in the presence of oxygen and perfectly functioning

mitochondria [68]. In fact, neoplastic cells preferably use glycolysis rather than oxidative metabolism. They have a glycolytic activity up to 200 times higher than that healthy cells even in the presence of normal oxygen concentrations; furthermore, the normal slowdown of glycolysis in the presence of oxygen does not occur in cancer cells. This difference in glycolytic flow velocities between healthy and cancerous cells has been called the "Warburg effect", named after the German physiologist Otto Heinrich Warburg who first observed it in the 1930s (**Figure 8**) [69] .

Considering the number of glucose molecules used to produce a given amount of ATP, glycolysis is less efficient than oxidative phosphorylation, however the rate of glucose metabolism is higher through aerobic glycolysis, so that the amount of ATP synthesized in a given period of time becomes superimposable regardless of the type of glucose metabolism that is used [70]. The "Warburg effect" was observed since the appearance of the first neoplastic cells and is necessary for tumor maintenance and growth. It was initially thought that this could represent a cause of tumor development. However, following the identification of numerous genetic alterations present in cancer cells, it is currently believed that this phenomenon represents a consequence rather than a cause of the tumor itself [71]. Despite years of studies on the energy metabolism of cancer cells, to date there are no published studies that analyze the energy metabolism of patients with MDS or clonal hematopoiesis.

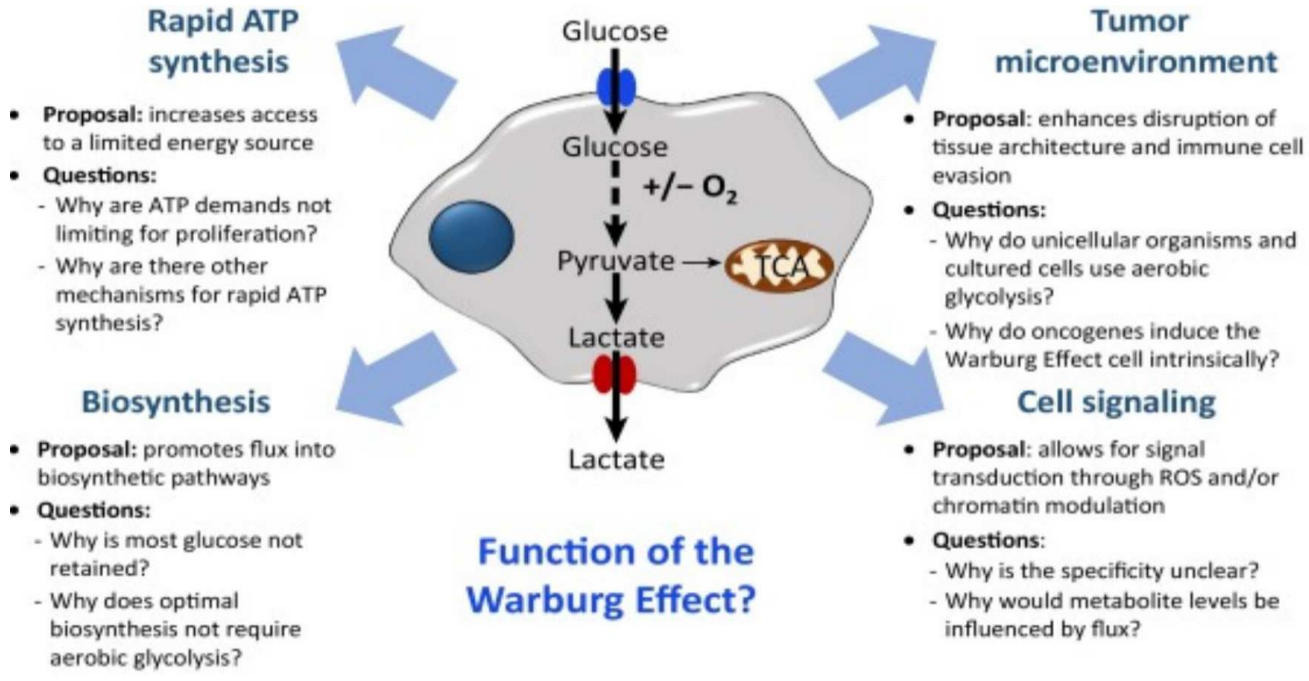

Figure 8: Hypothesized functions of the Warburg effect, i.e., possible advantages for the cancer cells in preferring glycolysis to the oxidative phosphorylation. Adapted from Liberti et al, Trends in biochemical sciences 2016 [68].

2.4 ROS

The role of different ROS in different MDS subgroups was addressed by Goncalves et al in a 2015 free radical research paper [72].

The ROS/antioxidant systems balance can induce apoptosis or stimulate proliferation, and hematopoietic cells are known to be particularly vulnerable to free radical accumulation [73] .

Goncalves' group analyzed levels of peroxide, superoxide, GSH and mitochondrial membrane potentials in various types of WHO MDS at diagnosis and control patients and different cell types (blasts, erythroid precursors, monocytes, granulocytes and monocytes).

As in many other papers, an increase in ROS levels has been seen in patients with MDS; more specifically, it was observed that all types of bone marrow cells from MDS patients, including lymphocytes, had increased intracellular peroxide levels and reduced GSH content compared to controls. The superoxide levels were not significantly different from the control samples.

Overall, hence, oxidative stress levels, expressed as peroxides/GSH and superoxide/GSH ratios in MDS patients were significantly higher in MDS patients, compared to controls.

Notably, peroxide levels were highest in RCMD blasts and monocytes and in the erythroid precursors of RA. RA and RCMD had the highest levels of oxidative stress, which could contribute to higher apoptosis rates.

Patients RAEB-1 and RAEB-2 were the MDS subtypes least affected by oxidative stress, but showed an increase in the superoxide/peroxide ratio, much higher than in low-grade MDS or controls.

As suggested by Pervaiz and Clement [74], when the superoxide / peroxide ratio favors peroxides, an apoptotic intracellular environment is established.

Conversely, in cells where superoxide is predominant, survival pathways are normally activated by direct or indirect mechanisms, such as phosphoinositide 3-kinase (PI3K-AKT). GSH levels decreased in all MDS subtypes and cell types compared to control.

Moreover, transfusion dependency negatively correlated with GSH content, while peroxide levels positively correlated with serum ferritin. Iron overload, in fact, causes an excess of non-transferrin bound iron, which can participate in Fenton and Haber Weiss reactions to generate highly reactive hydroxyl radicals that deplete GSH content.

Pervaiz's group subsequently correlated oxidative stress levels in MDS with hypermethylation. Hypermethylation is one of the most common molecular alterations found in MDS patients; CpG island methylation in the regulatory regions of many tumor suppressor genes has been shown to promote carcinogenesis [75,76].

Gonçalves et al. demonstrated a correlation between P15 and P16 gene promoters hypermethylation with the levels of intracellular ROS, as well as the ratios of peroxides/GSH and superoxide/GSH in MDS patients [77].

The mechanisms are not yet clear; it has been described that hydrogen peroxide can modulate DNA through the formation and relocation of a silencing complex, consisting of DNMT1, DNMT3B, SIRT1 and members of polycomb repressive complex 4, which stimulates cancer-specific hypermethylation [78].

Furthermore, the superoxide anion can directly deprotonate cytosine at carbon 5 position, allowing direct methylation, independent of DNMT [79]. Gonçalves hypothesizes that the hematological improvement observed during iron chelation therapy could be due to the reduction of induced oxidative stress from these drugs and, indirectly, to the reduction of methylation.

2.5 Iron overload

Iron overload in MDS is due to both multiple red blood cell transfusions and hepcidin suppression caused by ineffective erythropoiesis. During normal physiology, the amount of iron absorbed (1-2 mg/d) is exactly proportional to that lost due to the desquamation of the intestinal mucosa and skin, as well as small amounts in the urine and bile. While the organism has strict regulation on iron, absorption has no meaningful way to get rid of it.Each unit of the transfused blood contains about 250 mg of iron, therefore, after the transfusion of about 20 units of blood, ferritin levels generally reach 1000 mg / dL. Transfusion-dependent MDS patients often have 2-3 units of blood per month, so they are likely to reach this value after less than 7-8 months. Furthermore, MDS with anemia belong to the so-called iron load anemias, such as intermediate non-transfusional beta thalassemia intermeia, these anemias are characterized by severe ineffectiveness erythropoiesis and pathological low levels of hepcidin [80].

Although the exact mechanism has not yet been elucidated for erythropoiesis, it is absolutely necessary in paraphysiological conditions that require an increase in the production of red blood cells and, therefore, in the absorption of iron: recovery from anemia after bleeding and secondary polycythemia in hypoxic condition.

However, when anemia is due to ineffective erythropoiesis, hepcidin inhibition leads exclusively to iron overload, with altered erythropoiesis. Many proteins related to blood production have been found to inhibit hepcidin: GDF15, a growth factor produced by erythroblasts during chronic anemia [81], PDGF-BB (platelet derived growth factor -BB), expressed by several cell types under hypoxia [82], and, more recently, erythroferrone (ERFE), whose production increases rapidly after EPO injection only in maturing erythroblasts [83].

For this reason iron overload is very common for MDS patients overload. In this case the toxicity of iron does not derive from storage iron or transferrin-bound iron.When transferrin saturation exceeds 75%, non-transferrin-bound iron species appear in the plasma. This labile iron is very prone to react with oxygen, strengthening the production of ROS and, in particular, of hydroxyl radicals.

ROS can have damaging effects on MDS cells, increased lipid peroxidation and organelle damage, leading to cell death and TGF-beta1-mediated fibrogenesis [84]; moreover ROS damages DNA, worsening the genomic instability of MDS and finally, and can also have anti-apoptotic activity, increasing the risk of leukemic evolution. The effects of iron overload and ROS in MDS are summarized in **Figure 9**.

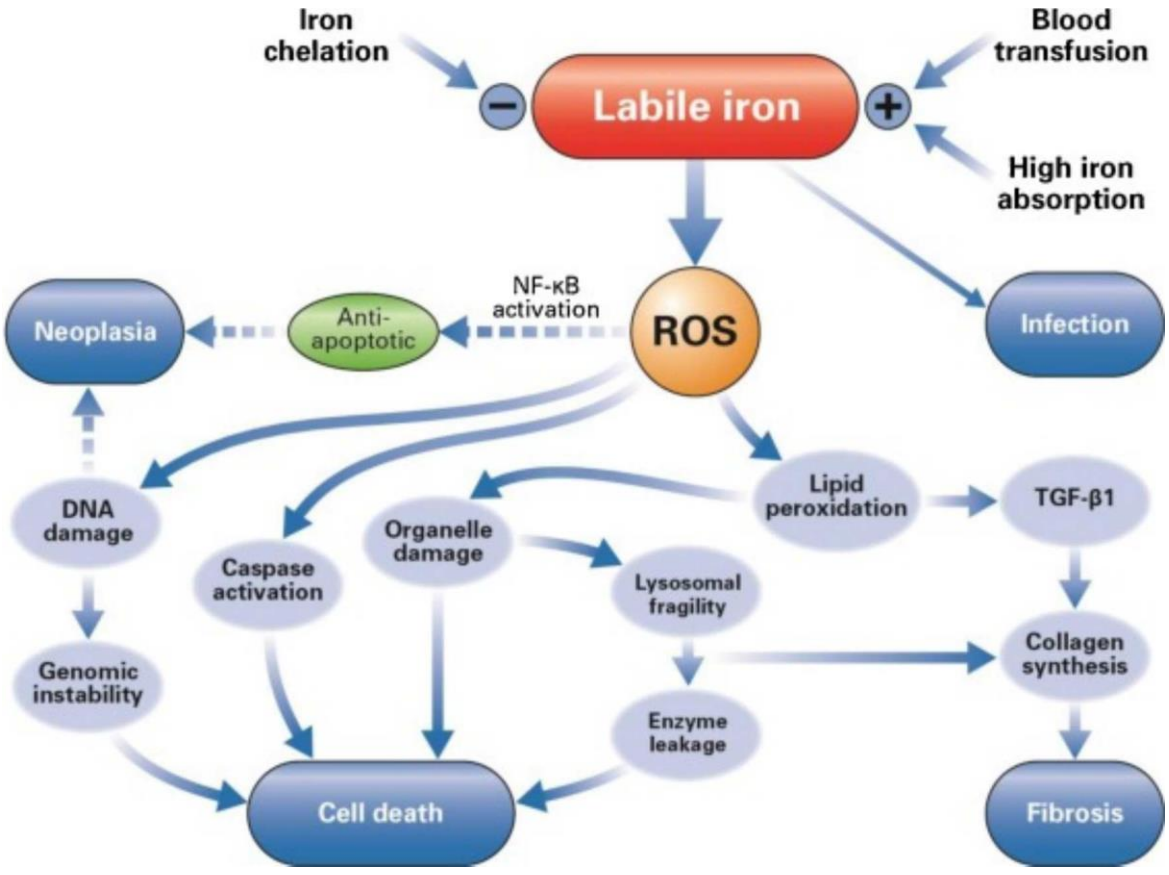

Figure 9: Pathological mechanisms and consequences of iron overload in MDS. Adapted from Kautz et al. 2014 [83].

2.6 Iron chelation in MDS

Iron chelation is an established treatment in patients with thalassemia, where the accumulation of iron begins in childhood and soon becomes a major cause of morbidity and mortality, if left untreated.
Although iron overload is a systemic phenomenon, iron tends to accumulate first in the liver, heart and endocrine glands, leading to cirrhosis, heart failure and endocrine disorders. However, iron overload can cause more subtle damage than cirrhosis or heart failure; it can worsen ineffective erythropoiesis and induce genomic instability, due to ROS production [85,86]. Furthermore, recent studies have reported potential effects of iron chelation therapy (ICT) on overall survival (OS) of leukemic patients, however this effect has not been observed in all the cohorts [87-91]. Experimental data generated in a murine model of MDS with IOL indicated that iron chelation affects the disease progression [92]. In this regard, the oral iron chelator has been demonstrated to improve the OS and to delay leukemic transformation [91,93,94].
The most commonly used iron chelators are deferoxamine (DSF), which can be administered subcutaneously or intravenously, deferasirox (DFX) and deferiprone, two oral medications.
Deferoxamine can cause skin lesions at the site injection and, more rarely, kidney damage; deferasirox can cause gastrointestinal upset and kidney failure; deferiprone can induce diffuse joint and muscle pain, as well as agranulocytosis, so it is not approved in MDS.
In MDS, iron chelation is still controversial: considering old age, the neoplastic genesis of anemia and, therefore, the relatively short life expectancy, it is quite a common belief that these patients will not live long enough to develop complications from iron overload.
Therefore, treatment of MDS with iron chelators could improve hematopoiesis and decrease the possibility of AML progression by improving prognosis. The first clinical data supporting these laboratory results are already available. Both DSF and DFX are able to modestly improve myelodysplastic hematopoiesis over time; this type of response is slow and occurs in parallel with the reduction of iron overload [95].
Furthermore, many studies have reported early hematological improvements with DFX, but not with DSF [96], depending on the study, erythroid response seems to vary from 6 to 44%, platelets response from 13 to 61% and ANC response from 3 to 76% [97-99].
As shown in **Table 4**, no significant correlation was found between hematopoietic response and serum ferritin decrease in any study; moreover, no predictive factor for response was identified in the GIMEMA study [100].
Molecular mechanisms underlying hematopoietic response to DFX are still to clarify, but recent studies found that:

1. DFX inhibits NF-Kb [101],
2. DFX inhibits mTOR signaling [102],
3. DFX favours apoptosis by increasing caspase 3/7[103],
4. After exposure to DFX, a gene expression profile analysis revealed an increase in the transcription of genes involved in cell cycle regulation, IFN pathway, apoptosis (Bcl6) and GDF15, a negative regulator of hepcidin [98].

All the mechanisms proposed so far seem to enhance apoptosis or limit proliferation; in this case, hematopoietic improvement would be secondary to the inhibition of the myelodysplastic clone. At the best of our knowledge, however, no strong reduction of the blasts' count or significant anatomopathological improvement after treatment with deferasirox has ever been reported in the literature.

Reference	**No. pts**	**HI-E**	**HI-plts**	**HI-PMN**	**Biological parameters**
EPIC [104,105]	247	53 (21.7 %) 11.8 % TI 8.9 % ↑ Hb	13 (13 %)	50 (22 %)	No significant changes in SF and LIP between responders and non-responders
US03 [106]	173	26 (15 %)	17/77 (22 %)	8/52 (15 %)	No significant changes in SF and LIP between responders and non-responders
GERMAN [107]	50	2/33 (6 %)	3/10 (30 %)	Not evaluated	Not evaluated
GIMEMA [100]	152	16/152 (11 %)	18/125 (15 %)	1/41 (3 %)	No significant changes in SF between responders and non-responders
REL [108]	53	19 (35.1 %)	8/13 (61 %)	13/17 (76.4 %)	No correlations
Italian cooperative group [99]	105	41/105 (44.5 %)	Not evaluated	Not evaluated	HI not related to SF changes

Table 4: Main clinical studies analyzing the erythroid response to DFX in MDS. TI transfusion independence, SF serum ferritin, Hi-E erythroid improvement, HI-Plts platelet improvement, HI-PMN neutrophil improvement, LIP labile iron pool. Adapted from Breccia et al, Annals of hematology 2015 [98].

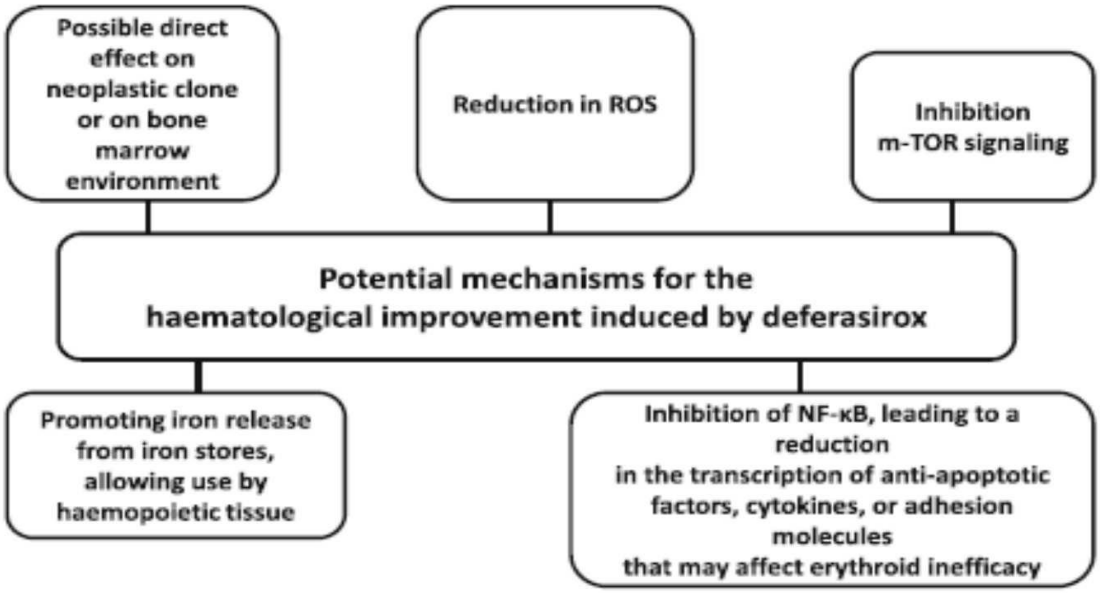

Figure 9: Potential mechanism for the hematological effect of deferasirox. Adapted from Breccia et al, Annals of hematology 2015 [98]

2.7 *Tp53* in MDS

Within this scenario, we focused our attention on p53, the oncosuppressor whose function is heavily related to apoptosis and to mitochondrial activity. Moreover, its stability is directly dependent and regulated by iron, indeed, iron depletion triggered p53 phosphorylation and stabilization, thus preventing its proteasomal degradation. Recently, Shen and colleagues demonstrated that intracellular iron overload shortens p53 half-life by promoting p53 nuclear export and cytosolic degradation [109]. All these findings provide insights into tumorigenesis associated with deregulated apoptosis, mitochondrial dysfunction and iron excess, suggesting that p53 family might represent an interesting target to be investigated during iron chelation therapy.

2.7.1 Role of p53 in Cell Cycle Control

- Lee and Bernstein [110] using transgenic mice found that the expression of one of the 2 mutant p53 alleles significantly increased the cellular resistance of a variety of hematopoietic cell lines to gamma radiation. They hypothesized that the wild type p53 could act as a "guardian of the genome", preventing the proliferation of a cell that has suffered genetic damage. Hence, cells without the wild-type p53 protein due to a dominant negative action of the p53 mutant may not undergo radiation-induced cell death, thereby increasing radiation resistance.

- El-Deiry et al. [111] found that induction of WAF1 (CDKN1A; 116899) was associated with wildtype but not mutant p53 gene expression in a human brain tumor cell line. WAF1 is also called CIP1 or p21, and Harper et al. [112] showed that it binds to cyclin complexes and inhibits the function of cyclin-dependent kinases. El-Deiry et al. [111] suggested that p53 is not required for normal development, but its expression is stimulated in certain cellular environments, such as DNA damage or cellular stress. In turn, p53 binds to WAF1 regulatory elements and transcriptionally activates its expression. WAF1 subsequently binds to and inhibits cyclin-dependent kinase activity, preventing phosphorylation of critical cyclin-dependent kinase substrates and blocking cell cycle progression. In tumor cells with inactive p53, this pathway would thereby be defective, permitting unregulated growth.
- After DNA damage, many cells appear to enter a sustained arrest in the G2 phase of the cell cycle. Bunz et al. [113] demonstrated that this arrest could be sustained only when p53 was present in the cell and capable of transcriptionally activating p21. After disruption of either p53 or p21, gamma-radiated cells progressed into mitosis and exhibited G2 DNA content only due to failure of cytokinesis. Bunz concluded that p53 and p21 are essential for maintaining the G2 checkpoint in human cells.
- Aylon et al. [114] found that LATS2 had a role in the p53-dependent G1/S arrest following damage to the mitotic spindle and centrosome dysfunction. LATS2 interacted physically with MDM2 to inhibit p53 ubiquitination and to promote p53 activation.
- Jiang et al. [115] showed that p53 represses the expression of the malic enzymes associated with the tricarboxylic acid cycle) and ME2 in human and murine cells. Both malic enzymes are important for NADPH production, lipogenesis and glutamine metabolism, but ME2 has a deeper effect. Through the inhibition of malic enzymes, p53 regulates metabolism and cell proliferation. Downregulation of ME1 and ME2 mutually activates p53 through distinct mechanisms of MDM2- (164785) and AMP-activated protein kinase (AMPK) in a feed-forward fashion, strengthening this pathway and enhancing p53 activation. Jiang [115] concluded that their results defined the physiological functions of malic enzymes, demonstrated a positive feedback mechanism supporting p53 activation, and revealed a p53-mediated connection between metabolism and senescence.

2.7.2 Role of p53 in Apoptosis

- Caelles in 1994 [116] developed immortalized somatotropic progenitor cells expressing a temperature-sensitive p53 mutant. In these cells, induction of apoptosis by DNA damage

depended strictly on p53 function. Temperature-shift experiments showed that the extent of apoptotic DNA cleavage was directly proportional to the period during which p53 was functional. A shift to the permissive temperature triggered apoptosis following UV radiation-induced DNA damage independently of new RNA or protein synthesis [116] suggested that, rather than activating apoptosis-mediator genes, p53 either represses genes necessary for cell survival or is a component of the enzymatic machinery for apoptotic cleavage or repair of DNA.

- According to Polyak et al. [117] p53 triggers apoptosis through the transcriptional induction of oxidation-related genes, followed by the formation of reactive oxygen species and oxidative degradation of mitochondrial components.
- Sablina et al. [118] found that p53 had an antioxidant function associated with highly responsive p53 target genes induced during nonlethal oxidative stress in several human cell lines. Prooxidant effects of p53 in gravely damaged cells were associated with delayed induction of proapoptotic genes. The p53-dependent increase in reactive oxygen species was secondary to induction of apoptosis and originated from mitochondrial leakage.
- In 1998 Conseiller [119] constructed a 'chimeric tumor suppressor-1' (CTS1) gene from wildtype p53 by removing the domains that mediate p53 inactivation. CTS1 enhanced transcriptional activity, was resistant to inactivation by MDM2, had the ability to suppress cell growth, and showed faster induction of apoptosis.
- In his work Ryan [120] examined the effect of p53 induction on activation of NF-kappa-B (NFKB), a transcription factor that can protect from or contribute to apoptosis. In human cells without NFKB activity, p53-induced apoptosis was abrogated. Ryan [120] found that p53 activated NFKB through the RAF /MEK1/p90(rsk) pathway rather than the TNFR1 /TRAF2 /IKK pathway used by TNF A . Inhibition of MEK1 blocked p53-induced NFKB activation and apoptosis, but not cell cycle arrest.
- Brodsky [121] identified a Drosophila p53 homolog and demonstrated that it could activate transcription from a promoter containing binding sites for human p53. Dominant-negative forms of Dmp53 inhibited transactivation in cultured cells and radiation-induced apoptosis in developing tissues. The cis-regulatory region of the proapoptotic gene 'reaper' contains a radiation-inducible enhancer that includes a consensus p53-binding site. Dmp53 could activate transcription from this site in yeast, and a multimer of this site was sufficient for radiation induction in vivo. These results indicated that reaper is a direct transcriptional target of Dmp53 following DNA damage.
- Chipuk et al. [122,123] found that cytosolic localization of endogenous wildtype or transactivation-deficient p53 was necessary and sufficient for apoptosis. p53 directly activated

the proapoptotic BCL2 protein BAX in the absence of other proteins to permeabilize mitochondria and engage the apoptotic program. p53 also released both proapoptotic multidomain proteins and BH3-only proteins that were sequestered by BCLXL. Transcription-independent activation of BAX by p53 occurred with similar kinetics and concentrations to those produced by activated BID. Chipuk [122,123] proposed that when p53 accumulates in the cytosol, it can function analogously to the BH3-only subset of proapoptotic BCL2 proteins to activate BAX and trigger apoptosis.

- Leu et al. [124] found that after cell stress, p53 interacted with BAK, resulting in oligomerization of BAK and release of cytochrome c from mitochondria. Formation of the p53-BAK complex coincided with loss of interaction between BAK and the antiapoptotic protein MCL1. Leu [124] suggested that p53 and MCL1 have opposing effects on mitochondrial apoptosis by modulating BAK activity.
- Nuclear p53 regulates proapoptotic genes, whereas cytoplasmic p53 directly activates pro apoptotic BCL2 proteins to permeabilized mitochondria and initiate apoptosis. Chipuk [125] found that a tripartite nexus between BCLXL, cytoplasmic p53, and PUMA coordinated these distinct p53 functions in mouse and human cells. After genotoxic stress, BCL XL sequestered cytoplasmic p53. Nuclear p53 caused expression of PUMA, which then displaced p53 from BCLXL, allowing p53 to induce mitochondrial permeabilization. Mutant BCL XL that bound p53, but not PUMA, rendered cells resistant to p53-induced apoptosis irrespective of PUMA expression. Thus, Chipuk [125] concluded that PUMA couples the nuclear and cytoplasmic proapoptotic functions of p53.

2.7.3 Regulation of p53 by MDM2 and Ubiquitination

- Fuchs et al. [126] stated that direct association of p53 with the cellular protein MDM2 results in ubiquitination and subsequent degradation of p53.
- Yin et al. in 2002 [127] found that MDM2 induced translation of p53 mRNA from 2 alternative initiation sites, resulting in full-length p53 and an N-terminally truncated protein, p53/47. p53/47 lacks the MDM2-binding site and the most N-terminal transcriptional activation domain of full-length p53. Translation induction required MDM2 to interact directly with the nascent p53 polypeptide and led to a change in the ratio of p53 to p53/47 by inducing translation of both proteins followed by selective degradation of full-length p53.
- By mass spectrometry of affinity-purified p53-associated factors, Li et al. [128] identified the herpesvirus-associated ubiquitin-specific protease (HAUSP) as a novel p53-interacting protein.

HAUSP strongly stabilized p53, even in the presence of excess MDM2, and induced p53-dependent cell growth repression and apoptosis. HAUSP had an intrinsic enzymatic activity that specifically deubiquitinated p53 both in vivo and in vitro. Expression of a catalytically inactive point mutation of HAUSP in cells increased the levels of p53 ubiquitination and also destabilized p53. Li [128] concluded that p53 can be stabilized by direct deubiquitination and suggested that HAUSP may function as a tumor suppressor in vivo through stabilization of p53.

- Both p53 and MDM2 interact with p300/CREB-binding protein (CBP) transcriptional coactivators. Purified p300 exhibited intrinsic ubiquitin ligase activity. In vitro, p300 with MDM2 catalyzed p53 polyubiquitination, whereas MDM2 alone catalyzed p53 monoubiquitination [129]. Generation of the polyubiquitinated forms of p53 that are targeted for proteasome degradation requires the intrinsic ubiquitin ligase activities of MDM2 and p300.
- Colaluca et al. [130] described a previously unknown function for human NUMB as a regulator of tumor protein p53. NUMB enters in a tricomplex with p53 and the E3 ubiquitin ligase MDM2 thereby preventing ubiquitination and degradation of p53. This results in increased p53 protein levels and activity, and in regulation of p53-dependent phenotypes
- Le Cam et al. [131] found that human E4F1 functioned as as a ubiquitin E3 ligase for p53 both in vitro and in vivo. E4F1-mediated ubiquitylation of p53 occurred at sites distinct from those targeted by MDM2, competed with PCAF-induced acetylation of p53, and did not target p53 for proteasomal degradation. E4F1-stimulated p53-ubiquitin conjugates were associated with chromatin, and their stimulation coincided with induction of a p53-dependent transcriptional program specifically involved in cell cycle arrest, but not apoptosis.
- Impeding ribosomal biogenesis generates ribosomal stress that activates p53 to stop cell growth. Dai et al. [132] stated that the ribosomal proteins L5 (RPL5), L11 (RPL11), and L23 (RPL23) interact with MDM2 and inhibit MDM2-mediated p53 ubiquitination and degradation in response to ribosomal stress. They found that L5 and L23 inhibited ubiquitination of both p53 and MDM2 in human cell lines. In contrast, L11 inhibited proteasome-mediated degradation of ubiquitinated MDM2, but not p53, resulting in stabilization of p53.
- Using Tctp (TPT1 -haploinsufficient mice and mouse cells and human cell lines, Amson et al. In 2012 [133] found that TCTP had an antiapoptotic function by promoting MDM2-dependent ubiquitination and proteasome-dependent degradation of p53. TCTP also interacted directly with NUMB, and Amson [133] suggested that TCTP may compete with NUMB for binding to the MDM2-p53 complex. On the other hand, p53 bound to the promoter region of TCTP and repressed TCTP transcription, suggesting a negative-feedback loop between TCTP and p53 for the control of cell and tumor growth.

3. AIM OF THE STUDY

Mitochondria, oxidative stress, and iron overload play a key role in the pathogenesis and progression of MDS. In addition, the energy metabolism is frequently altered in cancer cells and this effect could represent an interesting therapeutic target. Nowadays, thanks to detailed studies on this field, there are a number of publications that analyze energy metabolism in MDS. Besides, recent identifications of iron overload induced damage, suggested a possible role of iron on MDS mitochondrial metabolism.

The aim of the study was therefore to analyze the mitochondrial status and the metabolism of MDS patient's cells before and after iron chelation. We assessed the availability of ATP in vitro (by measuring the levels of ATP and AMP and by calculating the ATP/AMP ratio), the mitochondrial efficiency (through P/O ratio, i.e. the balance between the ATP produced and the oxygen used, as a result of stimulation of the respiratory chain with pyruvate/malate and succinate), the process of glycolysis (through LDH levels) and lipid peroxidation (through MDA). These analyzes were initially performed in healthy subjects stratified by age and subsequently in subjects with iron overload and in patients with MDS (evolved or not in LAM). The same parameters were analyzed and compared after in vitro incubation of samples with two iron chelating drugs, deferasirox, and deferoxamine. We, therefore, sought to establish the role of ferrochelation in the energy metabolism of subjects with MDS.

Finally, we investigated the potential anti-leukemic effect of DFX, by analyzing three different leukemia cell lines (i.e.: HL60, NB4, and MOLM-13) and human primary cells derived from MDS/AML patients.

4. MATERIALS AND METHODS

4.1 Patients and controls

The FISM-BIOFER-12 study has been approved by the local ethic committee San Luigi Gonzaga (number of approval: 14/2013). All methods were performed in accordance with the relevant guidelines and regulations. Ten centers participated in the study. This prospective study enrolled MDS patients with transfusion dependent iron overload. Peripheral Blood (PB) samples were collected at the time of starting iron chelation therapy (ICT). After written informed consent, PB samples from 40 MDS patients, and 80 healthy controls have been collected. Not all the samples were

analyzed for the experiments described below, mainly because of peripheral cytopenia. Normal controls (CTRL) are divided into the following age groups: 22 young controls (mean age 12 yrs ± 2.9), 24 adult controls (mean age 38 yrs ±12.2), and 34 elderly controls (mean age 73 yrs ±8.4). MDS risk was classified according to the Revised International Prognostic Scoring System (R-IPSS) [134,135].

According to the WHO classification, the MDS group included: 20 MDS with single lineage dysplasia (MDS-SLD), 7 MDS with multilineage dysplasia (MDS-MLD), 7 refractory anemia with excess of blasts type I (RAEB-I), 5 RAEB II, and 1 case of isolated 5q-. All MDS samples were derived from patients with a high level of iron before being included in a protocol with iron chelation treatment. The general characteristics of these patients are summarized in **Table 5**. The mean age of the MDS patients was 75±6.8.

Mononuclear cells (MNCs) were isolated from 10 ml of PB on a Ficoll gradient. All samples were sent to the laboratory and analysed within 24 hours from collection.

For the second part of the study we used the local ethics committee of San Luigi Gonzaga (protocol 0003267, permission code 17/2016, 24 February 2016), in accordance with the Declaration of Helsinki. After written informed consent, bone marrow (BM) and PB specimens were collected from 25 MDS patients, with a median age of 77 years (range 53–90), whose clinical and molecular features are summarized in Table 6. White blood cells (WBCs) were isolated by buffy coat. In vitro primary cultures were incubated with DFX (50 μM) for 48 h in complete ISCOVE's medium and subsequently, apoptosis assay and *CDKN1A* and *PUMA* gene expression were evaluated as described below. p53 and p73 protein levels were evaluated by immunohistochemistry technique before and after DFX treatment in 5 additional patients, selected for the availability of samples before ICT and within one year of ICT, without any additional treatment including erythropoietic stimulating agents.

UPN	**DIAGNOSIS**	**AGE**	**R-IPSS**	**CYTOGENETIC**	**SERUM FERRITIN ng/mL**
1	MDS-MLD	80	low	normal	2400
2	MDS-MLD	79	int	normal	1460
3	MDS-MLD	67	low	normal	280
4	MDS-MLD	78	int	trisomy 8	2800
5	MDS-MLD	80	low	normal	5220
6	MDS-MLD	79	low	normal	4870
7	MDS-MLD	69	int	del(7q)	890
8	MDS-EB-2	79	very high	del(7q)	4800
9	MDS-EB-2	84	very high	normal	NA
10	MDS-EB-1	74	high	del(20q)	1450
11	MDS-EB-1	81	int	normal	1090
12	MDS-EB-1	76	NA	NA	12800
13	MDS-EB-1	77	high	normal	2760

14	MDS-EB-1	77	int	normal	1700
15	MDS-EB-1	76	Int	normal	6670
16	MDS-SLD	80	low	normal	6520
17	MDS-SLD	85	low	normal	2400
18	MDS-SLD	74	low	normal	3380
19	MDS-SLD	61	int	del(7q)	NA
20	MDS-SLD	65	low	normal	2230
21	MDS-SLD	86	low	normal	7400
22	MDS-SLD	75	int	trisomy 8	1800
23	MDS-SLD	77	int	normal	4700
24	MDS-SLD	77	int	-7	NA
25	MDS-SLD	67	NA	NA	5240
26	MDS-SLD	75	low	normal	7400
27	MDS-SLD	73	very low	del(11q)	1700
28	MDS-SLD	80	low	normal	4000
29	MDS-SLD	83	NA	NA	6440
30	MDS-SLD	69	low	normal	2100
31	MDS-SLD	72	low	normal	1420
32	MDS-SLD	68	NA	NA	2270
33	MDS-SLD	68	very low	normal	1380
34	Isolated del (5q)	57	very low	del(5q)	3670
35	MDS-SLD	73	low	normal	1820
36	MDS-SLD	84	NA	NA	2770
37	MDS-EB-1	82	high	normal	1889
38	MDS-EB-2	65	Very high	complex	3880
39	MDS-EB-2	83	very high	complex	2800
40	MDS-EB-2	80	very high	normal	3600

Table n. 5: Clinical characteristics of the MDS patients.

Abbreviation: MDS-SLD, MDS with single lineage dysplasia; AML, acute myeloid leukemia; MDS-RS-SLD, MDS with ring sideroblasts with single lineage dysplasia; MDS-MLD: MDS with multilineage dysplasia; MDS EB I: MDS with excess of blast type me; MDS EB II: MDS with excess of blast type II; N/A: not available.

UPN	**DIAGNOSIS**	**AGE**	**R-IPSS**	**CYTOGENETIC**	**SERUM FERRITIN ng/mL**
1	MDS-SLD	81	low	Normal	2400
2	Isolated del (5q)	58	low	del(5q)	1191
3	AML	67	NA	Normal	2250
4	MDS-MLD	78	low	del(9q)	2292
5	MDS-RS-SLD	70	int	trisomy 8	2587
6	MDS-EB-II	82	int	Normal	975
7	MDS-EB-II	69	int	NA	700
8	MDS-MLD	56	low	NA	4706
9	MDS-EB-I	78	int	Normal	1207
10	MDS-SLD	69	NA	NA	2643
11	MDS-MLD	64	low	Normal	1314
12	MDS-SLD	71	low	Normal	N/A
13	Isolated del (5q)	79	low	del(5q)	746
14	MDS-EB-I	82	int	Normal	N/A

15	AML	81	NA	NA	2272
16	MDS-RS	83	low	Normal	3805
17	MDS-EB-I	77	low	Normal	2008
18	MDS-RS	78	int	Normal	5350
19	MDS-EB-I	77	low	Normal	5785
20	MDS-EB-I	76	low	Normal	1750
21	MDS-EB-I	72	int	Normal	1179
22	MDS-RS	53	int	N/A	4514
23	MDS-EB-II	81	low	Normal	1184
24	MDS-EB-I	80	low	Normal	800
25	MDS-EB-I	90	low	del(Y)	687
	Healthy donor 1	63	-	Normal	200
	Healthy donor 2	52	-	Normal	13
	Healthy donor 3	56	-	Normal	80
	Healthy donor 4	57	-	Normal	83
	Healthy donor 5	53	-	Normal	49

Table 6: Clinical characteristics of the MDS patients and controls.WBCs were treated with DFX 50 uM for 48h.

Abbreviation: MDS-SLD, MDS with single lineage dysplasia; AML, acute myeloid leukemia; MDS-RS-SLD, MDS with ring sideroblasts with single lineage dysplasia; MDS-MLD: MDS with multilineage dysplasia; MDS EB I: MDS with excess of blast type me; MDS EB II: MDS with excess of blast type II; N/A: not available.

4.2 Iron chelation

Twenty PB from healthy controls (10 young subjects with a mean age of 20±3.6, 10 elderly subjects with a mean age 67±5.5) and 25 myelodysplastic patients with a mean age of 75±6.8) were incubated with two iron chelators: Deferasirox (DFX) and Deferoxamine (DFO), for 24hours, both at 50 μM concentration. All MDS patients had an iron overload due to blood transfusions (all of them have received at least 20 U of red blood cells), with a serum ferritin level higher than 1000ng/mL and a transferrin saturation higher than 70%. All samples were taken before starting iron chelation therapy.

4.3 Cell Culture conditions

MOLM, NB4, and HL60 cell lines were purchased from American Type Culture Collection (ATCC, Manassas, VA, USA). MOLM and NB4 cells were grown in RPMI 1640 medium supplemented with 200 nmol/L Glutamine (EuroClone), 10% inactivated fetal bovine serum (FBS) (Sigma-Aldrich, St. Louis, MO, USA), and 0.1% penicillin/streptomycin. HL60 cells were grown in ISCOVE's medium

supplemented with 200 nmol/L Glutamine (EuroClone, Milan, Italy), 10% inactivated FBS, and 0.1% penicillin/streptomycin. All cell lines were maintained at 37 ◦C with 5% CO2.

4.4 F1 ATP synthase activity

ATP synthesis, trough F_0-F_1 ATP synthase, was performed according to published method [136].The reaction was monitored in a luminometer (GloMax® 20/20n Luminometer, Promega Italia, Milano, Italy), by the luciferin/luciferase chemiluminescent method, with ATP standard solutions between 10–8 and 10–5M (luciferin/luciferase ATP bioluminescence assay kit CLS II, Roche, Basel, Switzerland).

4.5 Evaluation of ATP/AMP intracellular level, lipid peroxidation and Lactate Dehydrogenase (LDH) assays

To evaluate the cellular energy status, the ATP/AMP ratio was calculated on the basis of the ATP and AMP intracellular level. ATP and AMP concentrations were measured spectrophotometrically at 340 nm, following the NADP reduction or NADH oxidation, respectively [137].

ATP and AMP were measured according to the enzyme coupling method, following the NADP reduction or NADH oxidation, at 340 nm, respectively26.

To assess lipid peroxidation, the malondialdehyde (MDA) level was evaluated by the thiobarbituric acid reactive substances (TBARS) test, at 532 nm [138]. LDH activity was measured as a marker of anaerobic glycolysis following the NADH oxidation, at 340 nm [138].

4.6 Oxygen consumption measurements

The oxygen consumption rate (OCR) was measured in a closed chamber, using an amperometric electrode (Unisense-Microrespiration, Unisense A/S, Tueager, Denmark) [139].

For each experiment, 100,000 cells, treated or not with 50 µM Deferasirox for 48 h, were permeabilized with 0.03% digitonin for 1 min. 5 mM pyruvate and 2.5 mM malate were used to stimulate the pathway composed by complexes I, III, and IV, while 20 mM succinate induced the pathway formed by complexes II, III, and IV. To observe the ADP-stimulated respiration rates, 0.08 mM ADP was added after pyruvate and malate or succinate addition.

4.7 Evaluation of the efficiency of mitochondrial energy metabolism

The OxPhos efficiency (P/O ratio) was calculated as the ratio between the concentration of the produced ATP and the amount of consumed oxygen in the presence of respiratory substrate and ADP. When the oxygen consumption is completely devoted to energy production, the P/O ratio should be around 2.5 and 1.5 after pyruvate + malate or succinate addition, respectively,[136,140].

4.8 Cell Treatment and Calcein Fluorescence Assay

Labile iron pool (LIP) was quantified by exploiting the iron ability to bind to calcein acetoxymethyl ester (CA-AM). Notably, 1×10^6 of cells and mononuclear cells isolated from patients at diagnosis were incubated in PBS with calcein (Invitrogen), for 15 min at 37°C, after 48 h of Deferasirox treatment. After three PBS washes, to remove excess reagent, we analyzed the samples by flow cytometry. LIP level was inversely proportional to measured fluorescence intensity. In normal condition, indeed, upon entering viable cells, calcein fluorescence is quenched by binding to cellular LIP. DFX acts by removing iron from its complex with CA. Therefore, the fluorescence emitted by the cells increases (measurable as Mean Fluorescence Intensity (MFI) with flow cytometry), thus confirming the occurred iron chelation.

4.9 Proliferation and Apoptosis Assay

Cell growth was evaluated by the MTT assay (Cell Proliferation Kit I (MTT), Sigma-Aldrich, St. Louis, MO, USA) [141], according to the manufacturer's instructions. 50,000 cells/per well were seeded in triplicate for each condition, in a 96-well plate. 48 h after DFX treatment, MTT reagent was added inside each well and, after appropriate incubation, the corresponding absorbance was measured.

Apoptosis was evaluated by flow cytometry after labeling with fluorescein isothiocyanate (FITC)-conjugated annexin V and propidium iodide (Annexin V-FITC Apoptosis Detection Kit, Immunostep, Salamanca, Spain), as previously described [142]. BD CellQuest software (BD Biosciences) was used for data analysis of Annexin V-positive cells.

4.10 RNA Extraction and qRT-PCR Analysis

Total RNA was extracted using TRIzol Reagent (Ambion, Thermo Fisher Scientific, Waltham, MA, USA) as previously described [143]. Briefly, 1 µg of total RNA was used as template for the reverse transcription reaction. Expression levels of *CDKN1A*, *PUMA*, *GADD45*, and *MDM2* were evaluated with TaqMan technology (TaqMan Universal Master Mix, Thermo Fisher Scientific, Waltham, MA, USA), through the C1000 Thermal Cycler CFX96 Real-Time System (Bio-Rad, Hercules, CA, USA).qRT-PCR data were analyzed by Bio-Rad CFX Manager 3.1 software (Bio-Rad, Hercules, CA, USA).

The analysis was performed in triplicate. Genes' expression was normalized with respect to the *ABL* housekeeping gene and expressed as 2–DDCt. Universal human references RNA (Stratagene, San Diego,CA, USA) was used to calibrate the assay.

4.11 MitoTracker Staining and Morphological Analysis of Mitochondria

MitoTracker Green FM (M7514) was dissolved in DMSO to obtain 1 mM stock solutions. To stain our cell lines, MitoTracker solution was added to the growth medium, after 48 h of incubation with DFX at 1:5000 dilution (to a final working concentration of 100 nM). After 40 min of incubation, cells were centrifuged and resuspended in fresh prewarmed medium, to be analyzed by confocal scanning microscope (LSM 5110; Carl Zeiss MicroImaging Inc., Oberkochen, Germany, 63× objective) [144]. The morphological analysis of mitochondria was performed in silico using existing ImageJ plug-ins following Valente et al.'s toolset, called MiNA (Mitochondrial Network Analysis). MiNA allows semi-automated analysis and consists in images' preprocessing, to ensure quality, conversion to binary image, and in the production of the final skeleton for quantitative analysis. Briefly, images were opened on ImageJ and processed as follows: 1-Process/Filters/Unsharp Mask; 2-Process/Enhance Local Contrast (CLAHE);

3 Process /Filters/Median; 4-Process/Binary/Make Binary; 5-Process/Binary/Skeletonize;

6 Analyze/Skeleton/Analyze Skeleton (2D/3D); 7-Plugins/StuartLab/MiNA Scripts/MiNA Analyze Morphology.

4.12 Immunofluorescence Assay

After cytospin, 50,000 cells were fixed in 4% PFA for 10 min [145]. Cells were permeabilized with 0.5% triton for 5 min, blocked for 45 min with PBS 10% BSA and subsequently incubated for 2 h with the specific primary antibodies p53 DO-1 (sc-126, Santa Cruz Biotechnology, Dallas, TX, USA) and p73 (PA5-35368, ThermoFisher Scientific, Waltham, MA, USA). Immunocomplex was detected by 40 min incubation with a secondary antibody (Alexa Fluor 488 or 543, Invitrogen). PI was used for nuclear staining. Cells were visualized with a confocal scanning microscope (LSM 5110; Carl Zeiss MicroImaging Inc., Oberkochen, Germany, 63× objective) and pictures were quantified by the Java (Image J) program.

4.13 Protein Extraction and Immunoblotting

To isolate total protein content, samples were lysed on ice with RIPA buffer (50 mmol/L Tris-HCl pH 8.0, 150 mmol/L NaCl, 1% Np 40, 0.5% DOC, 0.1% SDS, freshly added to protease and phosphatase [146] 15 of 22 inhibitors cocktail). Cell debris were removed by centrifugation at 14,000× *g* at 4 ◦C for 15 min. Protein concentration was determined by Bio-Rad Protein Assay Bio-Rad, Hercules, CA, USA) [147]. Fifty µg of each total cell lysate were loaded, resolved through SDS-PAGE 8% or 12% gel, and electro blotted onto 0.2 µm nitrocellulose membranes (Bio-Rad, Hercules, CA, USA). After blocking with 5% BSA (Sigma-Aldrich, St. Louis, MO, USA) in TBS (Tris-HCl pH 7.4, 150 mM NaCl), 0.3% Tween-20 for at least 1 h at RT, membranes were incubated overnight (ON) at 4 ◦C with the primary antibodies (Aconitase 2, #6922, Cell Signaling Technology, Danvers, MA, USA, p21 sc-6246, Santa Cruz Biotechnology, Dallas, TX, USA, MDM2, sc-13161, Santa Cruz Biotechnology, Dallas, TX, USA, Cleaved Caspase 3, #9664, Cell Signaling Technology, Danvers, MA, USA, GAPDH, sc-365062, Santa Cruz Biotechnology, Dallas, TX, USA). For each antibody, a dilution of 1:1000 was used. As secondary antibodies, we used peroxidase-conjugated goat anti-mouse IgG-HRP (Santa Cruz Biotechnology, sc-2005) or goat anti-rabbit IgG-HRP (Santa Cruz Biotechnology, sc2004), both at 1:8000 dilutions for 1 h at RT. Immuno-reactive bands were visualized by using chemiluminescent enhanced reagent (Clarity Western ECL Substrate #170-5061, Bio-Rad). Quantification was performed using the Image Lab program (BioRad Laboratories, Hercules, CA, USA) [148].

4.14 Gene Expression Profiling Analysis in Deferasirox-Treated Cells

Gene expression profiling of DFX-treated leukemic cells by Affymetrix GeneChip (U133 Plus 2.0, Santa Clara, CA, USA) was retrieved from GEO (GSE11670). Treated samples (GSM296615, GSM296616) with Deferasirox 50 µM for 16 h and untreated controls (GSM296608, GSM296609) were analyzed by the GEO2R tool. Original submitter-supplied processed data tables were imputed into R using GEOquery [149]. Linear Models for Microarray Analysis (Limma) R package from the Bioconductor project were used to compute differential expression [150]. Differentially expressed probes (p-value < 0.001) were annotated with the Ensembl BioMart tool and the GRCh38.p12 as a reference genome assembly [151].

In case of multiple probe sets corresponding to the same gene annotation, the probe set with lower p-value was used. Identified differentially expressed genes were submitted to a pathway analysis using the tool EnrichR [152]. The first 10 enriched terms from the National Cancer Institute Nature (NCI-Nature) Pathway Interaction Database (PID) 2016 were ordered by ascending adjusted p-value and reported [153]. Differentially expressed genes involved in the identified pathways were visualized and hierarchically clustered by using the Clustergrammer web-tool integrated in EnrichR.

4.15 Immunohistochemistry on MDS Bone Marrow Samples

Immunohistochemistry experiments were performed on formalin-fixed [136], paraffin-embedded serial sections of 4 µm thick, derived from 5 MDS patients at diagnosis and within one year of iron chelation treatment (ICT). FFPE tissue sections were previously deparaffinized. p73 (dilution 1:100, ab40658) and p53 (dilution 1:200, MA5-12453) labelling was performed using the UltraView Universal DAB Detection Kit (Ventana Medical Systems, Orovalley, AZ, USA) on Benchmark ULTRA (Roche, Ventana, Meylan, France). Slides were scored independently by 2 pathologists.

4.16 Statistical analysis

Statistical analyses were performed using the paired t-test. All the experiments were performed in triplicate and analyses with confidence level greater than 95% are indicated as significant and marked as follows: * $p \leq 0.05$, ** $p \leq 0.01$, and *** $p \leq 0.001$. Biochemical data were analyzed by one-way analysis of variance (ANOVA) followed by Tukey's multiple comparison test, using GraphPad Prism version 7.00. p-value < 0.05 was considered significant.

5. RESULTS

Oxidative stress, iron overload, and consequently mitochondrial dysfunction, appear as emerging key players in MDS pathogenesis and progression. Therefore, we analyzed the energy metabolism status of MDS and its link with oxidative stress and iron overload. In particular, we studied the production of aerobic ATP, glycolysis, mitochondrial efficiency, and lipid peroxidation of mononuclear cells (MNC) isolated from patients with MDS, comparing the results obtained with those obtained with MNC from healthy young and old subjects. Furthermore, we have analyzed the same parameters after treatment with two iron chelators.

5.1 Cellular energy status decreases in MDS mononuclear cells

The cellular energy state was studied in terms of ATP / AMP ratio, which represents the balance between available energy (ATP) and energy used (AMP). The measured ATP derives from both anaerobic glycolysis and OxPhos metabolism. In patients with MDS the cellular energy state significantly decreases. As shown in **Figure 10**, the ATP / AMP ratio progressively decreases from young controls (8-20 years) to adult controls (21–60 years) and elderly controls (61-86 years). Interestingly, MDS subjects show a further decrease in this ratio, indicating a further reduction in energy availability (young CTRL vs elderly CTRL $p < 0.0001$ e CTRL elderly vs MDS $p < 0.0001$). More specifically, the mean ATP / AMP ± SEM ratio in young CTRLs is 3.3 ± 0.2, in adults, the CTRL is 2.5 ± 0.2 and in the elderly, the CTRL is 1.3 ± 0.1, while it is 0.2 ± 0.03 in subjects with MDS.

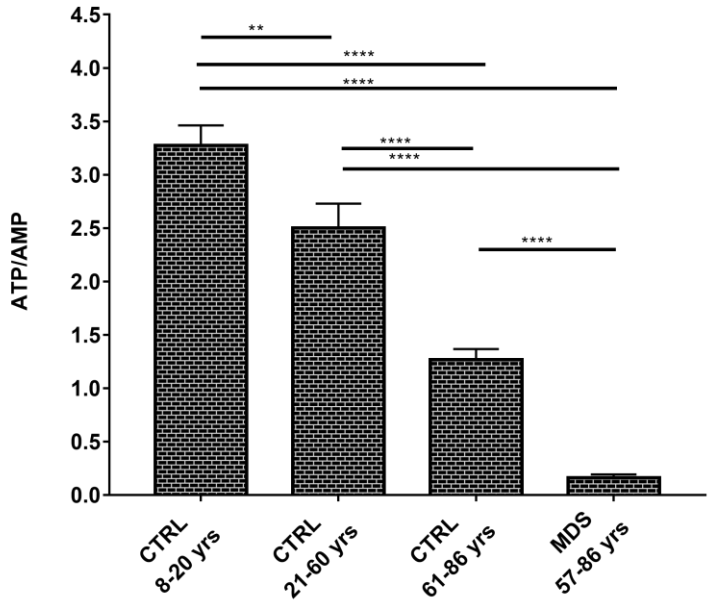

Figure 10: ATP/AMP ratio. ATP/AMP ratio in MNCs isolated from young healthy subjects (CTRL 8–20 yrs), adult healthy subjects (CTRL 21–60 yrs), elderly healthy subjects (CTRL 61–86 yrs) and MDS patients with iron overload. Each column represents the mean ± SEM. Data are analyzed by one-way ANOVA followed by Tukey's multiple comparison test. ** indicates a significant difference for p < 0.0001 between MDS sample and the healthy controls.**

5.2 OxPhos is defective in MDS mononuclear cells

To evaluate whether the decrement of ATP/AMP ratio in elderly and MDS subjects was due to a dysfunction of mitochondrial energy metabolism, we analyzed the OxPhos activity. Oxygen consumption has been assayed after stimulation with pyruvate/malate (P/M) or succinate, to activate the pathways composed by complexes I, III, and IV or complexes II, III, and IV, respectively. As shown in **Figure 11**, the oxygen consumption increases progressively with age, and the respiration of MDS-MNCs appears no-significantly different from those of adult and elderly controls.

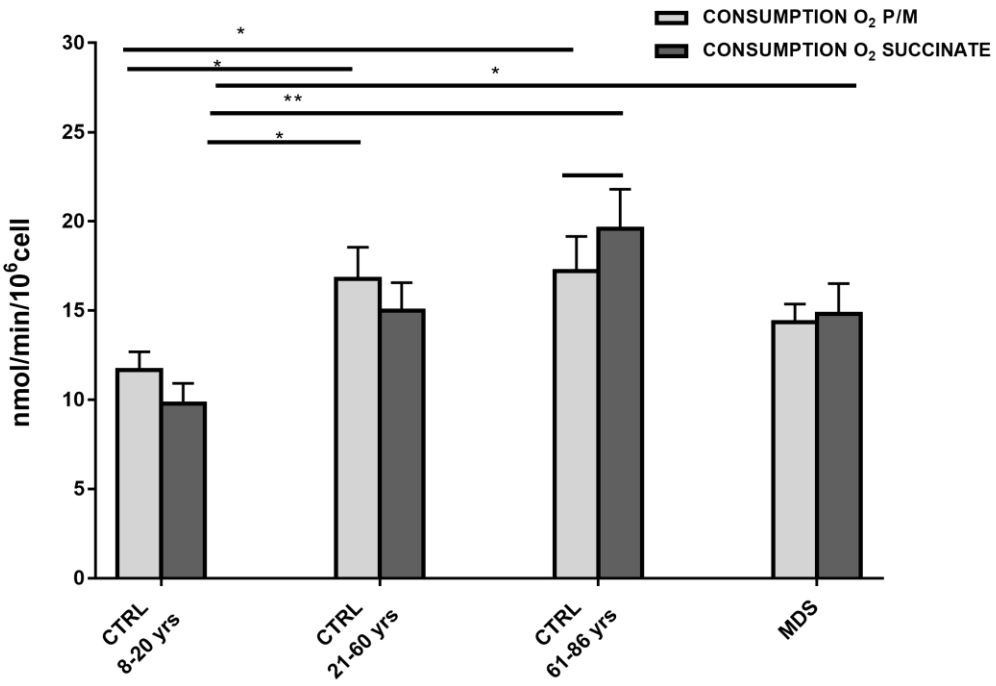

Figure 11: Oxygen consumption, ATP synthesis and P/O value in the presence of pyruvate/malate or succinate. Oxygen consumption after stimulation with pyruvate/malate (P/M) (light grey column) or succinate (dark gray) in MNCs isolated from young healthy subjects (CTRL 8–20 yrs, n=18), adult healthy subjects (CTRL 21–60 yrs; n=18), elderly healthy subjects (CTRL 61–86 yrs, n=25) and MDS patients with iron overload (n=22).

Conversely, ATP synthesis is significantly reduced in elderly control and, less marked, in MDS with respect to young and adult, confirming a significant involvement of complexes I, III, and IV (**Figure 12**), which are the most efficient pathways implicated and the main ROS producers [51]. In details, the oxygen consumption, expressed as mean ± SEM, after stimulation with pyruvate/malate is 10.3±0.7 in young CTRL, 14.3±0.7 in adult CTRL, 18.9±1.9 in elderly CTRL, and it is 15.3±0.7 in MDS subjects. The oxygen consumption after stimulation with succinate is 8.8±0.7 in young CTRL, 15.8±1.6 in adult CTRL, 19.4±1.9 in elderly CTRL, and 15.7±1.7 in MDS subjects. Regarding the ATP synthesis, we observed an ATP production of about 28.5±2.7 in young CTRL, 29.9±2.7 in adult CTRL, 12.6 ± 1.5 in elderly CTRL, and 16.6 ± 1.8 in MDS subjects after stimulation with pyruvate/malate; a similar effect was observed after stimulation with succinate with values of 16.0±1.2 in young CTRL, 15.9±1 in adult CTRL, 12,5±1 in elderly CTRL, and 11.2±1.4 in MDS subjects.

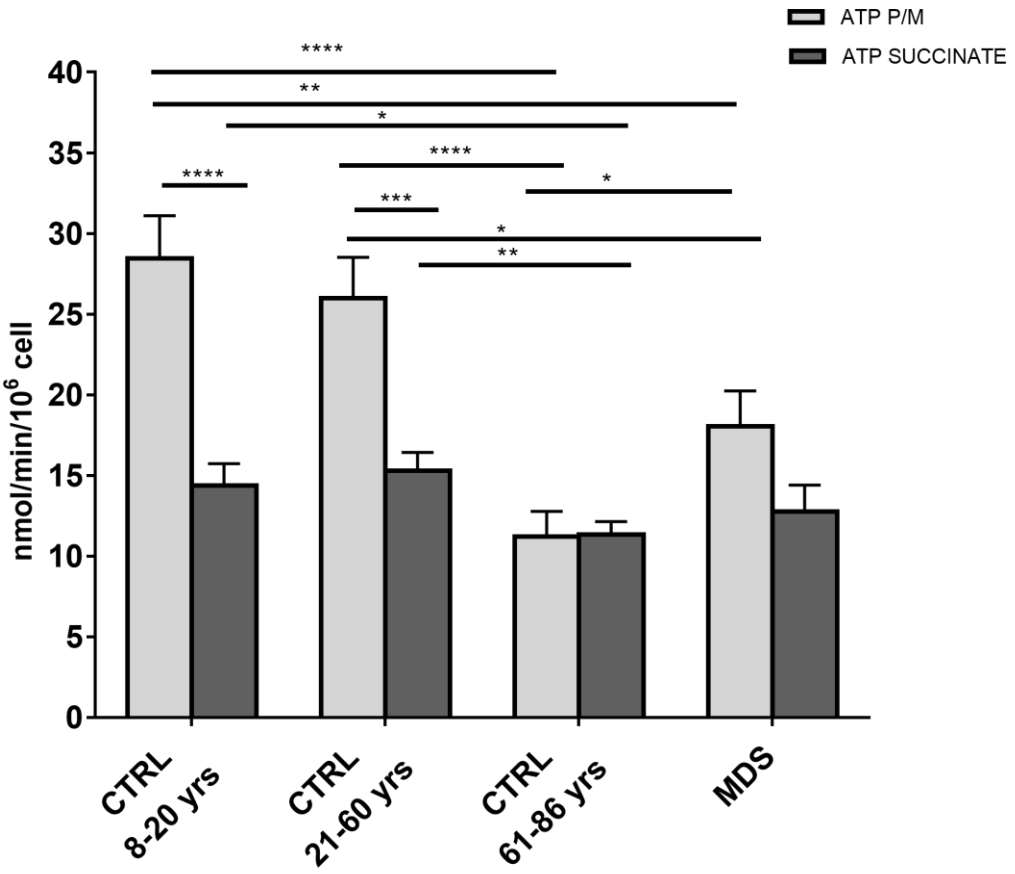

Figure 12: aerobic ATP synthesis after stimulation with P/M (light grey column) or succinate (dark gray) in MNCs isolated from young healthy subjects (CTRL 8–20 yrs, n=18), adult healthy subjects (CTRL 21–60 yrs; n= 18), elderly healthy subjects (CTRL 61–86 yrs, n=25) and MDS patients with iron overload (n= 22).

To obtain a more precise picture of the mitochondrial efficiency, we calculated the P/O value, as the ratio between the produced ATP and the oxygen consumption (**Figure 13**). The P/O ratio is clearly reduced in elderly CTRL and MDS compared to young or adult CTRL. In particular, the P/O ratio in young CTRL is 2.6 ± 0.1 for P/M and 1.5 ± 0.1 for succinate (similarly to the values reported in the literature [140]), while in the other groups decreases proportionally with the age: 2.3 ± 0.1 for adult CTRL, 1 ± 0.2 for elderly CTRL, 1.3 ± 0.1 for MDS, after P/M induction, and 1.4 ± 0.1 for adult CTRL, 0.9 ± 0.1 for elderly CTRL, 1 ± 0.1 for MDS, after succinate stimulation. Notably, the difference is again more pronounced in the presence of P/M compared to that obtained after succinate induction.

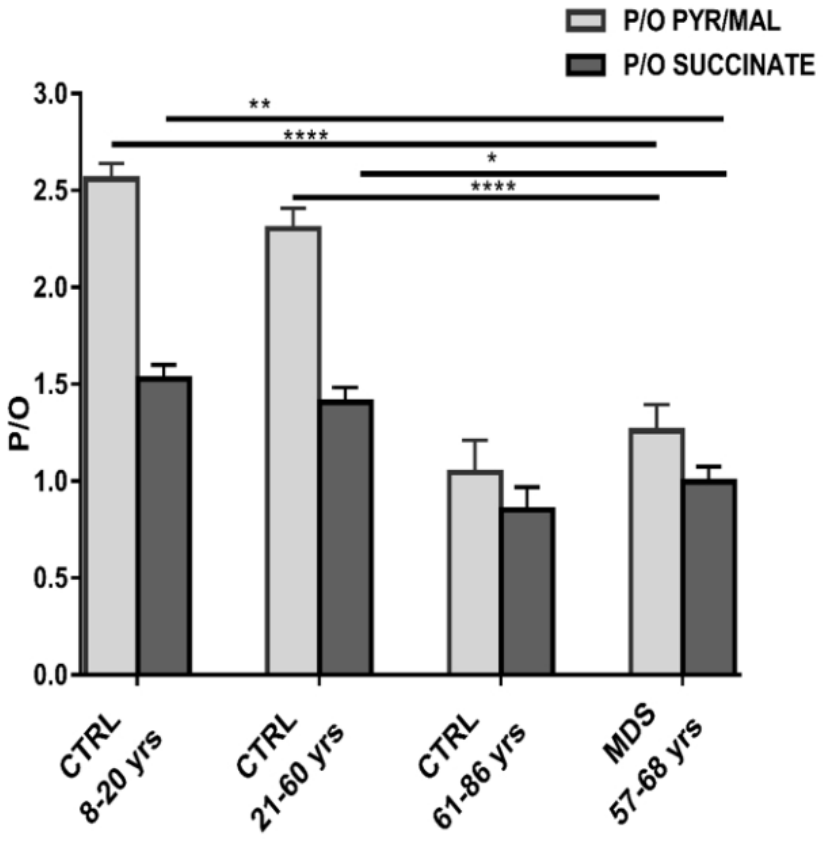

Figure 13: P/O ratio, as marker of OxPhos efficiency, in MNCs isolated from young healthy subjects (CTRL 8–20 yrs, n =18), adult healthy subjects (CTRL 21–60 yrs; n= 18), elderly healthy subjects (CTRL 61–86 yrs, n=25) and MDS patients with iron overload (n = 22). Data are expressed as mean ± SEM. Data are analyzed by one-way ANOVA followed by Tukey's multiple comparison test. *, **, *, **** indicate a significant difference for p <0.05, p < 0.01, p<0.001, p < 0.0001, respectively, between MDS sample and the healthy controls**

5.3 Lactate fermentation is enhanced in MDS mononuclear cells

To evaluate the contribution of the anaerobic glycolysis to the cell energy status, we evaluated the lactate dehydrogenase (LDH) activity, which converts pyruvate to lactate, when oxygen is absent or in short supply. In our samples, LDH activity is higher in MDS and elderly CTRL, as compared to young and adult controls ($p<0.0001$) (**Figure 14**). More in details, in young CTRL the mean LDH activity ± SEM is 188.5 ± 8.7 mU/mg, in adult CTRL is 205.6 ± 15.9 mU/mg, in elderly CTRL is 281.7 ±13.4 mU/mg and in MDS is 337 ±9.6 mU/mg.

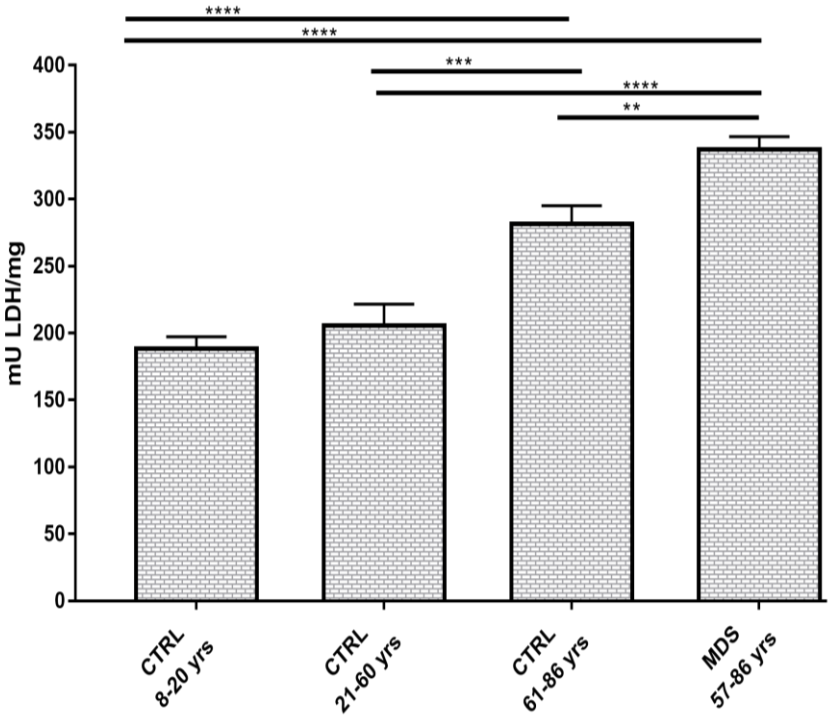

Figure 14: LDH activity assay. LDH activity has been evaluated as marker of anaerobic glycolysis in MNCs isolated from young healthy subjects (CTRL 8–20 yrs, n= 18), adult healthy subjects (CTRL 21–60 yrs; n =20), elderly healthy subjects (CTRL 61–86 yrs, n=25) and MDS patients with iron overload (n =16). Each column represents the mean ± SEM. Data are analyzed by one-way ANOVA followed by Tukey's multiple comparison test. * indicates a significant difference for $p < 0.05$ between MDS and CTRL 61–86 yrs; ** indicates a significant difference for $p < 0.0001$ between MDS sample and the CTRL 8–20 or the CTRL 21–60.**

5.4 Oxidative stress is increased in mononuclear cells from MDS patients

Since the OxPhos inefficiency is linked to an increment of oxidative stress production, we have evaluated the MDA level, as a marker of lipid peroxidation. MDA levels increase in elderly controls compared to young controls and appear even higher in MDS samples: $p < 0.001$ for MDS vs elderly CTRL, $p < 0.0001$ for elderly CTRL vs adult CTRL, $p < 0.0001$ for adult CTRL vs young CTRL. Going into details, the mean ± SEM MDA levels are: 1.2 ± 0.2μM/mg in young CTRL, 4 ± 0.7 μM/mg in adult CTRL, 9.3 ± 0.6 μM/mg in elderly CTRL, and 13.9 ± 1 μM/mg in MDS patients (**Figure 15**).

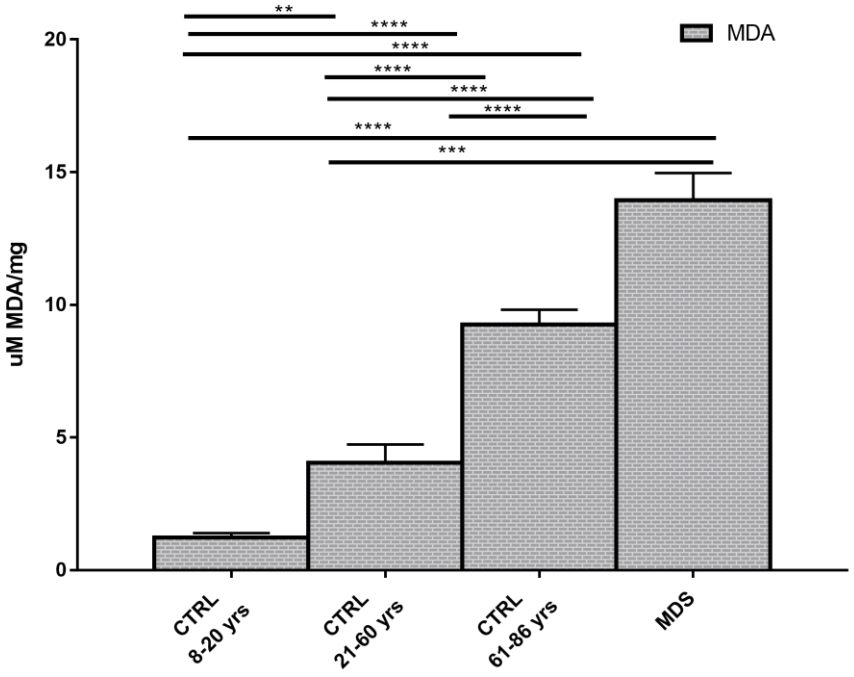

Figure 15: Lipid peroxidation evaluated through the malondialdehyde levels. Malondialdehyde (MDA) levels have been evaluated in MNCs isolated from young healthy subjects (CTRL 8–20 yrs, n= 18), adult healthy subjects (CTRL 21–60 yrs; n=24), elderly healthy subjects (CTRL 61–86 yrs, n= 28) and MDS patients with iron overload (n =30). Each column represents the mean ± SEM. Data are analyzed by one-way ANOVA followed by Tukey's multiple comparison test. ** indicates a significant difference for p <0.0001 between MDS sample and the healthy controls.**

5.5 Mitochondrial Morphology on Acute Myeloid Leukemia Cell Lines

After confirming the alteration of mitochondrial activity in MDS specimens, we tried to find a link between this phenomenon and iron overload, event commonly involved in the generation of intracellular Reactive Oxygen Species (ROS), in the increase of genomic instability, of lipid peroxidation and consequently in the reduction of mitochondrial function.
Indeed, we decided to treat the AML cell lines, HL60, NB4, and MOLM-13, with 50 µM of DFX for 48h and to examine mitochondria dynamics.

5.6 MiNA Toolset: iron chelation induces the Fragmentation of Mitochondrial Network and Dysfunction in the Oxidative Phosphorylation in acute Myeloid Leukemia Cell Lines

The analysis of the mitochondria shapes was performed by using the MiNA toolset [144], which allows obtaining parameters to quantitatively capture the morphology of the mitochondrial network. In all cell lines under physiological conditions, mitochondria were interconnected, thus forming an intracellular network (**Figure 16 A**). By contrast, when compared to the respective controls, DFX treatment caused a severe alteration of the mitochondrial network, as highlighted by the skeletal images and by the mitochondria footprint quantification (**Figure 16 B**).

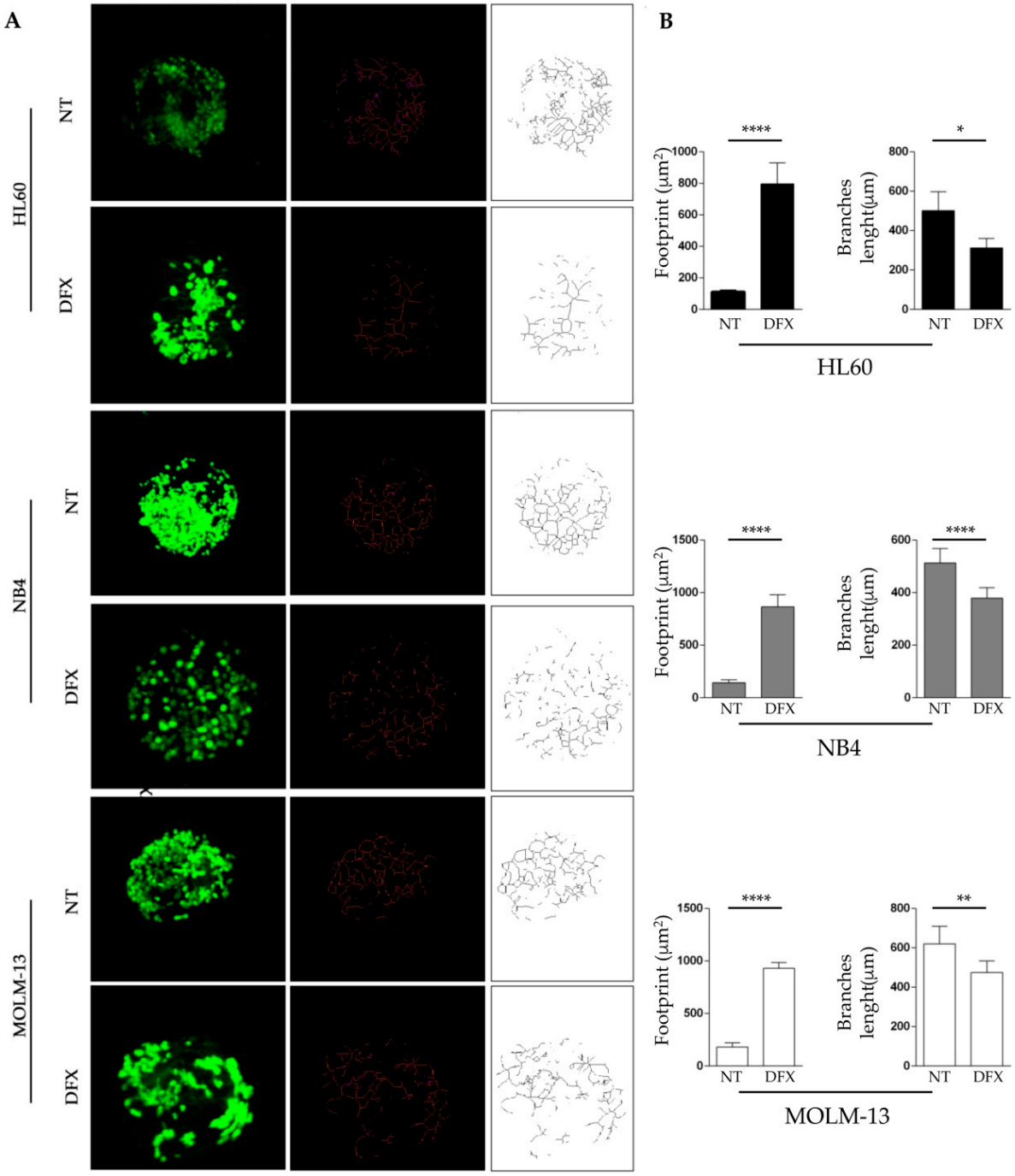

Figure 16: Iron chelation induces an altered network in acute myeloid leukemia cell lines. HL60, NB4, and MOLM-13 were treated for 48 h with 50 µM of DFX and subsequently incubated with 100 nM of MitoTracker green for mitochondrial network analysis. (A) The original green image obtained with a confocal microscope is a three-dimensional (3D) image created with a z-stack project (63× magnification). It has been processed using the MiNA toolset to generate an accurate skeleton. In red and black and white, the skeleton of mitochondria of the three cell lines treated with DFX is visible, compared to respective control. (B) Quantification of mitochondria footprint and branches length, which corresponds respectively to the area and connection of mitochondria expressed in µm. Abbreviations: NT, not treated; DFX, Deferasirox. * $p \leq 0.05$, ** $p \leq 0.01$, and **** $p \leq 0.0001$.

Indeed, DFX-treated cells showed a higher mitochondrial area compared to non-treated cells, while the mean mitochondria branch length is shorter in treated cells. Both morphological information clearly indicated an alteration of mitochondrial dynamics, in turn affecting the mitochondrial network and potentially, the function.

5.7 Mitochondrial metabolism in leukemic cell lines

These morphological alterations seem to be associated with a dysfunctional activity of oxidative phosphorylation (OxPhos). In particular, all myeloid leukemia cell lines treated with DFX displayed a reduction of oxygen consumption rate (OCR) and ATP synthesis through F0-F1 ATP synthase (**Table 7**). Moreover, the residual OxPhos activity appeared less efficient since the P/O value is lower concerning those observed in the untreated sample (**Table 7**).

	HL60		**NB4**		**MOLM-13**	
	NT	**DFX**	**NT**	**DFX**	**NT**	**FDFX**
OCR_P/M (nmol O/min/106 cells)	33.86 ± 1.25	19.51 ± 1.84 ****	30.98 ± 1.74	14.03 ± 1.23 ****	18.55 ± 1.19	9.96 ± 0.89 ***
ATPsynth_P/M (nmol ATP/min/106 cells)	82.89 ± 0.91	37.46 ± 1.86 ****	75.98 ± 3.11	16.58 ± 1.84 ****	44.96 ± 1.77	11.24 ± 0.93 ***
P/O_P/M	2.45 ± 0	1.62 ± 0.03 ****	2.45 ± 0.12	1.18 ± 0.04 ****	08 2.43 ± 0.08	1.13 ± 0.04 ***
OCR_Succ (nmol O/min/106 cells)	22.50 ± 1.08	12.87 ± 0.73 ****	20.52 ± 1.02	9.26 ± 0.85 ****	12.58 ± 0.54	6.78 ± 0.47 ****
ATPsynth_Succ (nmol ATP/min/106 cells)	4.96 ± 2.	85 14.95 ± 0.58 ****	32.05 ± 0.68	6.99 ± 0.31 ****	18.97 ± 1.45	4.73 ±0.66 ****
P/O_Succ	1.56 ± 0.09	1.00 ± 0.05 ****	1.57 ± 0.07	0.76 ± 0.04 ****	1.55 ± 0.09	0.72 ± 0.04 ****

Table 7: Iron chelation induced a decrement of oxygen consumption, ATP synthesis and a less efficient OxPhos in acute myeloid leukemia cell lines. The table reports the oxygen consumption rate (OCR) and the ATP synthesis (ATPsynth) through F0-F1 ATP synthase in acute myeloid leukemia cell lines untreated (NT) or treated with DFX. These activities have been evaluated in the presence of pyruvate/malate (P/M) or succinate (Succ), to investigate the OxPhos pathways triggered by complex I or complex II, respectively. The P/O value is calculated as the ratio between ATPsynth and OCR and represents a marker of mitochondrial efficiency. Literature reports that a complete efficiency is observed when the P/O ratios are 2.5 or 1.5 in the presence of pyruvate/malate or succinate, respectively. Data are expressed as mean + standard deviation (SD) and are representative of three independent

experiments. * or **** indicate a $p < 0.001$ or $p < 0.0001$ respectively, between the same untreated or DFX-treated samples.**

In addition, as a consequence of this metabolic alteration, the ATP/AMP ratio, a marker of cellular energy metabolism was very low in the DFX-treated samples in comparison to the controls, due to a decrement of ATP and an increment of AMP intracellular levels (**Table 8**).
Subsequently, investigating by Western blot the expression of the mitochondrial Aconitase 2 (Aco2), we observed a significant protein reduction (**Figure 17**), thus proving the importance of mitochondrial morphogenesis machinery components on mitochondrial function and activity. All these results demonstrate that iron chelation affects mitochondria in leukemic cells, representing a new attractive anti-leukemic strategy.

	HL60		NB4		MOLM-13	
	NT	**DFX**	**NT**	**DFX**	**NT**	**FDFX**
ATP (mM/mg)	2.39 ± 0.09	1.58 ± 0.22 ***	2.24 ± 0.10	1.29 ± 0.04 ***	2.17 ± 0.06	1.23 ± 0.04 ***
AMP (mM/mg)	0.84 ± 0.03	1.21 ± 0.04 ***	0.83 ± 0.04	1.40 ± 0.06 ***	0.95 ± 0.05	1.47 ± 0.02 ***
ATP/AMP	2.86 ± 0.07	1.45 ± 0.18 ****	2.71 ± 0.21	0.92 ± 0.06 ****	2.28 ± 0.16	0.84 ± 0.03 ****

Table 8: Iron chelation induced a decrement of cellular energy status in acute myeloid leukemia cell lines. The table reports the intracellular level of ATP and AMP, and the consequent ATP/AMP ratio to investigate the cellular energy status. Data are expressed as mean + SD and are representative of three independent experiments. * or **** indicate a $p < 0.001$ or $p < 0.0001$ respectively, between the same untreated or DFX-treated samples.**

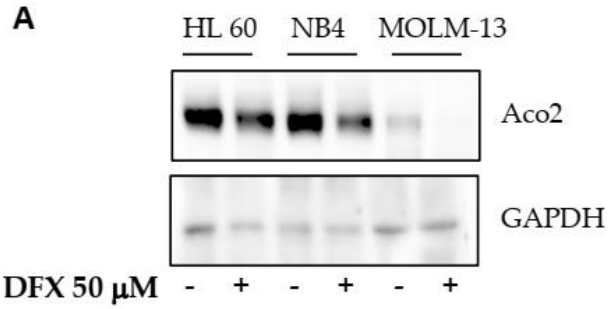

Figure 17: Aconitase 2 was analyzed by western blot in HL60, NB4 and MOLM-13 after treatment with 50 mM of DFX.

5.8 Deferasirox Exerts In Vitro Anti-Leukemic Activity on Acute Myeloid Leukemia Cell Lines

To assess whether the morphological alterations and dysfunctional activity of mitochondria were associated with cell viability, we analyzed the rate of cell proliferation and apoptosis after iron chelation treatment. Initially, we treated MOLM-13, HL60, and NB4 cell lines with 10, 25, 50, or 100 µM of DFX for 48 h. DFX inhibited the growth of all tested cell lines in a dose-dependent manner, reaching the maximum effect at 100 µM, with a reduction in proliferation close to 70% in all cells tested (**Figure 18**).

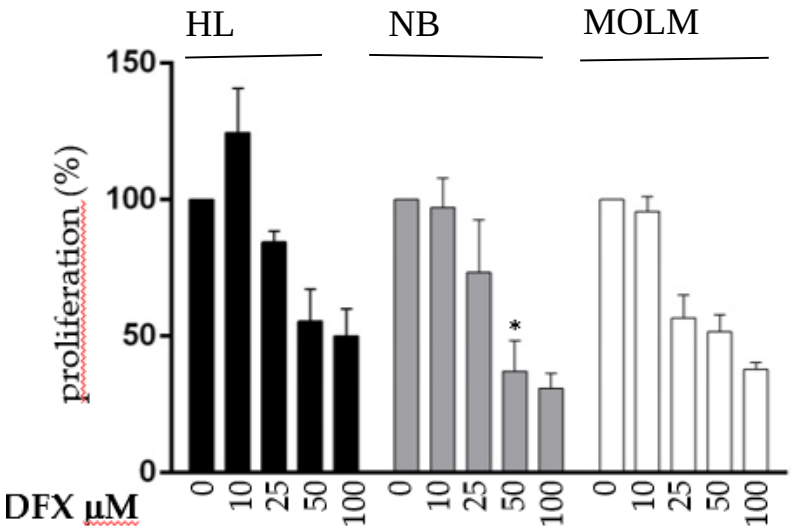

Figure 18: Deferasirox exerts an anti-leukemic activity on AML cell lines and on MDS patients' cells. HL60, NB4, and MOLM-13 were treated with 0, 10, 25, 50, or 100 µM DFX for 48 h and the MTT assay was performed to evaluate the proliferation index. The percentage of proliferation is expressed after normalizing with untreated cells (100%).

These promising results were confirmed by viability assay performed by Fluorescence Activated Cell Sorting (FACS) (**Figure 19**), with a significant dose-dependent reduction of viability after DFX exposition when compared to untreated cells.

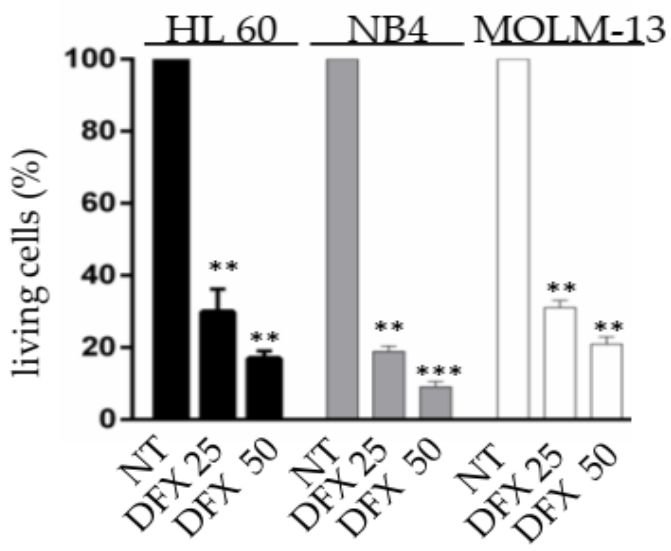

Figure 19: HL60, NB4 and MOLM-13 living cells were counted at FACS after DFX treatment.

To validate our experimental protocol, we investigated iron levels after 48 h of DFX treatment, at a concentration of 25 and 50 µM, that appeared to be the most tolerated concentrations, also capable of heavily decrease the percentage of proliferation, using the calcein fluorescence assay. In the presence of the chelator, a dose-dependent increase in intracellular calcein fluorescence signal confirmed the reduction in the content of labile iron pool (LIP), validating our experimental tools and suggesting a clear relationship between iron chelation and anti-proliferative effects in acute leukemia cells (**Figure 20**).

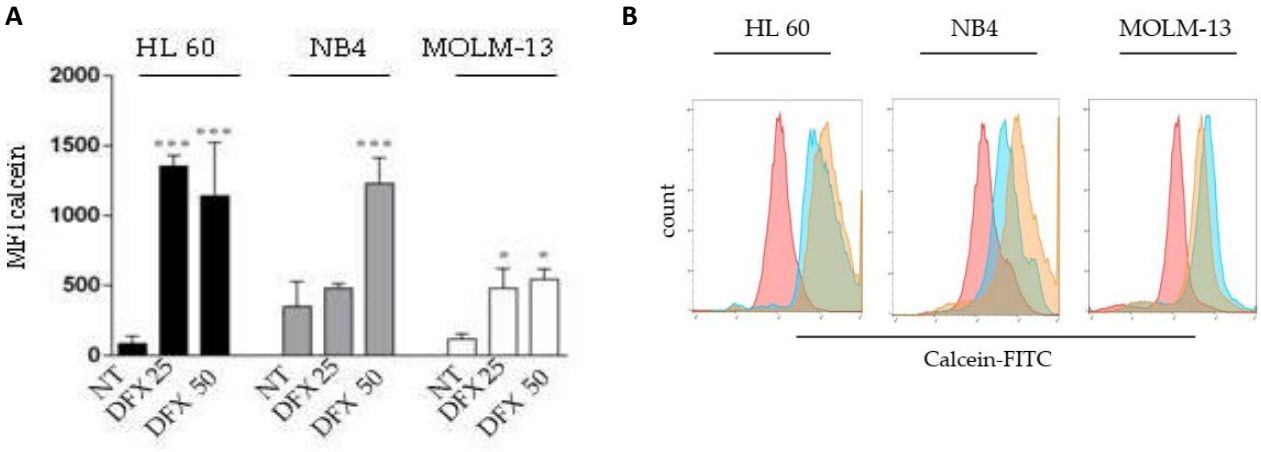

Figure 20: A) Mean fluorescence intensity (MFI) of FITC-calcein signal obtained after 48 h of DFX treatment. LIP level was inversely proportional to measured fluorescence intensity. B) Istograms overlay of FITC-calcein signal after 48 hours of DFX treatment. LIP level was inversely proportional to measured fluorescence intensity.

Consistently, we also noticed an induction of apoptosis. In more detail, flow cytometric evaluation of Annexin V/PI-stained cells demonstrated a significant induction of cell death in all the tested cell lines, with a percentage of apoptotic cells reaching 20–30% at 50 μM (**Figure 21**).

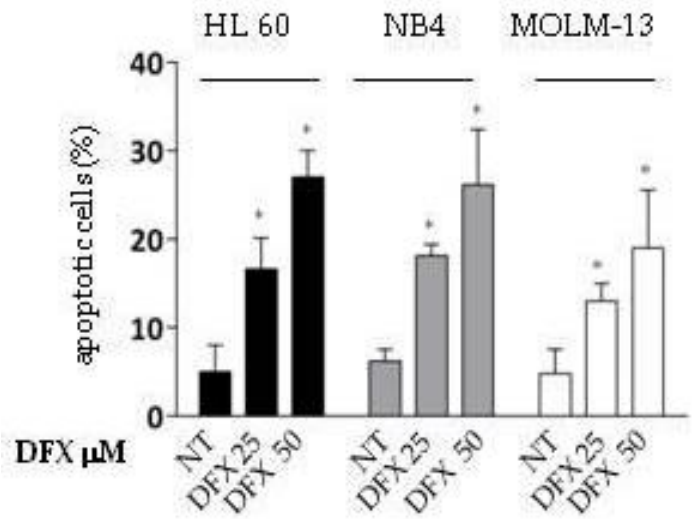

Figure 21: Percentage of apoptosis evaluated by flow cytometry after FITC Annexin-V assay on HL60, NB4, and MOLM-13 treated with 25 and 50 μM of DFX.

As shown in **Figure 22**, cleaved caspase-3 levels, analyzed by Western blot, increased dramatically in DFX-treated cells, according to the drug concentration.

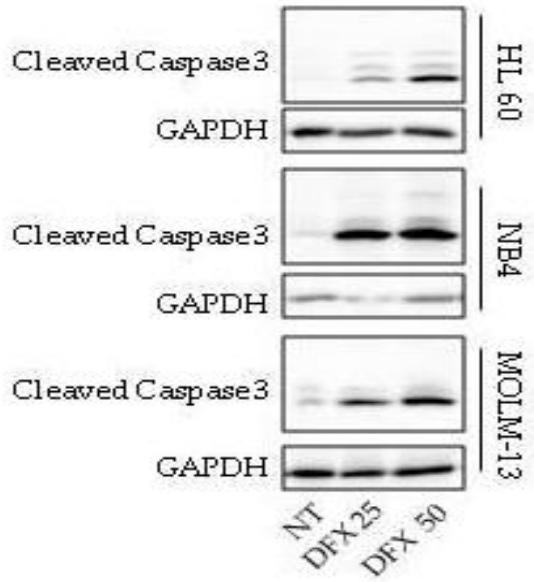

Figure 22: Western Blot analysis of cleaved caspase 3 revealed that its amount increased in a DFX dose-dependent fashion, in HL60, NB4, and MOLM-13.

5.9 Deferasirox Activates p53 Targets on Acute Myeloid Leukemia Cell Lines

Being p53 a key player in the regulation of the mitochondrion activity and apoptosis process, we investigated the p53 status and its potential involvement in the MDS/AML impaired functionality. Our hypotheses were supported by data already reported, indicating that p53 can move to mitochondria and to induce caspase activation during the apoptosis process [154]. In addition, p53 can play a role in mitochondrial dynamics by regulating genes such as *DRP1* [155]. Furthermore, it is known that iron depletion increases p53 protein amount by preventing its proteasomal degradation [156]. On this basis, to investigate if iron chelation may exert its activity on acute leukemia samples in a p53-dependent manner, we analyzed the expression of well-known p53 target genes in three acute myeloid leukemia cell lines characterized by a peculiar p53 genotype. Indeed, MOLM cells harbor a wild-type p53 locus, whereas HL-60 and NB4 are p53 null and p53 R248Q, respectively. Treatment with DFX induced a sharp increase in the expression of cell cycle-dependent kinase inhibitor *CDKN1A* and of the pro-apoptotic *PUMA* genes, the most representative genes dependent on p53 (**Figure 23 and 24**). Surprisingly, the transcriptional regulation was sensitive to DFX treatment independently from the p53 mutational status, since the increased expression was observed in all the cell lines tested. This innovative result suggests that DFX effects could depend from a p53 family member other than p53 itself. Instead, *GADD45* did not appear to be significantly modified after iron chelation (**Figure 23**).

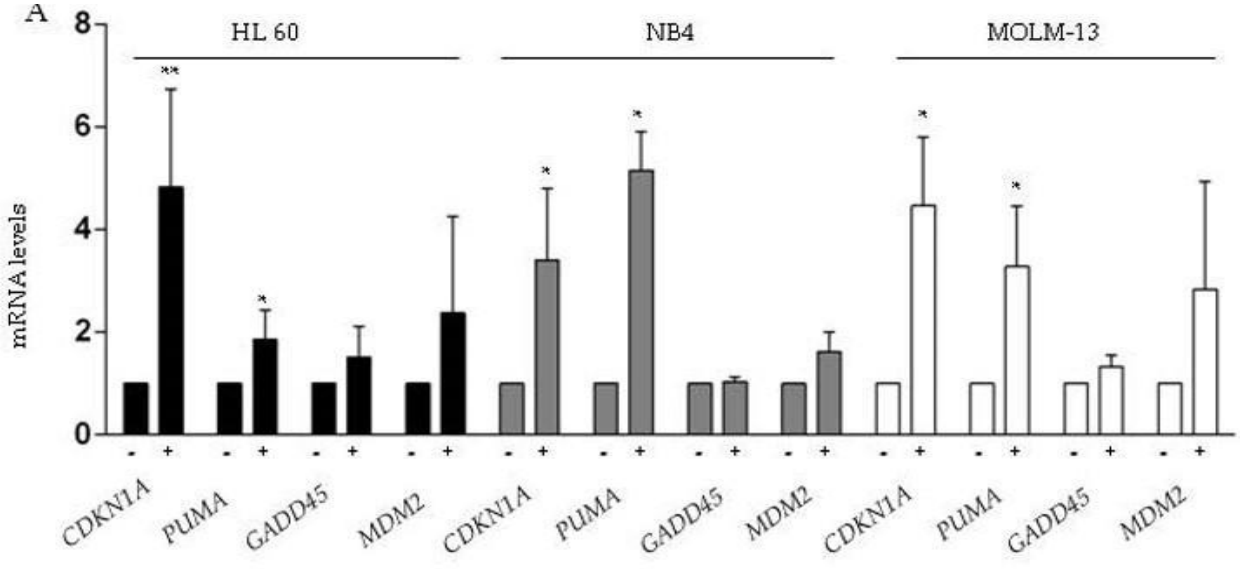

Figure 23: Deferasirox activates p53 targets on acute myeloid leukemia cell lines and MDS/AML patients Deferasirox activates p53 targets on acute myeloid leukemia cell lines and MDS/AML patients. *CDKN1A*, *PUMA*, *GADD45*, and *MDM2* gene expression were assayed by qRT-PCR in HL60, NB4, and MOLM-13 after 48 h treatment with DFX 50 µM. The amount is expressed as fold changes compared to untreated cells after normalizing on the ABL housekeeping gene.

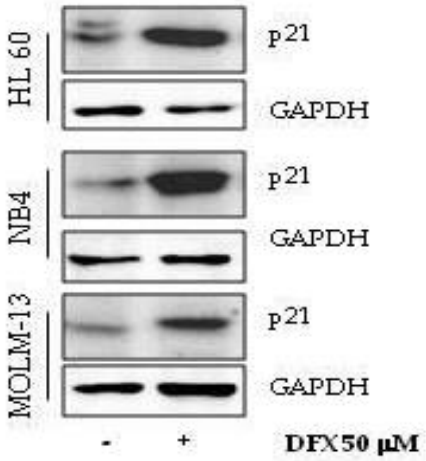

Figure 24: Western blot analysis of target proteins p21 after iron chelation treatment confirmed the effects of DFX on the p53 pathway.

On the contrary, we noticed a discrepancy for MDM2. In more detail, with some minor differences between the tested cell lines, we observed that DFX increased the mRNA (**Figure 23**) but lowered the protein level of MDM2 compared to untreated cells (**Figure 25**). Nevertheless, these results corroborated the dynamic p53-MDM2 negative feedback loop.

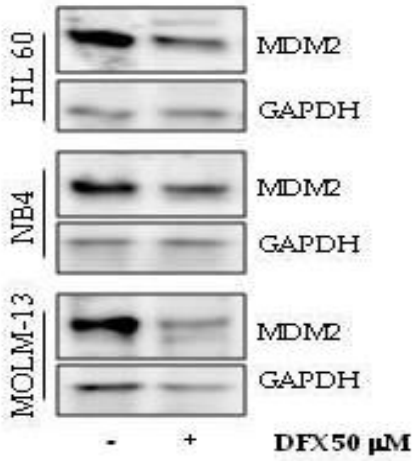

Figure 25: Western blot analysis of target proteins MDM2 after iron chelation treatment confirmed the effects of DFX on the p53 pathway.

5.10 Deferasirox regulates p53 and p73 Protein Stability

The p53 family includes two additional closely related members, p63 and p73. They share a high degree of structural homology with p53 and can activate the transcription of most p53-sensitive genes. In addition, the stability of both p53 and p73 is tightly controlled by the ubiquitin-proteasome system through the MDM2 E3 ubiquitin-ligase [157]. For that reason, and in order to identify a plausible explanation for the unexpected gene expression pattern observed even in HL60 and NB4 p53-deficient cell lines, we examined the p53 and p73 protein levels, and their subcellular localization, in the three cell lines after treatment with 50 μM Deferasirox. The results obtained by immunofluorescence showed that DFX increased p73 levels by inducing a sharp nuclear protein accumulation (**Figure 26**).

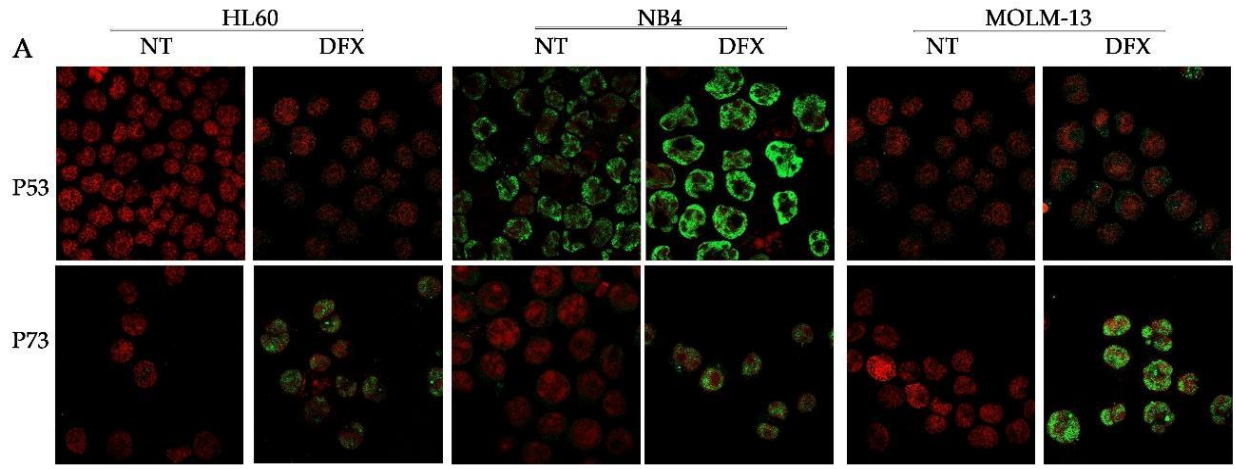

Figure 26: Deferasirox regulates p53 and p73 protein stability. Immunofluorescence of p53 and p73 after DFX treatment. The green signal corresponds to p53 or p73 while the red propidium is used to detect nuclei (63× magnification).

p53 also appears to be increased, even if with less intensity, except for the p53 null HL60 cell line. These results were further confirmed by determining the levels of cellular fluorescence from fluorescence microscopy images (**Figure 27A**), and by analyzing total protein levels by Western blot (**Figure 27B**).

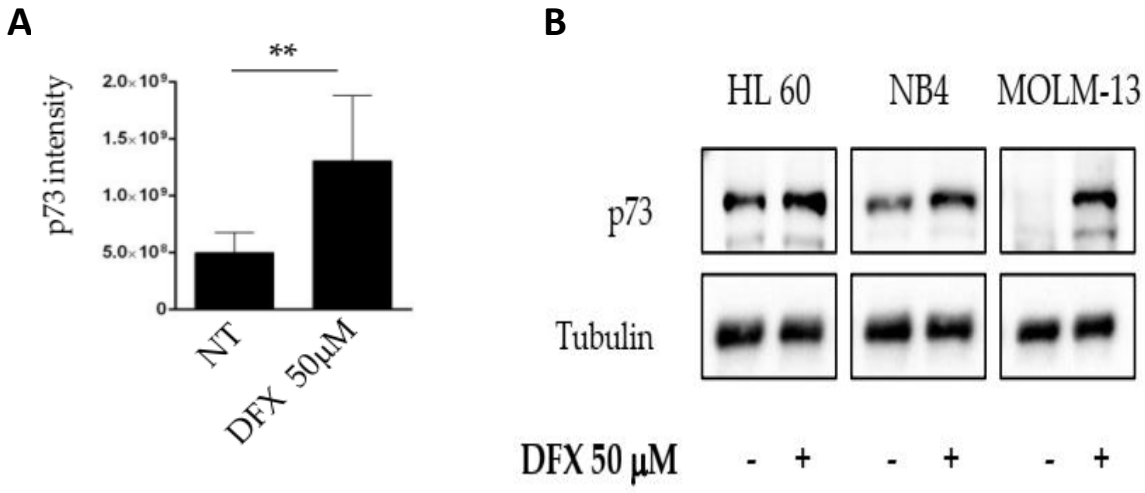

Figure 27: (A) p73 immunofluorescence signals intensity was quantified by the Java (Image J) program (B) p73 was analyzed by Western Blot in HL60, NB4 and MOLM-13 after treatment with 50 mM of DFX. Abbreviations: -: not treated, +: DFX 50 mM, NT: not treated, * $p \leq 0.05$, ** $p \leq 0.01$.

5.11 Effect of iron chelation on the transcriptional levels by analyzing a microarray dataset

To further strengthen our results, we investigated the effect of iron chelation on the transcriptional levels, by analyzing a microarray dataset from the p53-truncated K562 leukemia cell line treated with DFX [102]. Then, we performed a pathway enrichment analysis by using the 258 genes that emerged as differentially expressed. Surprisingly, although the cell line analyzed was p53-deficient, the gene [146] ontology analysis performed highlighted an enrichment related to effectors of p53, p73, and p63 networks arisen among the most significant enriched clusters (**Figure 28**). Since most of the p53 direct outputs are common to other family members [158,159], our findings indicate that iron depletion-triggered signaling, in the absence of p53, is overtaken by other family members (i.e., p73 and p63). This conclusion was significant for our previous findings concerning p53 family activation, reinforcing our hypothesis. Indeed, *TP53INP1* resulted as a highly expressed gene after iron chelation treatment. Several studies confirmed the ability of p73 to induce *TP53INP1* expression in p53-deficient cells, by enhancing the capacity of p73 to regulate cell cycle progression and apoptosis, regardless of p53. *PMAIP1*, also known as NOXA, contributes to p53 family-dependent apoptosis by a direct action on MCL1 and subsequent activation of mitochondrial membrane changes. Finally, this

analysis revealed that *CDKN1A* was commonly activated by all p53 family proteins after DFX treatment, just like our experimental results.

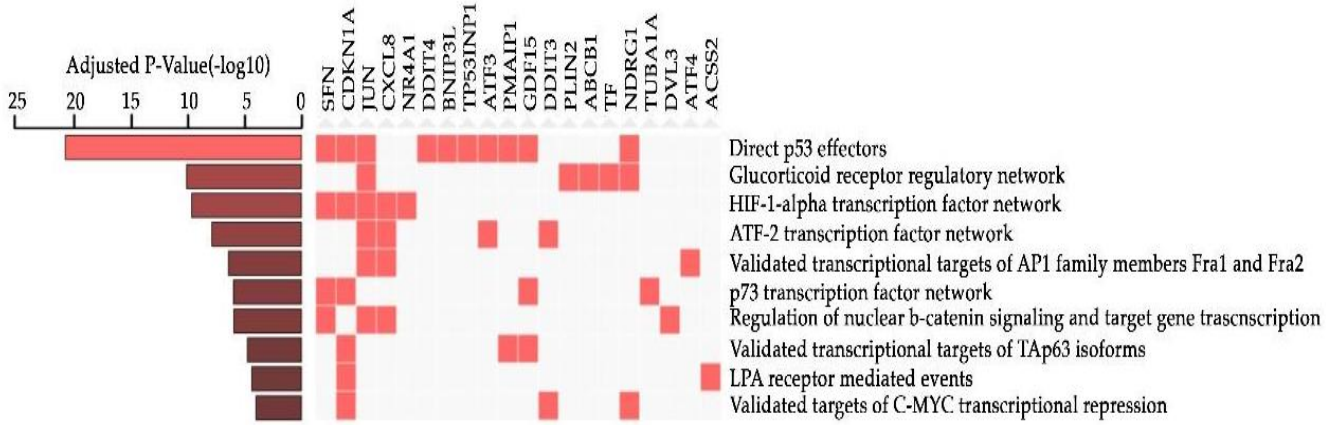

Figure 28: Differentially expressed genes clusters enriched according to Gene Ontology terms and ordered by ascending adjusted *p*-value.

5.12 Primary cell culture

We next attempted to validate our data in MDS/AML primary cells. Our objective was to:
1) confirm the effect of DFX on MDS cells in term of restoration of mitochondrial activity
2) confirm the effect of DFX on MDS cells in terms of anti-leukemic activity and p53 involvement.

5.13 Iron chelation partially restores the energy balance in MDS mononuclear cells

Since MDS patients display a high iron accumulation, which can contribute to oxidative stress production and to alteration of energy metabolism, we incubated MNCs *in vitro* for 24 or 48 hours, with two iron chelators: deferasirox (DFX) or deferoxamine (DFO). Regarding the energy balance, DFX and DFO determined a decrease in the ATP/AMP ratio in cells from young and elderly CTRL, more evident in the age range between 8–20 years old. Conversely, the treatment induced an increment of energy availability in MNCs from MDS patients, as shown in **Figure 29**. Moreover, DFX seems to be more efficient than DFO in increasing this ratio. More in detail, the ATP/AMP ratio decreases in young CTRL from a mean value of 3.19 ±0.37 to 1.24 ±0.13 with DFX and 1.66±0.23 with DFO ($p<0.0001$ and $p<0.001$, respectively). In elderly, it decreases from a mean value of 1.12 ± 0.08 to 0.87 ± 0.05 with DFX and 0.95 ± 0.06 with DFO ($p< 0.05$ only for DFX). By contrast, in

MDS the ATP/AMP ratio increases significantly from 0.12 ± 0.01 to 0.33 ± 0.02 with DFX and 0.24 ± 0.01 with DFO ($p < 0.0001$ for both). The negative effect on young healthy subjects could depend by the chelation of the iron necessary for normal mitochondrial function. On the contrary, in MDS the iron chelation improved the mitochondrial activity highly damaged by excessive iron.

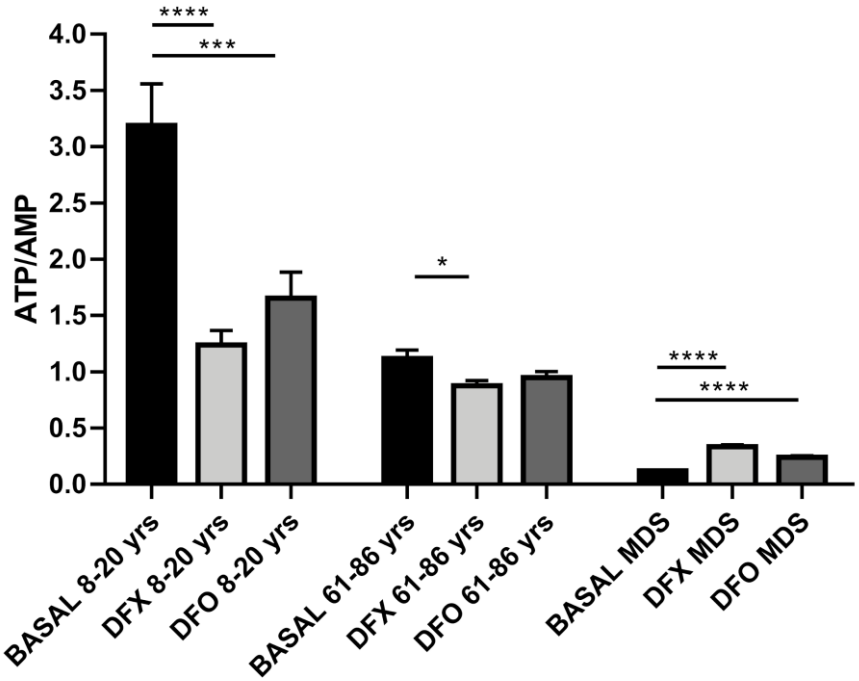

Figure 29: Evaluation of energy metabolism and lipid peroxidation after the treatment with iron chelators. MNCs treated for iron chelation with deferasirox (DFX, light grey column) or deferoxamine (DFO, grey column). BASAL is for untreated samples (black column). ATP/AMP ratio in MNCs isolated from young controls (CTRL 8–20 yrs, n=9), elderly controls (CTRL 61–86 yrs, n=7) and MDS patients (MDS, n =19). Each column represents the mean ± SEM. Data are analyzed by one-way ANOVA followed by Tukey's multiple comparison test. *, **, *, **** indicate a significant difference for p <0.05, 0.01, 0.001 or 0.0001, respectively, between the untreated sample and the MNCs treated with iron chelators.**

5.14 OxPhos improves in MDS after iron chelation

As expected, the improvement of the ATP/AMP ratio in MDS patients after iron chelation is associated with the increased efficiency of the mitochondrial respiration. After incubation with DFX or DFO, oxygen consumption decreased in MDS patients, after stimulation either with P/M or succinate, while ATP synthesis increased, indicating a better coupling of OxPhos machinery. This hypothesis is confirmed by the improvement of the P/O ratio in MDS with both DFX and DFO after

stimulation with P/M (**Figure 30A**) or succinate (**Figure 30B**). Conversely, the P/O ratio in the presence of two chelators decreased in healthy controls, justifying the impairment of the ATP/AMP ratio reported above. Interestingly, both the negative and the positive effects of chelators' treatment are more evident on the OxPhos metabolism induced by pyruvate/ malate. More in detail, the P/M P/O ratio decreases in young CTRL from 2.39 ± 0.04 to 1.54 ± 0.03 with DFX and 1.93 ± 0.03 with DFO ($p < 0.0001$ for both). In elderly healthy subjects, it decreases from a mean value of 0.85 ± 0.06 to 0.68 ± 0.02 with DFX and 0.73 ± 0.03 with DFO ($p < 0.05$ only for DFX). In MDS, the P/M P/O ratio increases significantly from 1.04 ± 0.06 to 1.74 ± 0.14 with DFX and 1.44 ± 0.09 with DFO ($p < 0.001$ and $p < 0,05$, respectively). Regarding the succinate P/O ratio, the value in young subjects passes from 1.51 ± 0.05 to 0.98 ± 0.01 with DFX and 1.15 ± 0.02 with DFO ($p < 0.0001$ for both). In the elderly subjects, it passes from 1.01 ± 0.03 to 0.93 ± 0.04 with DFX and 0.96 ± 0.04 with DFO (no significant differences). In MDS MNCs, the P/O value increases from 1.01 ± 0.03 to 1.23 ±0.03 with DFX and 1.17 ±0.01 with DFO ($p < 0.001$ and $p <0.01$, respectively).

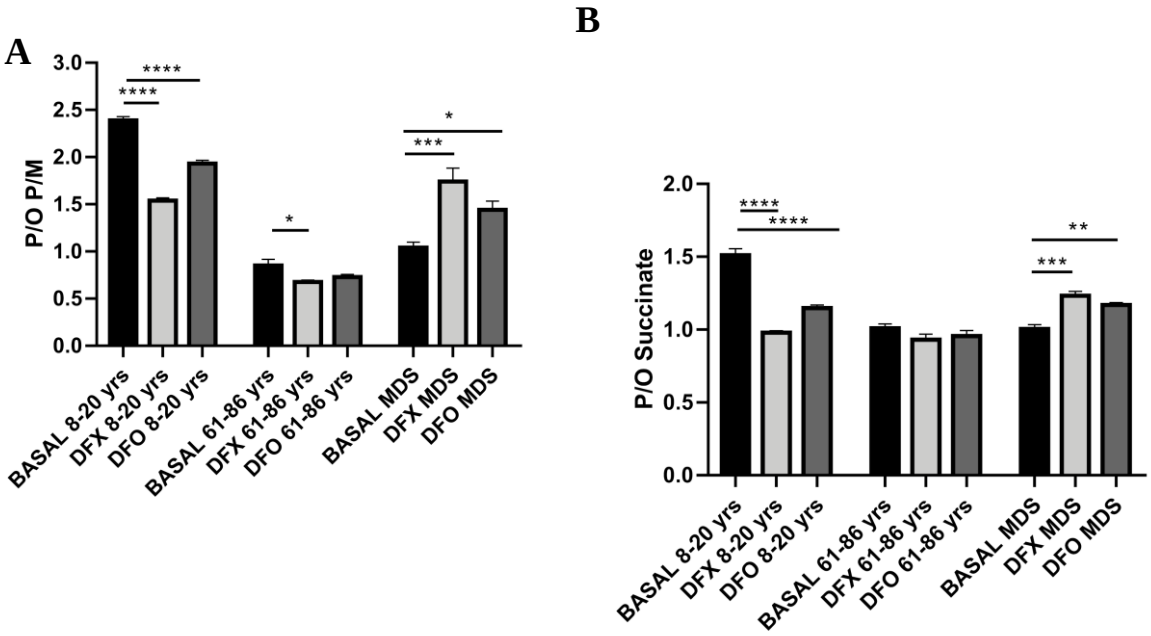

Figure 30: Evaluation of energy metabolism after the treatment with iron chelators. MNCs treated for iron chelation with deferasirox (DFX, light grey column) or deferoxamine (DFO, grey column). BASAL is for untreated samples (black column).

(A) P/O ratio after stimulation with pyruvate/malate (P/M) in MNCs isolated from young controls (CTRL 8–20 yrs, n=9), elderly controls (CTRL 61–86 yrs, n =7) and MDS patients (MDS, n =19).

(B) P/O ratio after stimulation with succinate in MNCs isolated from young controls (CTRL 8–20 yrs, n=9), elderly controls (CTRL 61–86 yrs, n=7) and MDS patients (MDS, n=19).

Each column represents the mean ± SEM. Data are analyzed by one-way ANOVA followed by Tukey's multiple comparison test. *, **, *, **** indicate a significant difference for p <0.05, 0.01, 0.001 or 0.0001, respectively, between the untreated sample and the MNCs treated with iron chelators.**

5.15 Anaerobic glycolysis decreases after iron chelation

As shown in **Figure 31**, after incubation with iron chelators, MNCs from MDS patients show a significant decrease in LDH activity ($p < 0.0001$ for DFX and $p < 0.001$ for DFO). Interestingly the reduction of LDH activity is more pronounced with DFX than DFO ($p < 0.0001$). By contrast, LDH activity is markedly increased in young controls ($p < 0.0001$ for DFX and 0.01 for DFO) and showed a slight enhancement in elderly CTRL, significant only for DFX treatment ($p < 0.05$). More in detail, the LDH activity decreases in young CTRL from 176.3 ± 3.7 to 240.4 ± 11.4 with DFX and 216.7 ± 6.6 with DFO. In elderly healthy subjects, the basal activity is 279.3 ± 4.7 and shifts to 300.2 ± 5.6 with DFX and 293.4±6.6 with DFO. In MDS MNCs, the basal LDH activity is 332.7±5.8 and passes to 274.6±4 with DFX and 303 ±5.4 with DFO.

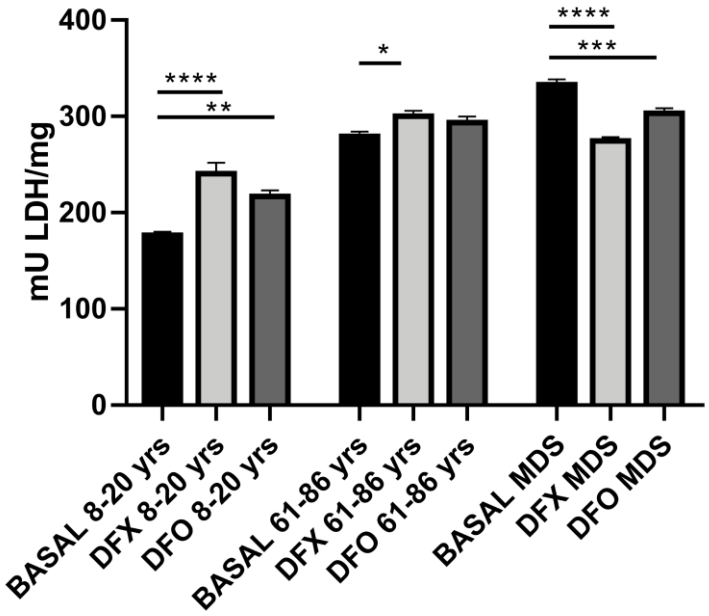

Figure 31: Evaluation of energy metabolism and lipid peroxidation after the treatment with iron chelators. Each Panel represents the data obtained on MNCs treated for iron chelation with deferasirox (DFX, light grey column) or deferoxamine (DFO, grey column). BASAL is for untreated samples (black column). LDH activity in MNCs isolated from young controls (CTRL 8–20 yrs, n= 9), elderly controls (CTRL 61–86 yrs, n=7) and MDS patients (MDS, n = 19). Each column represents the mean ± SEM. Data are analyzed by one-way ANOVA followed by Tukey's multiple comparison test. *, **, *, ****

indicate a significant difference for p <0.05, 0.01, 0.001 or 0.0001, respectively, between the untreated sample and the MNCs treated with iron chelators.

5.16 Lipid peroxidation decreases after iron chelation in MDS

Analyzing the lipid peroxidation in response to iron chelating treatment, we have observed a significant decrement of MDA levels ($p < 0.0001$ for both DFX and DFO) (**Figure 32**). By contrast, there was a trend towards increasing MDA levels in healthy controls, although statistically significant only for the young subject ($p < 0.001$ for DFX and $p < 0.05$ for DFO), probably because iron chelators induced indirect damage to the respiratory chain by removing the necessary iron. More in detail, the MDA in young CTRL is 2.3±0.5, 4.76± 0.4 with DFX and 4.2±0.4 with DFO. In elderly healthy subjects, the basal value is 9.0 ± 0.4 and passes to 10.9± 0.7 with DFX, and 10.4 ± 0.9 with DFO. In MDS MNCs, MDA basal value is 12.3 ±0.4, 8.7 ±0.2 with DFX, and 9.5 ±0.3 with DFO.

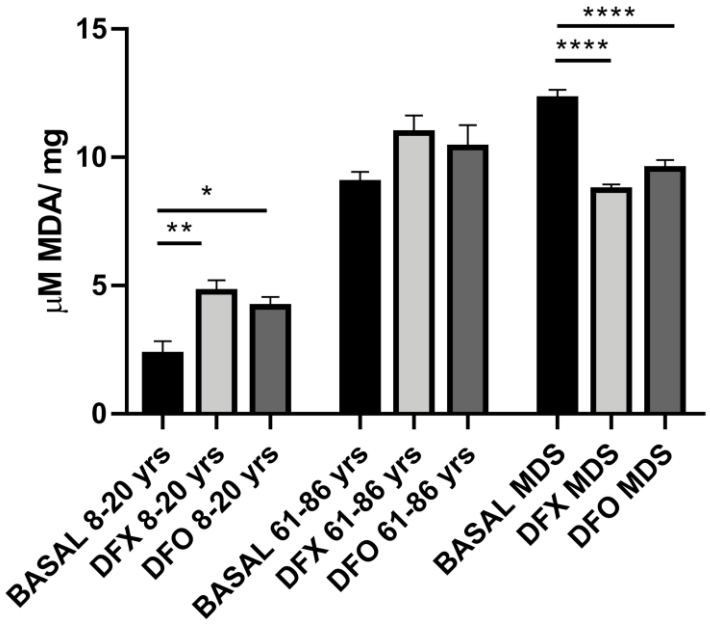

Figure 32: Evaluation of energy metabolism and lipid peroxidation after the treatment with iron chelators. Each Panel represents the data obtained on MNCs treated for iron chelation with deferasirox (DFX, light grey column) or deferoxamine (DFO, grey column). BASAL is for untreated samples (black column). MDA levels in MNCs isolated from young controls (CTRL 8–20 yrs, n= 9), elderly controls (CTRL 61–86 yrs, n =7) and MDS patients (MDS, n =19). Each column represents the mean ± SEM. Data are analyzed by one-way ANOVA followed by

Tukey's multiple comparison test. *, **, *, **** indicate a significant difference for p <0.05, 0.01, 0.001 or 0.0001, respectively, between the untreated sample and the MNCs treated with iron chelators.**

5.17 Correlation between mitochondrial dysfunction, disease characteristics and systemic iron overload

Finally, we tried to correlate our results both with the disease features and with the markers of systemic iron overload. In particular, we investigated hemoglobin (Hb) levels, bone marrow blast percentage, and R-IPSS. No significant correlation is found between our data and the parameters mentioned above for pre-treatment conditions. Cellular ATP deficiency, lactate dehydrogenase activity, mitochondrial function, and MDA levels are not associated with any disease feature. In addition, we have looked for links between our data and ferritin or transferrin saturation, finding a strong correlation between MDA and serum ferritin levels with a Pearson product-moment correlation coefficient (PCC) of zero.

Primary cells from 5 patients at diagnosis belonging to the different World Health Organization (WHO) categories, whose clinical and cytogenetic features are illustrated in **Table 6** (**Sample 1**–**5**), were used for proliferation and apoptosis assays. Five healthy subjects were already used as controls and their characteristics are reported in **Table 6**.

Interestingly, ferritin levels, which is a standard indirect parameter of iron content, were extremely high and totally different from MDS and normal controls, confirming that the iron content of WBC isolated from normal samples was greatly reduced. In this regard, DFX inhibited the vitality of MDS primary cells, reaching the maximum effect at 100 µM, by a reduction close to 50%. At the same time, we didn't observe a significant reduction of viability on healthy subjects' specimens (**Figure 33**).

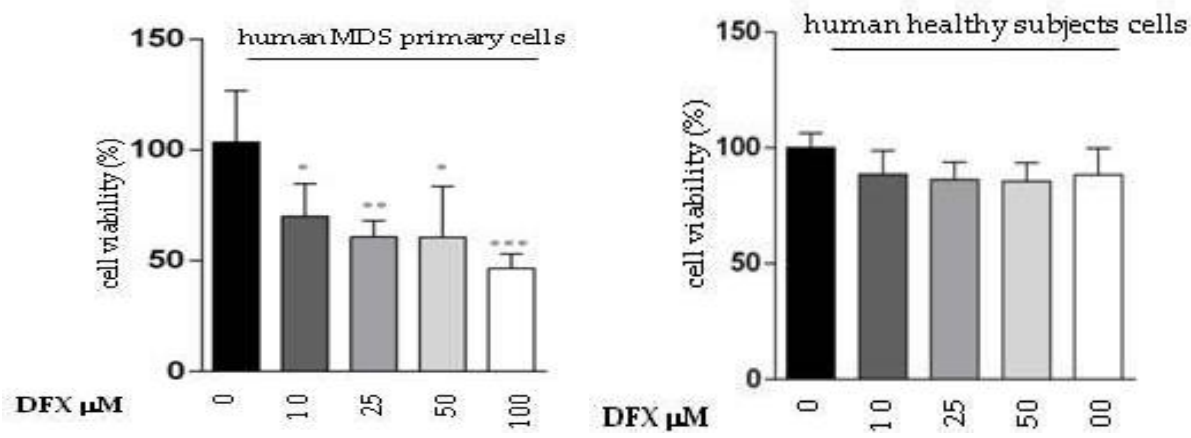

Figure 33: Five MDS/AML patients or 5 healthy subjects were treated with 10, 25, 50, or 100 µM of DFX for 48 h and the MTT assay was performed. Each column represents the mean ± SEM. Data are analyzed by one-way ANOVA followed by Tukey's multiple comparison test. *, **, *, **** indicate a significant difference for p <0.05, 0.01, 0.001 or 0.0001, respectively, between the untreated sample and the MNCs treated with iron chelators.**

This effect was confirmed by monitoring apoptosis in MDS and healthy cells by flow cytometry (**Figure 34**). All these results suggested a clear relationship between iron chelation and anti-proliferative/pro-apoptotic effects in leukemia cells. The lack of effect on healthy donors' cells increased the relevance of our work and suggested that iron overload may represent a new target to exploit by iron chelation, to obtain a specific anti-leukemic effect.

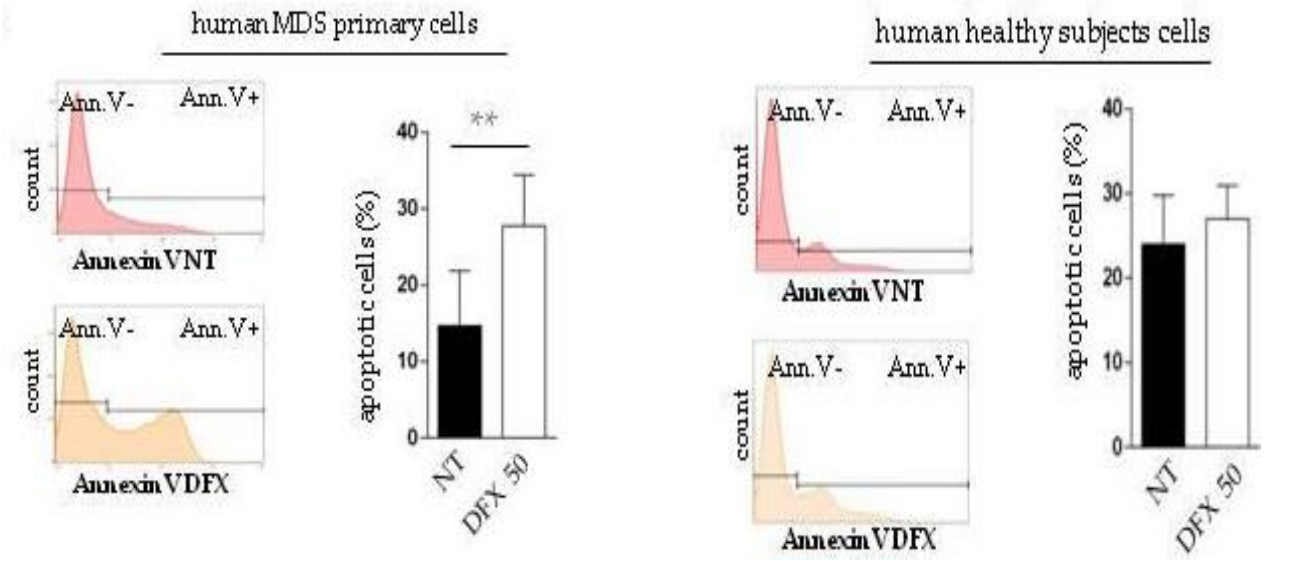

Figure 34: Representative histograms and % of apoptosis evaluated by flow cytometry after FITC Annexin-V assay on 5 MDS/AML patients or 5 healthy subjects treated with 50 µM of DFX. Abbreviations: NT, not treated; DFX, Deferasirox; Ann V, Annexin V. * $p \leq 0.05$, ** $p \leq 0.01$, and *** $p \leq 0.001$.

5.18 Deferasirox Activates p53 Targets on Acute Myeloid Leukemia in Primary MDS/AML cells

Primary cells of 25 MDS/AML patients, whose clinical and cytogenetic features are illustrated in **Table 6**, were used to evaluate the effect of DFX on the expression of the *CDKN1A* and *PUMA* genes. Like what we observed in leukemia cell lines, the *CDKN1A* and *PUMA* gene expression significantly increased after DFX incubation (**Figure 35**).

Therefore, these data led us to propose that also in MDS/AML primary cells, DFX could activate specific p53-dependent gene transcription.

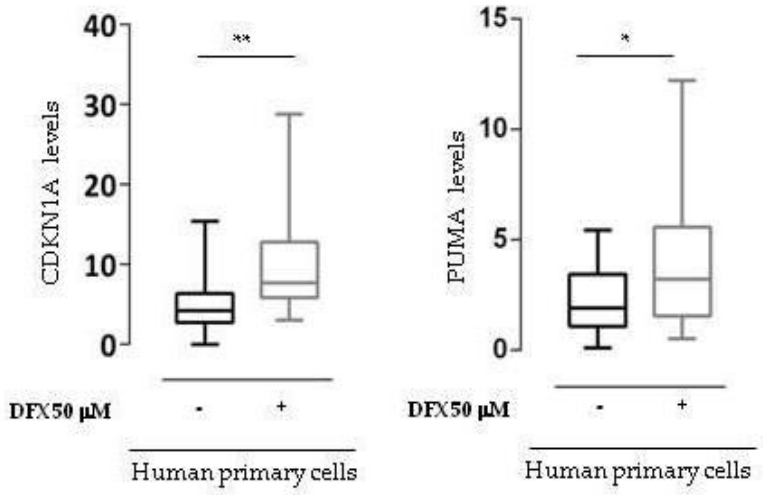

Figure 35: *CDKN1A* and *PUMA* gene expression was assayed by qRT-PCR on 15 patients' cells after 48 h in vitro treatment with DFX 50 µM. The mRNA quantity is expressed as 2-DDCt after normalization with the ABL housekeeping gene. Abbreviationes: -, not treated, + treated with DFX 50 µM. * $p \leq 0.05$, $p \leq 0.01$.

5.19 Deferasirox regulates p53 and p73 Protein Stability in Primary MDS/AML cells

We next moved to investigate p53 and p73 proteins by IHC in 5 BM MDS patients at diagnosis (DX) and within one year of iron chelation treatment (ICT) with DFX. Despite the paucity of the cohort, 80% of patients (even if with different intensity among them) displayed behavior similar to that observed in cell lines culturing. p73 signal significantly increased (**Figure 36 and Figure 37**) after treatment. A similar result was obtained in the same specimens, by immunofluorescence technique, against p53 and p73 respectively (**Figure 38**). In our specimens, the p53 signal resulted difficult to detect. We have assumed that since it is extremely crucial to several cellular processes, therefore, even small changes in its amount are enough to activate a specific response.

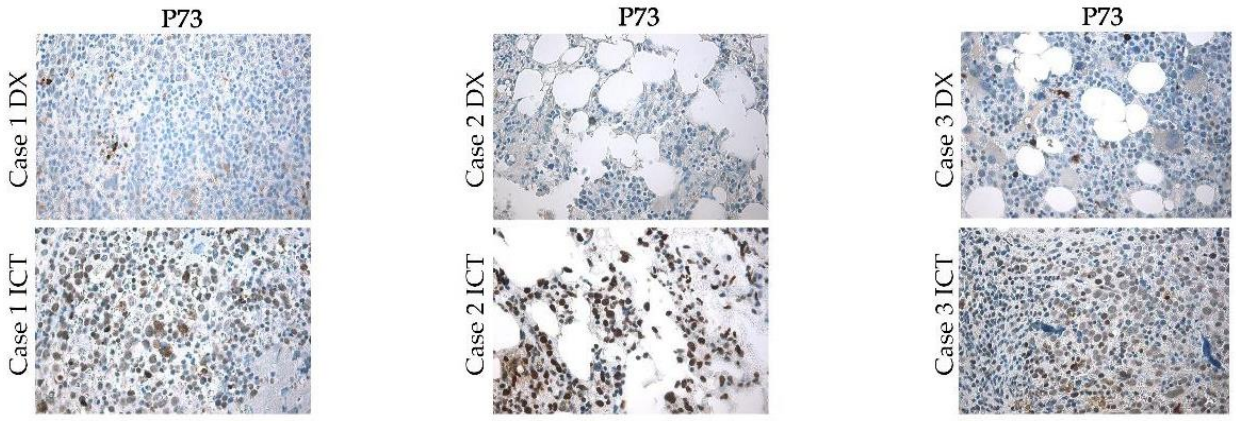

Figure 36: p73 Immunohistochemistry on MDS bone marrow samples derived from 3 different patients at diagnosis (DX) and within one year of iron chelation treatment (ICT) (10× magnification).

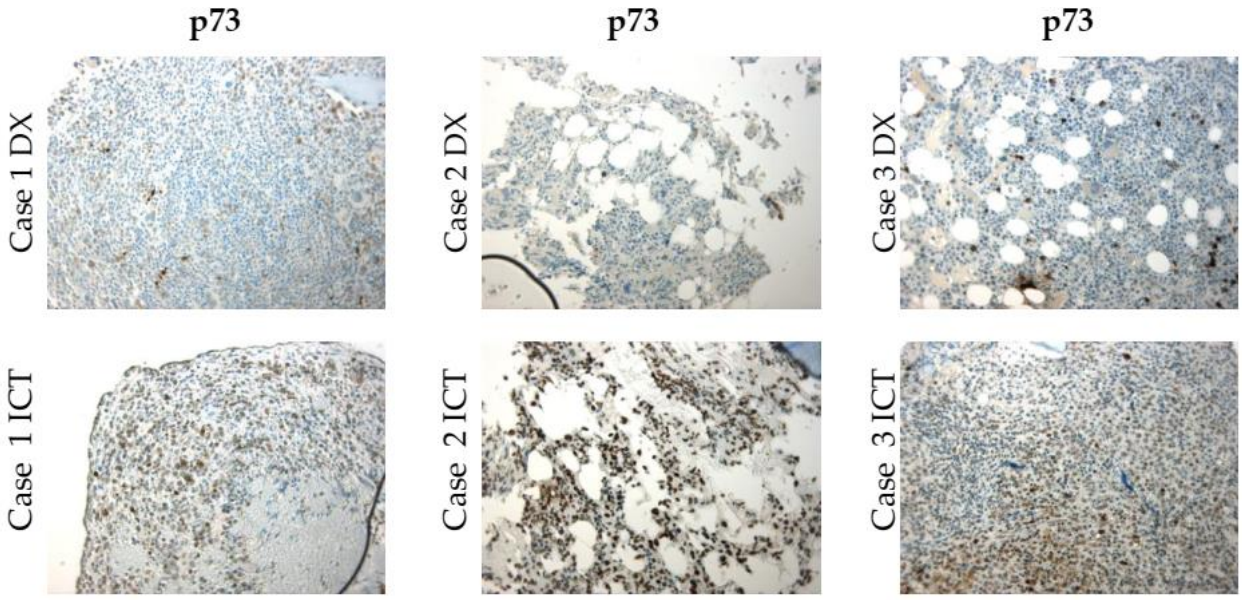

Figure 37: p73 Immunohistochemistry on MDS bone marrow samples derived from 3 different patients at diagnosis (DX) and within one year of iron chelation treatment (ICT) (20x magnification). Abbreviations: DX: diagnosis, ICT: iron chelation treatment.

Cases	Samples	SCORE p73
Case 1	Sample 1-DX	40%
	Sample 1-DFX	70%
Case 2	Sample 2-DX	<1%
	Sample 2-DFX	90%
Case 3	Sample 3-DX	10%
	Sample 3-DFX	20%
Case 4	Sample 4-DX	<1%
	Sample 4-DFX	10%
Case 5	Sample 5-DX	90%
	Sample 5-DFX	90%

Table 9: Table illustrating MDS samples used for IHC analysis and p73 scores. Slides were scored independently by 2 pathologists

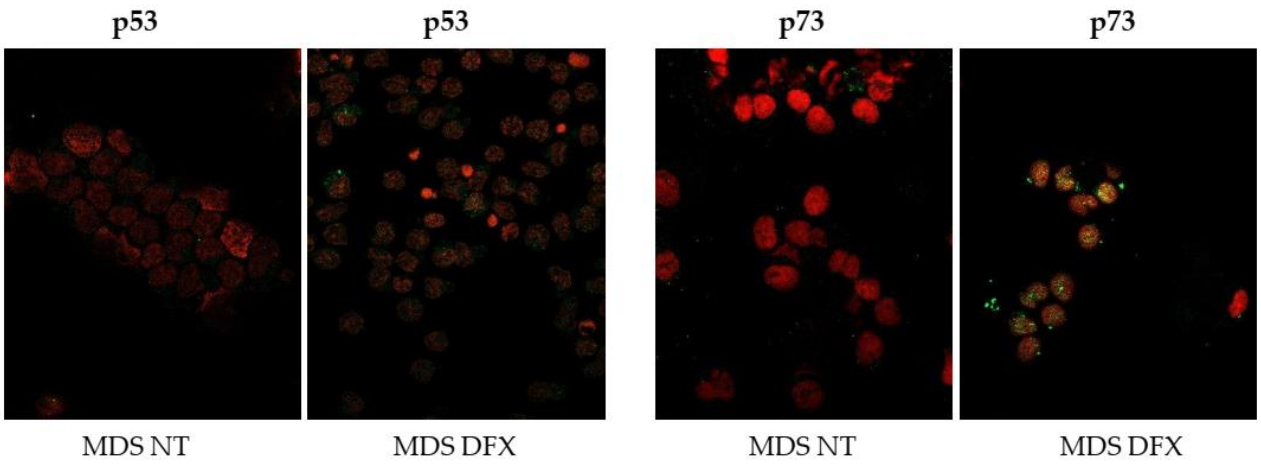

Figure 38: Immunofluorescence of p53 and p73 in one MDS sample after DFX treatment. The green signal corresponds to p53 or p73 while the red propidium is used to detect nuclei (63x magnification).

6. CONCLUSION

Finally, in **Figure 39**, we resumed our hypothesis about the strategic role of iron chelation on mitochondrial activity and p53 family stability, in order to propose new attractive targets to investigate in DFX-treated patients.

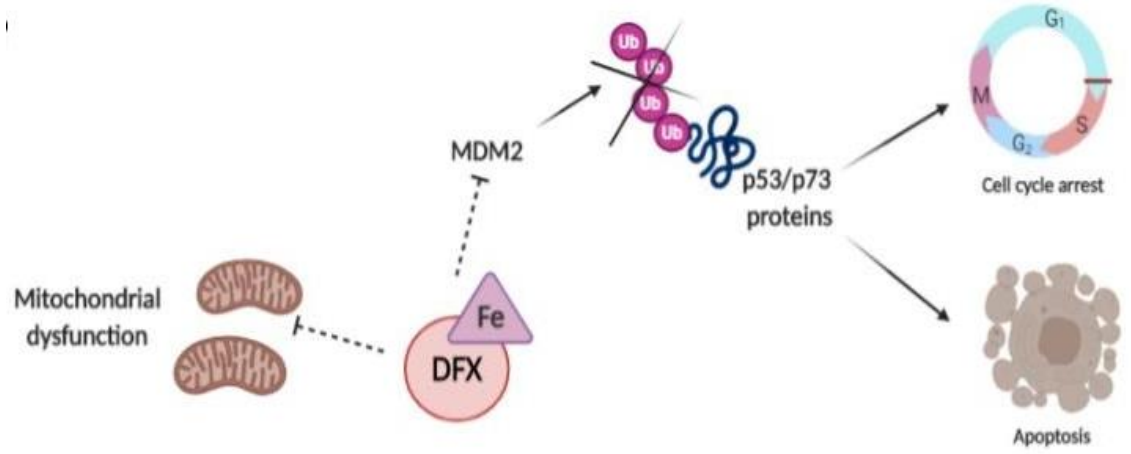

Figure 39: hypothesis about the strategic role of iron chelation on mitochondrial activity and on p53 family stability.

7. DISCUSSION

Myelodysplastic syndromes are a heterogeneous group of diseases characterized by increased apoptosis in the bone marrow cells and subsequent ineffective erythropoiesis. Within this scenario mitochondria, organelles involved in metabolic processes and apoptosis, play a crucial role. Several lines of evidence linked mitochondrial dysfunction to dyserythropoiesis, including results obtained by animal models carrying mitochondrial DNA mutations [59]. Mitochondria are organelles that play a vital role in metabolic processes. Their dysfunction is related to many human diseases from cancer to dementia [160,161] and the preservation of a viable pool of mitochondria is crucial for cell function. In this regard, it was found that mitochondrial DNA is frequently mutated in MDS [60], and nuclear-encoded mitochondrial proteins have been found altered [64]. Mitochondria are also sites of iron storage, a process that occurs frequently in MDS, favoring the production of ROS.

ROS, in turn, can have detrimental effects on cell survival: they increase lipid peroxidation and impair organelles, leading to cell death [84] and, can also damage DNA, promoting genomic instability, contributing to leukemic evolution.

In addition to these data, we must remember that mitochondria are considered the main source of energy and site of OxPhos. Energy metabolism is known to be altered in cancer cells and may represent an attractive therapeutic target, but little few data in literature evaluate the direct energy metabolism involvement in hematological malignancies and especially in MDS.

Schildgen et al.[65] indirectly addressed this problem by demonstrating that the transcription rate of four pivotal subunits of the mitochondrial respiratory chain in myelodysplastic $CD34^+$ cells was reduced and that mitochondrial mRNA stoichiometry was impaired.

We then analyzed in detail the energy metabolism of MDS, trying to link this issue to oxidative stress and iron overload. In particular, we compared energy balance, anaerobic glycolysis rate, OxPhos activity and efficiency, and lipid peroxidation in MNC from patients with MDS, comparing those results with those obtained on healthy controls.

Our data show that the ATP/AMP ratio decreases proportionally with aging, despite this the MNCs of patients with MDS showed a lower energy status than the healthy subjects of the same age, suggesting an alteration in the energy balance. To understand the origins of this energy shortage, we, therefore analyzed the metabolism of OxPhos induced by P/M or succinate, observing an increase in oxygen consumption, accompanied by a decrease in ATP synthesis, both in healthy elderly subjects and in patients with MDS, compared to young controls. This phenomenon causes the progressive deterioration of the OxPhos efficiency, as indicated by the decrease in the P/O value, both after P/M and succinate induction. We, therefore, observed an increase in oxidative stress, since decoupled respiration is associated with the production of reactive oxygen species (ROS).

Moreover, the impairment of aerobic energy metabolism is associated with an increment of lactate dehydrogenase (LDH) activity, both in MDS patients and in elderly subjects with respect to the younger control, suggesting an attempt to restore the energy balance.

Interestingly, despite the P/O values appear similar in MDS and elderly healthy subjects, MDS-MNCs display a very low energy status, which can be only partially justified by the OxPhos impairment. This apparent discrepancy could be explained by the high energy expenditure necessary to contrast the increment of oxidative stress production, which characterized the MDS cells [77].

Our data demonstrate in addition a higher lipid peroxidation in MDS samples than in age-matched control samples. This finding appears to be associated with iron overload as the MDA level decreases significantly after incubation with iron binders. However, this event could also be due to an imbalance between the enzymatic activities of adenylate kinase that convert AMP to ADP and ATP, and vice versa, [162] or from the increase in inflammatory processes associated with iron overload. The involvement of iron overload in the imbalance of energy metabolism is confirmed by the positive effects on MDS-MNC after in vitro treatment with two different iron chelators, deferasirox, and

deferoxamine. In particular, iron chelators were able to improve the ATP/AMP ratio, partially restore mitochondrial function and reduce the level of MDA. Interestingly, the effects of iron chelation on healthy controls were opposite, especially for younger subjects, probably causing a reduction in mitochondrial activity and in the ATP/AMP ratio because chelation removed the iron necessary for the activity of respiratory cytochrome complexes. Finally, no significant correlation was found between clinical parameters and energy metabolism except one: serum ferritin levels correlated with MDA production, thus confirming the harmful role of iron overload in lipids peroxidation.

In summary, our data show that MDS cells exhibit altered mitochondrial metabolism associated with uncontrolled production of oxidative stress, which causes a strong energy deficit. This event seems related to iron overload, as suggested by the partial restoration of MDS-MNC energy metabolism observed after the iron chelating treatment.

Based on these results we considered that further experiments were needed to investigate more in detail the potential anti-leukemic effect of iron chelation [134]. As already introduced, iron is essential for the normal functioning of almost all cell types. The necessity of iron is even higher in cancer cells, due to their rapid cell growth and proliferation. Previous studies have shown that iron administration in mice can induce the generation of tumors [163]. In addition, iron overloading has been shown to exert a negative impact on the overall survival of patients suffering from acute leukemia treated with hematopoietic stem cell transplantation (HSCT). Increased levels of NTBI (iron not bound to transferrin) and LPI, during hematopoietic stem cell transplantation, were correlated with poor survival. On the contrary, different epidemiological studies have shown that a reduced incidence of cancer is associated with iron deficiency [164]. In line with these data, recent studies have described the improved leukemia free survival in patients with AML and MDS treated with iron chelation [87-91]. Then, following the first clinical case of a patient with acute leukemia that has reached remission with iron chelation [94], several studies have addressed the potential anti-leukemic properties of iron chelation [87-89]. The results obtained are divergent in some respects, except for the capacity of chelation therapy to delay leukemic progression. The biological mechanisms responsible for this event are still quite obscure. Accumulated evidence suggests that iron plays a critical role in mitochondrial functions, including energy metabolism and oxidative phosphorylation [137,165]. Mitochondria are sensitive to iron deprivation and the dynamic transition from fission to fusion is highly dependent on this form of cellular stress [166]. In our specimens, iron chelation induces mitochondrial network fragmentation and oxidative phosphorylation dysfunction. From the analysis of mitochondria shapes we found that in all cell lines under physiological conditions, the mitochondria were interconnected, thus forming an intracellular network, while, compared to the respective controls, DFX treatment caused severe alteration of the mitochondrial network.

A further important aspect is described by, Shen and colleagues [109]. They demonstrated that iron overload can reduce p53 activity and that iron chelation can stabilize p53, and the related p63 and p73 proteins [167], suggesting a biological rationale for the relationship between iron overload and increased risk of cancer. Indeed, in order to identify such involvement in the leukemia field too, we clearly demonstrated that iron chelation triggers apoptosis and impairs cell growth by enhancing the p53 transcriptional activity, in leukemic blasts and cell lines. *CDKN1A* and *PUMA*, master regulators of proliferation and apoptosis respectively, represent the most activated genes. The regulation of CDKN1A by iron chelation has already been reported [168,169]. Our study confirms that CDKN1A and PUMA expression occurs independently from p53 status, suggesting that stress signals, including iron chelation, could act through p53-related proteins p63 or p73, thus compensating for the lack of p53 function.

Similar results were obtained by analyzing a microarray dataset concerning a p53-truncated leukemia cell line treated with DFX. The p53 family protein network is heavily enriched, further indicating that the signal triggered by iron depletion, in the absence of p53, is overtaken by the other family members. To better clarify the mechanism of p53 family reactivation, we investigated MDM2, which controlled the p53 and p73 stability by the ubiquitin-proteasome system [170]. After cellular stress, p53-enhanced expression is achieved through different mechanisms, including (*Int. J. Mol. Sci.* 2020, *21*, 7674 12 of 22) phosphorylation, acetylation, and methylation, which reduced its interaction with MDM2, thus favoringp53 activity [171,172]. Iron-dependent regulation of MDM2 influenced p53 activity in liver cancer cells [173]. Moreover, hypoxia-inducible factor 1 alpha (HIF1a) enforced p53 protein stability [174].

In this study, we demonstrated that MDM2 protein, but not mRNA, decreased after iron chelation, thus stabilizing p53 and p73, as suggested by their strong nuclear accumulation after DFX treatment. The fact that DFX exerts activity on MDM2 seems very interesting in view of an anti-leukemic property. The importance of MDM2 inhibition in leukemia is suggested by the clinical results obtained from a small molecule, idasanutlin, designed to block MDM2 and to consequently increase p53 levels [175]. Our findings revealed a direct link between iron and stability/functions of p53 family members, providing a new fascinating opportunity for cancer treatment based on iron deprivation. Additionally, MDM2 is a potential binding partner able to directly link and block complexes composed of mutant R175H p53 and p73, thus resulting in a loss of the functional wild-type p73 [140]. Hence, reduction of MDM2 inhibitory ability on p53-p73 complex after iron chelation could further promote p73 transcriptional activity. Moreover, the NB4 cell line that we used is characterized by R248Q mutation, classified as a DNA binding mutant, which differed from other structurally unfolded mutants. Even if both types of mutants have been shown to inhibit p63 and p73 function, the unfolded

p53 mutants seem to be more severe and capable to interact with p63 and p73 [176]. Consequently, the GOF of mutant p53 related to p63 and p73 inhibition could be less pronounced in our p53 mutated cell line model. Furthermore, we demonstrated that iron chelation drastically increased the level of p73 itself, and this phenomenon may further reduce the inhibitory binding effect of mutant p53 on p73.

Moreover, being p53 a key player in the regulation of the mitochondrion activity, our results suggested that the p53 family reactivation after DFX might be connected to mitochondrial impairment observed in leukemia cells after iron chelation. Indeed, structural mitochondrial elements such as OPA1 and Drp1, respectively responsible for mitofusion or mitofission, regulate their activity according to the level of iron and are directly involved, together with p53 members, in the activation of the apoptotic signaling pathway [177-179]. Moreover, previous reports have suggested that the inhibition of mitochondrial fission significantly causes growth arrest, and cell cycle inhibition and activation of p53 and p21 appears to be primarily responsible for this phenomenon [155,177,179].

Besides, the Aco2 reduction observed in our experimental set could be an interesting pathway to be investigated in the field of leukemia. Indeed, Aco2 is the enzyme responsible for the isomerization of citrate to isocitrate in the Krebs Cycle [146] 13 of 22 and it binds one [4Fe-4S] cluster per subunit. The binding of a [3Fe-4S] cluster leads to an inactive enzyme. Aco2 is a sensitive redox sensor of reactive oxygen and nitrogen species in cells and its function is directly associated with iron levels [180]. Therefore, Aco2 could become a new interesting protein to investigate to identify a new vulnerable process to target in leukemia cells. On the other hand, the iron chelation seems to cause an alteration in the mitochondrial OxPhos activity, which appears lower and less efficient in comparison to the untreated samples. This negative effect could depend directly on the chelation of iron, a fundamental component of the cytochromes composing the electron transport chain, and on the disruption of the mitochondrial network since it was demonstrated that isolated mitochondria are less efficient in terms of energy production [142,181].

Finally, all together these data could justify one potential anti-leukemic effect of iron chelation antileukemic effect, mediated partly by the reactivation of p53 family proteins and partly by the restoring of functional mitochondria. The identification of common mitochondrial and p53 family targets could be attractive for new therapeutic approaches to exploit, alone or in combination with other drugs, in patients with AML or MDS to improve responses or to delay progression.

8. BIBLIOGRAPHY:

1. Hoffman, R. *Hematology : basic principles and practice*, 6th ed.; Saunders/Elsevier: Philadelphia, PA, 2013; pp. xxxi, 2343 p.
2. Winnik, S.; Raptis, D.A.; Walker, J.H.; Hasun, M.; Speer, T.; Clavien, P.A.; Komajda, M.; Bax, J.J.; Tendera, M.; Fox, K., et al. From abstract to impact in cardiovascular research: factors predicting publication and citation. *European heart journal* **2012**, *33*, 3034-3045, doi:10.1093/eurheartj/ehs113.
3. Ma, X. Epidemiology of myelodysplastic syndromes. *The American journal of medicine* **2012**, *125*, S2-5, doi:10.1016/j.amjmed.2012.04.014.
4. Vardiman, J.W.; Thiele, J.; Arber, D.A.; Brunning, R.D.; Borowitz, M.J.; Porwit, A.; Harris, N.L.; Le Beau, M.M.; Hellstrom-Lindberg, E.; Tefferi, A., et al. The 2008 revision of the World Health Organization (WHO) classification of myeloid neoplasms and acute leukemia: rationale and important changes. *Blood* **2009**, *114*, 937-951, doi:10.1182/blood-2009-03-209262.
5. Schanz, J.; Tuchler, H.; Sole, F.; Mallo, M.; Luno, E.; Cervera, J.; Granada, I.; Hildebrandt, B.; Slovak, M.L.; Ohyashiki, K., et al. New comprehensive cytogenetic scoring system for primary myelodysplastic syndromes (MDS) and oligoblastic acute myeloid leukemia after MDS derived from an international database merge. *Journal of clinical oncology : official journal of the American Society of Clinical Oncology* **2012**, *30*, 820-829, doi:10.1200/JCO.2011.35.6394.
6. Arber, D.A.; Orazi, A.; Hasserjian, R.; Thiele, J.; Borowitz, M.J.; Le Beau, M.M.; Bloomfield, C.D.; Cazzola, M.; Vardiman, J.W. The 2016 revision to the World Health Organization classification of myeloid neoplasms and acute leukemia. *Blood* **2016**, *127*, 2391-2405, doi:10.1182/blood-2016-03-643544.
7. Valent, P.; Horny, H.P. Minimal diagnostic criteria for myelodysplastic syndromes and separation from ICUS and IDUS: update and open questions. *European journal of clinical investigation* **2009**, *39*, 548-553, doi:10.1111/j.1365-2362.2009.02151.x.
8. Bain, B.J. The bone marrow aspirate of healthy subjects. *British journal of haematology* **1996**, *94*, 206-209, doi:10.1046/j.1365-2141.1996.d01-1786.x.
9. Malcovati, L.; Papaemmanuil, E.; Ambaglio, I.; Elena, C.; Galli, A.; Della Porta, M.G.; Travaglino, E.; Pietra, D.; Pascutto, C.; Ubezio, M., et al. Driver somatic mutations identify distinct disease entities within myeloid neoplasms with myelodysplasia. *Blood* **2014**, *124*, 1513-1521, doi:10.1182/blood-2014-03-560227.
10. Pellagatti, A.; Boultwood, J. The molecular pathogenesis of the myelodysplastic syndromes. *European journal of haematology* **2015**, *95*, 3-15, doi:10.1111/ejh.12515.
11. Ebert, B.L.; Pretz, J.; Bosco, J.; Chang, C.Y.; Tamayo, P.; Galili, N.; Raza, A.; Root, D.E.; Attar, E.; Ellis, S.R., et al. Identification of RPS14 as a 5q- syndrome gene by RNA interference screen. *Nature* **2008**, *451*, 335-339, doi:10.1038/nature06494.
12. Gangat, N.; Patnaik, M.M.; Tefferi, A. Myelodysplastic syndromes: Contemporary review and how we treat. *American journal of hematology* **2016**, *91*, 76-89, doi:10.1002/ajh.24253.
13. Papaemmanuil, E.; Gerstung, M.; Malcovati, L.; Tauro, S.; Gundem, G.; Van Loo, P.; Yoon, C.J.; Ellis, P.; Wedge, D.C.; Pellagatti, A., et al. Clinical and biological implications of driver mutations in myelodysplastic syndromes. *Blood* **2013**, *122*, 3616-3627; quiz 3699, doi:10.1182/blood-2013-08-518886.
14. Walter, M.J.; Ding, L.; Shen, D.; Shao, J.; Grillot, M.; McLellan, M.; Fulton, R.; Schmidt, H.; Kalicki-Veizer, J.; O'Laughlin, M., et al. Recurrent DNMT3A mutations in patients with myelodysplastic syndromes. *Leukemia* **2011**, *25*, 1153-1158, doi:10.1038/leu.2011.44.
15. Bejar, R.; Stevenson, K.; Abdel-Wahab, O.; Galili, N.; Nilsson, B.; Garcia-Manero, G.; Kantarjian, H.; Raza, A.; Levine, R.L.; Neuberg, D., et al. Clinical effect of point mutations in myelodysplastic syndromes. *The New England journal of medicine* **2011**, *364*, 2496-2506, doi:10.1056/NEJMoa1013343.

16. Thol, F.; Friesen, I.; Damm, F.; Yun, H.; Weissinger, E.M.; Krauter, J.; Wagner, K.; Chaturvedi, A.; Sharma, A.; Wichmann, M., et al. Prognostic significance of ASXL1 mutations in patients with myelodysplastic syndromes. *Journal of clinical oncology : official journal of the American Society of Clinical Oncology* **2011**, *29*, 2499-2506, doi:10.1200/JCO.2010.33.4938.
17. Soriano, A.O.; Yang, H.; Faderl, S.; Estrov, Z.; Giles, F.; Ravandi, F.; Cortes, J.; Wierda, W.G.; Ouzounian, S.; Quezada, A., et al. Safety and clinical activity of the combination of 5-azacytidine, valproic acid, and all-trans retinoic acid in acute myeloid leukemia and myelodysplastic syndrome. *Blood* **2007**, *110*, 2302-2308, doi:10.1182/blood-2007-03-078576.
18. Itzykson, R.; Kosmider, O.; Cluzeau, T.; Mansat-De Mas, V.; Dreyfus, F.; Beyne-Rauzy, O.; Quesnel, B.; Vey, N.; Gelsi-Boyer, V.; Raynaud, S., et al. Impact of TET2 mutations on response rate to azacitidine in myelodysplastic syndromes and low blast count acute myeloid leukemias. *Leukemia* **2011**, *25*, 1147-1152, doi:10.1038/leu.2011.71.
19. Traina, F.; Visconte, V.; Elson, P.; Tabarroki, A.; Jankowska, A.M.; Hasrouni, E.; Sugimoto, Y.; Szpurka, H.; Makishima, H.; O'Keefe, C.L., et al. Impact of molecular mutations on treatment response to DNMT inhibitors in myelodysplasia and related neoplasms. *Leukemia* **2014**, *28*, 78-87, doi:10.1038/leu.2013.269.
20. Patnaik, M.M.; Hanson, C.A.; Hodnefield, J.M.; Lasho, T.L.; Finke, C.M.; Knudson, R.A.; Ketterling, R.P.; Pardanani, A.; Tefferi, A. Differential prognostic effect of IDH1 versus IDH2 mutations in myelodysplastic syndromes: a Mayo Clinic study of 277 patients. *Leukemia* **2012**, *26*, 101-105, doi:10.1038/leu.2011.298.
21. Zhang, L.; McGraw, K.L.; Sallman, D.A.; List, A.F. The role of p53 in myelodysplastic syndromes and acute myeloid leukemia: molecular aspects and clinical implications. *Leukemia & lymphoma* **2017**, *58*, 1777-1790, doi:10.1080/10428194.2016.1266625.
22. Hunter, A.M.; Sallman, D.A. Targeting TP53 Mutations in Myelodysplastic Syndromes. *Hematology/oncology clinics of North America* **2020**, *34*, 421-440, doi:10.1016/j.hoc.2019.11.004.
23. Bode, A.M.; Dong, Z. Post-translational modification of p53 in tumorigenesis. *Nature reviews. Cancer* **2004**, *4*, 793-805, doi:10.1038/nrc1455.
24. Harms, K.L.; Chen, X. The functional domains in p53 family proteins exhibit both common and distinct properties. *Cell death and differentiation* **2006**, *13*, 890-897, doi:10.1038/sj.cdd.4401904.
25. Toledo, F.; Wahl, G.M. Regulating the p53 pathway: in vitro hypotheses, in vivo veritas. *Nature reviews. Cancer* **2006**, *6*, 909-923, doi:10.1038/nrc2012.
26. Bourdon, J.C. p53 and its isoforms in cancer. *British journal of cancer* **2007**, *97*, 277-282, doi:10.1038/sj.bjc.6603886.
27. Vousden, K.H.; Lane, D.P. p53 in health and disease. *Nature reviews. Molecular cell biology* **2007**, *8*, 275-283, doi:10.1038/nrm2147.
28. Hamada, M.; Fujiwara, T.; Hizuta, A.; Gochi, A.; Naomoto, Y.; Takakura, N.; Takahashi, K.; Roth, J.A.; Tanaka, N.; Orita, K. The p53 gene is a potent determinant of chemosensitivity and radiosensitivity in gastric and colorectal cancers. *Journal of cancer research and clinical oncology* **1996**, *122*, 360-365, doi:10.1007/BF01220804.
29. Stengel, A.; Kern, W.; Haferlach, T.; Meggendorfer, M.; Fasan, A.; Haferlach, C. The impact of TP53 mutations and TP53 deletions on survival varies between AML, ALL, MDS and CLL: an analysis of 3307 cases. *Leukemia* **2017**, *31*, 705-711, doi:10.1038/leu.2016.263.
30. Kulasekararaj, A.G.; Smith, A.E.; Mian, S.A.; Mohamedali, A.M.; Krishnamurthy, P.; Lea, N.C.; Gaken, J.; Pennaneach, C.; Ireland, R.; Czepulkowski, B., et al. TP53 mutations in myelodysplastic syndrome are strongly correlated with aberrations of chromosome 5, and correlate with adverse prognosis. *British journal of haematology* **2013**, *160*, 660-672, doi:10.1111/bjh.12203.
31. Iwasaki, T.; Murakami, M.; Sugisaki, C.; Sobue, S.; Ohashi, H.; Asano, H.; Suzuki, M.; Nakamura, S.; Ito, M.; Murate, T. Characterization of myelodysplastic syndrome and aplastic anemia by immunostaining of p53 and hemoglobin F and karyotype analysis: differential diagnosis between refractory anemia and aplastic anemia. *Pathology international* **2008**, *58*, 353-360, doi:10.1111/j.1440-1827.2008.02236.x.

32. Kaneko, H.; Misawa, S.; Horiike, S.; Nakai, H.; Kashima, K. TP53 mutations emerge at early phase of myelodysplastic syndrome and are associated with complex chromosomal abnormalities. *Blood* **1995**, *85*, 2189-2193.
33. Yoshizato, T.; Nannya, Y.; Atsuta, Y.; Shiozawa, Y.; Iijima-Yamashita, Y.; Yoshida, K.; Shiraishi, Y.; Suzuki, H.; Nagata, Y.; Sato, Y., et al. Genetic abnormalities in myelodysplasia and secondary acute myeloid leukemia: impact on outcome of stem cell transplantation. *Blood* **2017**, *129*, 2347-2358, doi:10.1182/blood-2016-12-754796.
34. Bejar, R.; Stevenson, K.E.; Caughey, B.A.; Abdel-Wahab, O.; Steensma, D.P.; Galili, N.; Raza, A.; Kantarjian, H.; Levine, R.L.; Neuberg, D., et al. Validation of a prognostic model and the impact of mutations in patients with lower-risk myelodysplastic syndromes. *Journal of clinical oncology : official journal of the American Society of Clinical Oncology* **2012**, *30*, 3376-3382, doi:10.1200/JCO.2011.40.7379.
35. Jadersten, M.; Saft, L.; Smith, A.; Kulasekararaj, A.; Pomplun, S.; Gohring, G.; Hedlund, A.; Hast, R.; Schlegelberger, B.; Porwit, A., et al. TP53 mutations in low-risk myelodysplastic syndromes with del(5q) predict disease progression. *Journal of clinical oncology : official journal of the American Society of Clinical Oncology* **2011**, *29*, 1971-1979, doi:10.1200/JCO.2010.31.8576.
36. Degterev, A.; Boyce, M.; Yuan, J. A decade of caspases. *Oncogene* **2003**, *22*, 8543-8567, doi:10.1038/sj.onc.1207107.
37. Verhagen, A.M.; Coulson, E.J.; Vaux, D.L. Inhibitor of apoptosis proteins and their relatives: IAPs and other BIRPs. *Genome biology* **2001**, *2*, REVIEWS3009, doi:10.1186/gb-2001-2-7-reviews3009.
38. Du, C.; Fang, M.; Li, Y.; Li, L.; Wang, X. Smac, a mitochondrial protein that promotes cytochrome c-dependent caspase activation by eliminating IAP inhibition. *Cell* **2000**, *102*, 33-42, doi:10.1016/s0092-8674(00)00008-8.
39. Suzuki, Y.; Takahashi-Niki, K.; Akagi, T.; Hashikawa, T.; Takahashi, R. Mitochondrial protease Omi/HtrA2 enhances caspase activation through multiple pathways. *Cell death and differentiation* **2004**, *11*, 208-216, doi:10.1038/sj.cdd.4401343.
40. Circu, M.L.; Aw, T.Y. Reactive oxygen species, cellular redox systems, and apoptosis. *Free radical biology & medicine* **2010**, *48*, 749-762, doi:10.1016/j.freeradbiomed.2009.12.022.
41. Lenaz, G.; Bovina, C.; D'Aurelio, M.; Fato, R.; Formiggini, G.; Genova, M.L.; Giuliano, G.; Merlo Pich, M.; Paolucci, U.; Parenti Castelli, G., et al. Role of mitochondria in oxidative stress and aging. *Annals of the New York Academy of Sciences* **2002**, *959*, 199-213, doi:10.1111/j.1749-6632.2002.tb02094.x.
42. Van Houten, B.; Woshner, V.; Santos, J.H. Role of mitochondrial DNA in toxic responses to oxidative stress. *DNA repair* **2006**, *5*, 145-152, doi:10.1016/j.dnarep.2005.03.002.
43. Will, O.; Mahler, H.C.; Arrigo, A.P.; Epe, B. Influence of glutathione levels and heat-shock on the steady-state levels of oxidative DNA base modifications in mammalian cells. *Carcinogenesis* **1999**, *20*, 333-337, doi:10.1093/carcin/20.2.333.
44. Hollins, D.L.; Suliman, H.B.; Piantadosi, C.A.; Carraway, M.S. Glutathione regulates susceptibility to oxidant-induced mitochondrial DNA damage in human lymphocytes. *Free radical biology & medicine* **2006**, *40*, 1220-1226, doi:10.1016/j.freeradbiomed.2005.11.011.
45. de la Asuncion, J.G.; Millan, A.; Pla, R.; Bruseghini, L.; Esteras, A.; Pallardo, F.V.; Sastre, J.; Vina, J. Mitochondrial glutathione oxidation correlates with age-associated oxidative damage to mitochondrial DNA. *FASEB journal : official publication of the Federation of American Societies for Experimental Biology* **1996**, *10*, 333-338, doi:10.1096/fasebj.10.2.8641567.
46. Cooper GM, H.R. *La cellula. Un approccio molecolare.* ; 2009.
47. Nacarelli, T.; Azar, A.; Sell, C. Mitochondrial stress induces cellular senescence in an mTORC1-dependent manner. *Free radical biology & medicine* **2016**, *95*, 133-154, doi:10.1016/j.freeradbiomed.2016.03.008.
48. Brand, M.D. Mitochondrial generation of superoxide and hydrogen peroxide as the source of mitochondrial redox signaling. *Free radical biology & medicine* **2016**, *100*, 14-31, doi:10.1016/j.freeradbiomed.2016.04.001.
49. Zhang, H.; Menzies, K.J.; Auwerx, J. The role of mitochondria in stem cell fate and aging. *Development* **2018**, *145*, doi:10.1242/dev.143420.

50. Echtay, K.S.; Roussel, D.; St-Pierre, J.; Jekabsons, M.B.; Cadenas, S.; Stuart, J.A.; Harper, J.A.; Roebuck, S.J.; Morrison, A.; Pickering, S., et al. Superoxide activates mitochondrial uncoupling proteins. *Nature* **2002**, *415*, 96-99, doi:10.1038/415096a.
51. Turrens, J.F. Mitochondrial formation of reactive oxygen species. *The Journal of physiology* **2003**, *552*, 335-344, doi:10.1113/jphysiol.2003.049478.
52. Levi, S.; Rovida, E. The role of iron in mitochondrial function. *Biochimica et biophysica acta* **2009**, *1790*, 629-636, doi:10.1016/j.bbagen.2008.09.008.
53. Zorov, D.B.; Krasnikov, B.F.; Kuzminova, A.E.; Vysokikh, M.; Zorova, L.D. Mitochondria revisited. Alternative functions of mitochondria. *Bioscience reports* **1997**, *17*, 507-520, doi:10.1023/a:1027304122259.
54. Farquhar, M.J.; Bowen, D.T. Oxidative stress and the myelodysplastic syndromes. *International journal of hematology* **2003**, *77*, 342-350, doi:10.1007/BF02982641.
55. Linnane, A.W.; Kios, M.; Vitetta, L. Healthy aging: regulation of the metabolome by cellular redox modulation and prooxidant signaling systems: the essential roles of superoxide anion and hydrogen peroxide. *Biogerontology* **2007**, *8*, 445-467, doi:10.1007/s10522-007-9096-4.
56. Morgan, M.J.; Liu, Z.G. Crosstalk of reactive oxygen species and NF-kappaB signaling. *Cell research* **2011**, *21*, 103-115, doi:10.1038/cr.2010.178.
57. Halliwell, B.; Gutteridge, J.M. Oxygen toxicity, oxygen radicals, transition metals and disease. *The Biochemical journal* **1984**, *219*, 1-14, doi:10.1042/bj2190001.
58. Dawson, M.A.; Davis, A.; Elliott, P.; Cole-Sinclair, M. Linezolid-induced dyserythropoiesis: chloramphenicol toxicity revisited. *Internal medicine journal* **2005**, *35*, 626-628, doi:10.1111/j.1445-5994.2005.00912.x.
59. Chen, M.L.; Logan, T.D.; Hochberg, M.L.; Shelat, S.G.; Yu, X.; Wilding, G.E.; Tan, W.; Kujoth, G.C.; Prolla, T.A.; Selak, M.A., et al. Erythroid dysplasia, megaloblastic anemia, and impaired lymphopoiesis arising from mitochondrial dysfunction. *Blood* **2009**, *114*, 4045-4053, doi:10.1182/blood-2008-08-169474.
60. Wulfert, M.; Kupper, A.C.; Tapprich, C.; Bottomley, S.S.; Bowen, D.; Germing, U.; Haas, R.; Gattermann, N. Analysis of mitochondrial DNA in 104 patients with myelodysplastic syndromes. *Experimental hematology* **2008**, *36*, 577-586, doi:10.1016/j.exphem.2008.01.004.
61. Levi, S.; Corsi, B.; Bosisio, M.; Invernizzi, R.; Volz, A.; Sanford, D.; Arosio, P.; Drysdale, J. A human mitochondrial ferritin encoded by an intronless gene. *The Journal of biological chemistry* **2001**, *276*, 24437-24440, doi:10.1074/jbc.C100141200.
62. Drysdale, J.; Arosio, P.; Invernizzi, R.; Cazzola, M.; Volz, A.; Corsi, B.; Biasiotto, G.; Levi, S. Mitochondrial ferritin: a new player in iron metabolism. *Blood cells, molecules & diseases* **2002**, *29*, 376-383, doi:10.1006/bcmd.2002.0577.
63. Invernizzi, R.; Travaglino, E.; Della Porta, M.G.; Galli, A.; Malcovati, L.; Rosti, V.; Bergamaschi, G.; Erba, B.G.; Bellistri, F.; Bastia, R., et al. Effects of mitochondrial ferritin overexpression in normal and sideroblastic erythroid progenitors. *British journal of haematology* **2013**, *161*, 726-737, doi:10.1111/bjh.12316.
64. Visconte, V.; Avishai, N.; Mahfouz, R.; Tabarroki, A.; Cowen, J.; Sharghi-Moshtaghin, R.; Hitomi, M.; Rogers, H.J.; Hasrouni, E.; Phillips, J., et al. Distinct iron architecture in SF3B1-mutant myelodysplastic syndrome patients is linked to an SLC25A37 splice variant with a retained intron. *Leukemia* **2015**, *29*, 188-195, doi:10.1038/leu.2014.170.
65. Schildgen, V.; Wulfert, M.; Gattermann, N. Impaired mitochondrial gene transcription in myelodysplastic syndromes and acute myeloid leukemia with myelodysplasia-related changes. *Experimental hematology* **2011**, *39*, 666-675 e661, doi:10.1016/j.exphem.2011.03.007.
66. D'Aurelio, M.; Gajewski, C.D.; Lenaz, G.; Manfredi, G. Respiratory chain supercomplexes set the threshold for respiration defects in human mtDNA mutant cybrids. *Human molecular genetics* **2006**, *15*, 2157-2169, doi:10.1093/hmg/ddl141.
67. Benard, G.; Faustin, B.; Passerieux, E.; Galinier, A.; Rocher, C.; Bellance, N.; Delage, J.P.; Casteilla, L.; Letellier, T.; Rossignol, R. Physiological diversity of mitochondrial oxidative phosphorylation. *American journal of physiology. Cell physiology* **2006**, *291*, C1172-1182, doi:10.1152/ajpcell.00195.2006.

68. Liberti, M.V.; Locasale, J.W. The Warburg Effect: How Does it Benefit Cancer Cells? *Trends in biochemical sciences* **2016**, *41*, 211-218, doi:10.1016/j.tibs.2015.12.001.
69. Warburg, O. [The effect of hydrogen peroxide on cancer cells and on embryonic cells]. *Acta - Unio Internationalis Contra Cancrum* **1958**, *14*, 55-57.
70. Shestov, A.A.; Liu, X.; Ser, Z.; Cluntun, A.A.; Hung, Y.P.; Huang, L.; Kim, D.; Le, A.; Yellen, G.; Albeck, J.G., et al. Quantitative determinants of aerobic glycolysis identify flux through the enzyme GAPDH as a limiting step. *eLife* **2014**, *3*, doi:10.7554/eLife.03342.
71. Fantin, V.R.; St-Pierre, J.; Leder, P. Attenuation of LDH-A expression uncovers a link between glycolysis, mitochondrial physiology, and tumor maintenance. *Cancer cell* **2006**, *9*, 425-434, doi:10.1016/j.ccr.2006.04.023.
72. Goncalves, A.C.; Cortesao, E.; Oliveiros, B.; Alves, V.; Espadana, A.I.; Rito, L.; Magalhaes, E.; Lobao, M.J.; Pereira, A.; Nascimento Costa, J.M., et al. Oxidative stress and mitochondrial dysfunction play a role in myelodysplastic syndrome development, diagnosis, and prognosis: A pilot study. *Free radical research* **2015**, *49*, 1081-1094, doi:10.3109/10715762.2015.1035268.
73. Ghaffari, S. Oxidative stress in the regulation of normal and neoplastic hematopoiesis. *Antioxidants & redox signaling* **2008**, *10*, 1923-1940, doi:10.1089/ars.2008.2142.
74. Pervaiz, S.; Clement, M.V. Superoxide anion: oncogenic reactive oxygen species? *The international journal of biochemistry & cell biology* **2007**, *39*, 1297-1304, doi:10.1016/j.biocel.2007.04.007.
75. Issa, J.P. Epigenetic changes in the myelodysplastic syndrome. *Hematology/oncology clinics of North America* **2010**, *24*, 317-330, doi:10.1016/j.hoc.2010.02.007.
76. Shen, L.; Kantarjian, H.; Guo, Y.; Lin, E.; Shan, J.; Huang, X.; Berry, D.; Ahmed, S.; Zhu, W.; Pierce, S., et al. DNA methylation predicts survival and response to therapy in patients with myelodysplastic syndromes. *Journal of clinical oncology : official journal of the American Society of Clinical Oncology* **2010**, *28*, 605-613, doi:10.1200/JCO.2009.23.4781.
77. Goncalves, A.C.; Cortesao, E.; Oliveiros, B.; Alves, V.; Espadana, A.I.; Rito, L.; Magalhaes, E.; Pereira, S.; Pereira, A.; Costa, J.M., et al. Oxidative stress levels are correlated with P15 and P16 gene promoter methylation in myelodysplastic syndrome patients. *Clinical and experimental medicine* **2016**, *16*, 333-343, doi:10.1007/s10238-015-0357-2.
78. O'Hagan, H.M.; Wang, W.; Sen, S.; Destefano Shields, C.; Lee, S.S.; Zhang, Y.W.; Clements, E.G.; Cai, Y.; Van Neste, L.; Easwaran, H., et al. Oxidative damage targets complexes containing DNA methyltransferases, SIRT1, and polycomb members to promoter CpG Islands. *Cancer cell* **2011**, *20*, 606-619, doi:10.1016/j.ccr.2011.09.012.
79. Afanas'ev, I. New nucleophilic mechanisms of ros-dependent epigenetic modifications: comparison of aging and cancer. *Aging and disease* **2014**, *5*, 52-62, doi:10.14336/AD.2014.050052.
80. Camaschella, C.; Pagani, A.; Nai, A.; Silvestri, L. The mutual control of iron and erythropoiesis. *International journal of laboratory hematology* **2016**, *38 Suppl 1*, 20-26, doi:10.1111/ijlh.12505.
81. Tanno, T.; Bhanu, N.V.; Oneal, P.A.; Goh, S.H.; Staker, P.; Lee, Y.T.; Moroney, J.W.; Reed, C.H.; Luban, N.L.; Wang, R.H., et al. High levels of GDF15 in thalassemia suppress expression of the iron regulatory protein hepcidin. *Nature medicine* **2007**, *13*, 1096-1101, doi:10.1038/nm1629.
82. Sonnweber, T.; Nachbaur, D.; Schroll, A.; Nairz, M.; Seifert, M.; Demetz, E.; Haschka, D.; Mitterstiller, A.M.; Kleinsasser, A.; Burtscher, M., et al. Hypoxia induced downregulation of hepcidin is mediated by platelet derived growth factor BB. *Gut* **2014**, *63*, 1951-1959, doi:10.1136/gutjnl-2013-305317.
83. Kautz, L.; Jung, G.; Valore, E.V.; Rivella, S.; Nemeth, E.; Ganz, T. Identification of erythroferrone as an erythroid regulator of iron metabolism. *Nature genetics* **2014**, *46*, 678-684, doi:10.1038/ng.2996.
84. Porter, J.B.; Garbowski, M. The pathophysiology of transfusional iron overload. *Hematology/oncology clinics of North America* **2014**, *28*, 683-701, vi, doi:10.1016/j.hoc.2014.04.003.
85. Leitch, H.A.; Chan, C.; Leger, C.S.; Foltz, L.M.; Ramadan, K.M.; Vickars, L.M. Improved survival with iron chelation therapy for red blood cell transfusion dependent lower IPSS risk MDS may be more significant in patients with a non-RARS diagnosis. *Leukemia research* **2012**, *36*, 1380-1386, doi:10.1016/j.leukres.2012.08.001.
86. Musto, P.; Maurillo, L.; Simeon, V.; Poloni, A.; Finelli, C.; Balleari, E.; Ricco, A.; Rivellini, F.; Cortelezzi, A.; Tarantini, G., et al. Iron-chelating therapy with deferasirox in transfusion-dependent, higher risk

myelodysplastic syndromes: a retrospective, multicentre study. *British journal of haematology* **2017**, *177*, 741-750, doi:10.1111/bjh.14621.
87. Rose, C.; Brechignac, S.; Vassilief, D.; Pascal, L.; Stamatoullas, A.; Guerci, A.; Larbaa, D.; Dreyfus, F.; Beyne-Rauzy, O.; Chaury, M.P., et al. Does iron chelation therapy improve survival in regularly transfused lower risk MDS patients? A multicenter study by the GFM (Groupe Francophone des Myelodysplasies). *Leukemia research* **2010**, *34*, 864-870, doi:10.1016/j.leukres.2009.12.004.
88. Raptis, A.; Duh, M.S.; Wang, S.T.; Dial, E.; Fanourgiakis, I.; Fortner, B.; Paley, C.; Mody-Patel, N.; Corral, M.; Scott, J. Treatment of transfusional iron overload in patients with myelodysplastic syndrome or severe anemia: data from multicenter clinical practices. *Transfusion* **2010**, *50*, 190-199, doi:10.1111/j.1537-2995.2009.02361.x.
89. Neukirchen, J.; Fox, F.; Kundgen, A.; Nachtkamp, K.; Strupp, C.; Haas, R.; Germing, U.; Gattermann, N. Improved survival in MDS patients receiving iron chelation therapy - a matched pair analysis of 188 patients from the Dusseldorf MDS registry. *Leukemia research* **2012**, *36*, 1067-1070, doi:10.1016/j.leukres.2012.04.006.
90. Delforge, M.; Selleslag, D.; Beguin, Y.; Triffet, A.; Mineur, P.; Theunissen, K.; Graux, C.; Trullemans, F.; Boulet, D.; Van Eygen, K., et al. Adequate iron chelation therapy for at least six months improves survival in transfusion-dependent patients with lower risk myelodysplastic syndromes. *Leukemia research* **2014**, *38*, 557-563, doi:10.1016/j.leukres.2014.02.003.
91. Hoeks, M.; Yu, G.; Langemeijer, S.; Crouch, S.; de Swart, L.; Fenaux, P.; Symeonidis, A.; Cermak, J.; Hellstrom-Lindberg, E.; Sanz, G., et al. Impact of treatment with iron chelation therapy in patients with lower-risk myelodysplastic syndromes participating in the European MDS registry. *Haematologica* **2019**, 10.3324/haematol.2018.212332, doi:10.3324/haematol.2018.212332.
92. Chen, J.; Lu, W.Y.; Zhao, M.F.; Cao, X.L.; Jiang, Y.Y.; Jin, X.; Xu, P.; Yuan, T.T.; Zhang, Y.C.; Chai, X., et al. Reactive oxygen species mediated T lymphocyte abnormalities in an iron-overloaded mouse model and iron-overloaded patients with myelodysplastic syndromes. *Annals of hematology* **2017**, *96*, 1085-1095, doi:10.1007/s00277-017-2985-y.
93. Leitch, H.A.; Parmar, A.; Wells, R.A.; Chodirker, L.; Zhu, N.; Nevill, T.J.; Yee, K.W.L.; Leber, B.; Keating, M.M.; Sabloff, M., et al. Overall survival in lower IPSS risk MDS by receipt of iron chelation therapy, adjusting for patient-related factors and measuring from time of first red blood cell transfusion dependence: an MDS-CAN analysis. *British journal of haematology* **2017**, *179*, 83-97, doi:10.1111/bjh.14825.
94. Fukushima, T.; Kawabata, H.; Nakamura, T.; Iwao, H.; Nakajima, A.; Miki, M.; Sakai, T.; Sawaki, T.; Fujita, Y.; Tanaka, M., et al. Iron chelation therapy with deferasirox induced complete remission in a patient with chemotherapy-resistant acute monocytic leukemia. *Anticancer research* **2011**, *31*, 1741-1744.
95. Cerchione, C.; Cerciello, G.; Avilia, S.; Della Pepa, R.; Pugliese, N.; Picardi, M.; Catalano, L.; Pane, F. Management of iron overload in myelodysplastic syndromes: combined deferasirox and deferoxamine in a patient with liver disease. *Blood transfusion = Trasfusione del sangue* **2018**, *16*, 32-35, doi:10.2450/2016.0137-16.
96. Messa, E.; Cilloni, D.; Messa, F.; Arruga, F.; Roetto, A.; Saglio, G. Deferasirox treatment improved the hemoglobin level and decreased transfusion requirements in four patients with the myelodysplastic syndrome and primary myelofibrosis. *Acta haematologica* **2008**, *120*, 70-74, doi:10.1159/000158631.
97. Guariglia, R.; Martorelli, M.C.; Villani, O.; Pietrantuono, G.; Mansueto, G.; D'Auria, F.; Grieco, V.; Bianchino, G.; Lerose, R.; Bochicchio, G.B., et al. Positive effects on hematopoiesis in patients with myelodysplastic syndrome receiving deferasirox as oral iron chelation therapy: a brief review. *Leukemia research* **2011**, *35*, 566-570, doi:10.1016/j.leukres.2010.11.027.
98. Breccia, M.; Voso, M.T.; Aloe Spiriti, M.A.; Fenu, S.; Maurillo, L.; Buccisano, F.; Tafuri, A.; Alimena, G. An increase in hemoglobin, platelets and white blood cells levels by iron chelation as single treatment in multitransfused patients with myelodysplastic syndromes: clinical evidences and possible biological mechanisms. *Annals of hematology* **2015**, *94*, 771-777, doi:10.1007/s00277-015-2341-z.
99. Messa, E.; Biale, L.; Castiglione, A.; Lunghi, M.; Bonferroni, M.; Salvi, F.; Allione, B.; Ferrero, D.; Calabrese, C.; De Gobbi, M., et al. Erythroid response during iron chelation therapy in a cohort of

patients affected by hematologic malignancies and aplastic anemia with transfusion requirement and iron overload: a FISM Italian multicenter retrospective study. *Leukemia & lymphoma* **2017**, *58*, 2752-2754, doi:10.1080/10428194.2017.1312385.

100. Angelucci, E.; Santini, V.; Di Tucci, A.A.; Quaresmini, G.; Finelli, C.; Volpe, A.; Quarta, G.; Rivellini, F.; Sanpaolo, G.; Cilloni, D., et al. Deferasirox for transfusion-dependent patients with myelodysplastic syndromes: safety, efficacy, and beyond (GIMEMA MDS0306 Trial). *European journal of haematology* **2014**, *92*, 527-536, doi:10.1111/ejh.12300.
101. Messa, E.; Carturan, S.; Maffe, C.; Pautasso, M.; Bracco, E.; Roetto, A.; Messa, F.; Arruga, F.; Defilippi, I.; Rosso, V., et al. Deferasirox is a powerful NF-kappaB inhibitor in myelodysplastic cells and in leukemia cell lines acting independently from cell iron deprivation by chelation and reactive oxygen species scavenging. *Haematologica* **2010**, *95*, 1308-1316, doi:10.3324/haematol.2009.016824.
102. Ohyashiki, J.H.; Kobayashi, C.; Hamamura, R.; Okabe, S.; Tauchi, T.; Ohyashiki, K. The oral iron chelator deferasirox represses signaling through the mTOR in myeloid leukemia cells by enhancing expression of REDD1. *Cancer science* **2009**, *100*, 970-977, doi:10.1111/j.1349-7006.2009.01131.x.
103. Martin-Sanchez, D.; Gallegos-Villalobos, A.; Fontecha-Barriuso, M.; Carrasco, S.; Sanchez-Nino, M.D.; Lopez-Hernandez, F.J.; Ruiz-Ortega, M.; Egido, J.; Ortiz, A.; Sanz, A.B. Deferasirox-induced iron depletion promotes BclxL downregulation and death of proximal tubular cells. *Scientific reports* **2017**, *7*, 41510, doi:10.1038/srep41510.
104. Gattermann, N.; Finelli, C.; Della Porta, M.; Fenaux, P.; Stadler, M.; Guerci-Bresler, A.; Schmid, M.; Taylor, K.; Vassilieff, D.; Habr, D., et al. Hematologic responses to deferasirox therapy in transfusion-dependent patients with myelodysplastic syndromes. *Haematologica* **2012**, *97*, 1364-1371, doi:10.3324/haematol.2011.048546.
105. Gattermann, N.; Coll, R.; Jacobasch, L.; Allameddine, A.; Azmon, A.; DeBonnett, L.; Bruederle, A.; Jin, J.; investigators, K.s. Effect of deferasirox + erythropoietin vs erythropoietin on erythroid response in Low/Int-1-risk MDS patients: Results of the phase II KALLISTO trial. *European journal of haematology* **2018**, 10.1111/ejh.13096, doi:10.1111/ejh.13096.
106. List, A.F.; Baer, M.R.; Steensma, D.P.; Raza, A.; Esposito, J.; Martinez-Lopez, N.; Paley, C.; Feigert, J.; Besa, E. Deferasirox reduces serum ferritin and labile plasma iron in RBC transfusion-dependent patients with myelodysplastic syndrome. *Journal of clinical oncology : official journal of the American Society of Clinical Oncology* **2012**, *30*, 2134-2139, doi:10.1200/JCO.2010.34.1222.
107. Nolte, F.; Hochsmann, B.; Giagounidis, A.; Lubbert, M.; Platzbecker, U.; Haase, D.; Luck, A.; Gattermann, N.; Taupitz, M.; Baier, M., et al. Results from a 1-year, open-label, single arm, multi-center trial evaluating the efficacy and safety of oral Deferasirox in patients diagnosed with low and int-1 risk myelodysplastic syndrome (MDS) and transfusion-dependent iron overload. *Annals of hematology* **2013**, *92*, 191-198, doi:10.1007/s00277-012-1594-z.
108. Molteni, A.; Riva, M.; Pellizzari, A.; Borin, L.; Freyrie, A.; Greco, R.; Ubezio, M.; Bernardi, M.; Fariciotti, A.; Nador, G., et al. Hematological improvement during iron-chelation therapy in myelodysplastic syndromes: the experience of the "Rete Ematologica Lombarda". *Leukemia research* **2013**, *37*, 1233-1240, doi:10.1016/j.leukres.2013.07.006.
109. Shen, J.; Sheng, X.; Chang, Z.; Wu, Q.; Wang, S.; Xuan, Z.; Li, D.; Wu, Y.; Shang, Y.; Kong, X., et al. Iron metabolism regulates p53 signaling through direct heme-p53 interaction and modulation of p53 localization, stability, and function. *Cell Rep 7*, 180-193.
110. Lee, J.M.; Bernstein, A. p53 mutations increase resistance to ionizing radiation. *Proceedings of the National Academy of Sciences of the United States of America* **1993**, *90*, 5742-5746, doi:10.1073/pnas.90.12.5742.
111. el-Deiry, W.S.; Tokino, T.; Velculescu, V.E.; Levy, D.B.; Parsons, R.; Trent, J.M.; Lin, D.; Mercer, W.E.; Kinzler, K.W.; Vogelstein, B. WAF1, a potential mediator of p53 tumor suppression. *Cell* **1993**, *75*, 817-825, doi:10.1016/0092-8674(93)90500-p.
112. Harper, J.W.; Adami, G.R.; Wei, N.; Keyomarsi, K.; Elledge, S.J. The p21 Cdk-interacting protein Cip1 is a potent inhibitor of G1 cyclin-dependent kinases. *Cell* **1993**, *75*, 805-816, doi:10.1016/0092-8674(93)90499-g.

113. Bunz, F.; Dutriaux, A.; Lengauer, C.; Waldman, T.; Zhou, S.; Brown, J.P.; Sedivy, J.M.; Kinzler, K.W.; Vogelstein, B. Requirement for p53 and p21 to sustain G2 arrest after DNA damage. *Science* **1998**, *282*, 1497-1501, doi:10.1126/science.282.5393.1497.
114. Aylon, Y.; Michael, D.; Shmueli, A.; Yabuta, N.; Nojima, H.; Oren, M. A positive feedback loop between the p53 and Lats2 tumor suppressors prevents tetraploidization. *Genes & development* **2006**, *20*, 2687-2700, doi:10.1101/gad.1447006.
115. Jang, W.I.; Yang, W.I.; Lee, C.I.; Kim, H.S.; Song, K.S.; Cho, M.Y.; Park, J.K.; Shim, Y.H. Immunohistochemical detection of p53 protein, c-erbB-2 protein, epidermal growth factor receptor protein and proliferating cell nuclear antigen in gastric carcinoma. *Journal of Korean medical science* **1993**, *8*, 293-304, doi:10.3346/jkms.1993.8.4.293.
116. Caelles, C.; Helmberg, A.; Karin, M. p53-dependent apoptosis in the absence of transcriptional activation of p53-target genes. *Nature* **1994**, *370*, 220-223, doi:10.1038/370220a0.
117. Polyak, K.; Xia, Y.; Zweier, J.L.; Kinzler, K.W.; Vogelstein, B. A model for p53-induced apoptosis. *Nature* **1997**, *389*, 300-305, doi:10.1038/38525.
118. Sablina, A.A.; Budanov, A.V.; Ilyinskaya, G.V.; Agapova, L.S.; Kravchenko, J.E.; Chumakov, P.M. The antioxidant function of the p53 tumor suppressor. *Nature medicine* **2005**, *11*, 1306-1313, doi:10.1038/nm1320.
119. Conseiller, E.; Debussche, L.; Landais, D.; Venot, C.; Maratrat, M.; Sierra, V.; Tocque, B.; Bracco, L. CTS1: a p53-derived chimeric tumor suppressor gene with enhanced in vitro apoptotic properties. *The Journal of clinical investigation* **1998**, *101*, 120-127, doi:10.1172/JCI1140.
120. Ryan, K.M.; Ernst, M.K.; Rice, N.R.; Vousden, K.H. Role of NF-kappaB in p53-mediated programmed cell death. *Nature* **2000**, *404*, 892-897, doi:10.1038/35009130.
121. Brodsky, M.H.; Nordstrom, W.; Tsang, G.; Kwan, E.; Rubin, G.M.; Abrams, J.M. Drosophila p53 binds a damage response element at the reaper locus. *Cell* **2000**, *101*, 103-113, doi:10.1016/S0092-8674(00)80627-3.
122. Chipuk, J.E.; Green, D.R. Cytoplasmic p53: bax and forward. *Cell cycle* **2004**, *3*, 429-431.
123. Chipuk, J.E.; Kuwana, T.; Bouchier-Hayes, L.; Droin, N.M.; Newmeyer, D.D.; Schuler, M.; Green, D.R. Direct activation of Bax by p53 mediates mitochondrial membrane permeabilization and apoptosis. *Science* **2004**, *303*, 1010-1014, doi:10.1126/science.1092734.
124. Leu, J.I.; Dumont, P.; Hafey, M.; Murphy, M.E.; George, D.L. Mitochondrial p53 activates Bak and causes disruption of a Bak-Mcl1 complex. *Nature cell biology* **2004**, *6*, 443-450, doi:10.1038/ncb1123.
125. Chipuk, J.E.; Bouchier-Hayes, L.; Kuwana, T.; Newmeyer, D.D.; Green, D.R. PUMA couples the nuclear and cytoplasmic proapoptotic function of p53. *Science* **2005**, *309*, 1732-1735, doi:10.1126/science.1114297.
126. Fuchs, S.Y.; Adler, V.; Buschmann, T.; Wu, X.; Ronai, Z. Mdm2 association with p53 targets its ubiquitination. *Oncogene* **1998**, *17*, 2543-2547, doi:10.1038/sj.onc.1202200.
127. Yin, Y.; Stephen, C.W.; Luciani, M.G.; Fahraeus, R. p53 Stability and activity is regulated by Mdm2-mediated induction of alternative p53 translation products. *Nature cell biology* **2002**, *4*, 462-467, doi:10.1038/ncb801.
128. Li, M.; Luo, J.; Brooks, C.L.; Gu, W. Acetylation of p53 inhibits its ubiquitination by Mdm2. *The Journal of biological chemistry* **2002**, *277*, 50607-50611, doi:10.1074/jbc.C200578200.
129. Grossman, S.R.; Deato, M.E.; Brignone, C.; Chan, H.M.; Kung, A.L.; Tagami, H.; Nakatani, Y.; Livingston, D.M. Polyubiquitination of p53 by a ubiquitin ligase activity of p300. *Science* **2003**, *300*, 342-344, doi:10.1126/science.1080386.
130. Colaluca, I.N.; Tosoni, D.; Nuciforo, P.; Senic-Matuglia, F.; Galimberti, V.; Viale, G.; Pece, S.; Di Fiore, P.P. NUMB controls p53 tumour suppressor activity. *Nature* **2008**, *451*, 76-80, doi:10.1038/nature06412.
131. Le Cam, L.; Linares, L.K.; Paul, C.; Julien, E.; Lacroix, M.; Hatchi, E.; Triboulet, R.; Bossis, G.; Shmueli, A.; Rodriguez, M.S., et al. E4F1 is an atypical ubiquitin ligase that modulates p53 effector functions independently of degradation. *Cell* **2006**, *127*, 775-788, doi:10.1016/j.cell.2006.09.031.

132. Dai, M.S.; Shi, D.; Jin, Y.; Sun, X.X.; Zhang, Y.; Grossman, S.R.; Lu, H. Regulation of the MDM2-p53 pathway by ribosomal protein L11 involves a post-ubiquitination mechanism. *The Journal of biological chemistry* **2006**, *281*, 24304-24313, doi:10.1074/jbc.M602596200.
133. Amson, R.; Pece, S.; Marine, J.C.; Di Fiore, P.P.; Telerman, A. TPT1/ TCTP-regulated pathways in phenotypic reprogramming. *Trends in cell biology* **2013**, *23*, 37-46, doi:10.1016/j.tcb.2012.10.002.
134. Lehmann, C.; Islam, S.; Jarosch, S.; Zhou, J.; Hoskin, D.; Greenshields, A.; Al-Banna, N.; Sharawy, N.; Sczcesniak, A.; Kelly, M., et al. The utility of iron chelators in the management of inflammatory disorders. *Mediators of inflammation* **2015**, *2015*, 516740, doi:10.1155/2015/516740.
135. Greenberg, P.L.; Tuechler, H.; Schanz, J.; Sanz, G.; Garcia-Manero, G.; Sole, F.; Bennett, J.M.; Bowen, D.; Fenaux, P.; Dreyfus, F., et al. Revised international prognostic scoring system for myelodysplastic syndromes. *Blood* **2012**, *120*, 2454-2465, doi:10.1182/blood-2012-03-420489.
136. Ravera, S.; Podesta, M.; Sabatini, F.; Fresia, C.; Columbaro, M.; Bruno, S.; Fulcheri, E.; Ramenghi, L.A.; Frassoni, F. Mesenchymal stem cells from preterm to term newborns undergo a significant switch from anaerobic glycolysis to the oxidative phosphorylation. *Cellular and molecular life sciences : CMLS* **2018**, *75*, 889-903, doi:10.1007/s00018-017-2665-z.
137. Pullarkat, V. Iron overload in patients undergoing hematopoietic stem cell transplantation. *Advances in hematology* **2010**, *2010*, doi:10.1155/2010/345756.
138. Cappelli, E.; Cuccarolo, P.; Stroppiana, G.; Miano, M.; Bottega, R.; Cossu, V.; Degan, P.; Ravera, S. Defects in mitochondrial energetic function compels Fanconi Anaemia cells to glycolytic metabolism. *Biochimica et biophysica acta. Molecular basis of disease* **2017**, *1863*, 1214-1221, doi:10.1016/j.bbadis.2017.03.008.
139. Ravera, S.; Vaccaro, D.; Cuccarolo, P.; Columbaro, M.; Capanni, C.; Bartolucci, M.; Panfoli, I.; Morelli, A.; Dufour, C.; Cappelli, E., et al. Mitochondrial respiratory chain Complex I defects in Fanconi anemia complementation group A. *Biochimie* **2013**, *95*, 1828-1837, doi:10.1016/j.biochi.2013.06.006.
140. Hinkle, P.C. P/O ratios of mitochondrial oxidative phosphorylation. *Biochimica et biophysica acta* **2005**, *1706*, 1-11, doi:10.1016/j.bbabio.2004.09.004.
141. Khurana, A.; Shafer, D.A. MDM2 antagonists as a novel treatment option for acute myeloid leukemia: perspectives on the therapeutic potential of idasanutlin (RG7388). *OncoTargets and therapy* **2019**, *12*, 2903-2910, doi:10.2147/OTT.S172315.
142. Dongiovanni, P.; Fracanzani, A.L.; Cairo, G.; Megazzini, C.P.; Gatti, S.; Rametta, R.; Fargion, S.; Valenti, L. Iron-dependent regulation of MDM2 influences p53 activity and hepatic carcinogenesis. *The American journal of pathology* **2010**, *176*, 1006-1017, doi:10.2353/ajpath.2010.090249.
143. Stindt, M.H.; Muller, P.A.; Ludwig, R.L.; Kehrloesser, S.; Dotsch, V.; Vousden, K.H. Functional interplay between MDM2, p63/p73 and mutant p53. *Oncogene* **2015**, *34*, 4300-4310, doi:10.1038/onc.2014.359.
144. Hage, S.; Stanga, S.; Marinangeli, C.; Octave, J.N.; Dewachter, I.; Quetin-Leclercq, J.; Kienlen-Campard, P. Characterization of Pterocarpus erinaceus kino extract and its gamma-secretase inhibitory properties. *Journal of ethnopharmacology* **2015**, *163*, 192-202, doi:10.1016/j.jep.2015.01.028.
145. Kravchenko, J.E.; Ilyinskaya, G.V.; Komarov, P.G.; Agapova, L.S.; Kochetkov, D.V.; Strom, E.; Frolova, E.I.; Kovriga, I.; Gudkov, A.V.; Feinstein, E., et al. Small-molecule RETRA suppresses mutant p53-bearing cancer cells through a p73-dependent salvage pathway. *Proceedings of the National Academy of Sciences of the United States of America* **2008**, *105*, 6302-6307, doi:10.1073/pnas.0802091105.
146. Calabrese, C.; Panuzzo, C.; Stanga, S.; Andreani, G.; Ravera, S.; Maglione, A.; Pironi, L.; Petiti, J.; Shahzad Ali, M.S.; Scaravaglio, P., et al. Deferasirox-Dependent Iron Chelation Enhances Mitochondrial Dysfunction and Restores p53 Signaling by Stabilization of p53 Family Members in Leukemic Cells. *International journal of molecular sciences* **2020**, *21*, doi:10.3390/ijms21207674.
147. Stanga, S.; Caretto, A.; Boido, M.; Vercelli, A. Mitochondrial Dysfunctions: A Red Thread across Neurodegenerative Diseases. *International journal of molecular sciences* **2020**, *21*, doi:10.3390/ijms21103719.

148. Panuzzo, C.; Jovanovski, A.; Pergolizzi, B.; Pironi, L.; Stanga, S.; Fava, C.; Cilloni, D. Mitochondria: A Galaxy in the Hematopoietic and Leukemic Stem Cell Universe. *International journal of molecular sciences* **2020**, *21*, doi:10.3390/ijms21113928.
149. Horowitz, M.P.; Greenamyre, J.T. Mitochondrial iron metabolism and its role in neurodegeneration. *Journal of Alzheimer's disease : JAD* **2010**, *20 Suppl 2*, S551-568, doi:10.3233/JAD-2010-100354.
150. Bhatti, J.S.; Bhatti, G.K.; Reddy, P.H. Mitochondrial dysfunction and oxidative stress in metabolic disorders - A step towards mitochondria based therapeutic strategies. *Biochimica et biophysica acta. Molecular basis of disease* **2017**, *1863*, 1066-1077, doi:10.1016/j.bbadis.2016.11.010.
151. Kim, Y.Y.; Um, J.H.; Yoon, J.H.; Lee, D.Y.; Lee, Y.J.; Kim, D.H.; Park, J.I.; Yun, J. p53 regulates mitochondrial dynamics by inhibiting Drp1 translocation into mitochondria during cellular senescence. *FASEB journal : official publication of the Federation of American Societies for Experimental Biology* **2020**, *34*, 2451-2464, doi:10.1096/fj.201901747RR.
152. Yoon, Y.S.; Yoon, D.S.; Lim, I.K.; Yoon, S.H.; Chung, H.Y.; Rojo, M.; Malka, F.; Jou, M.J.; Martinou, J.C.; Yoon, G. Formation of elongated giant mitochondria in DFO-induced cellular senescence: involvement of enhanced fusion process through modulation of Fis1. *Journal of cellular physiology* **2006**, *209*, 468-480, doi:10.1002/jcp.20753.
153. Gardner, P.R.; Nguyen, D.D.; White, C.W. Aconitase is a sensitive and critical target of oxygen poisoning in cultured mammalian cells and in rat lungs. *Proceedings of the National Academy of Sciences of the United States of America* **1994**, *91*, 12248-12252, doi:10.1073/pnas.91.25.12248.
154. Carturan, S.; Petiti, J.; Rosso, V.; Calabrese, C.; Signorino, E.; Bot-Sartor, G.; Nicoli, P.; Gallo, D.; Bracco, E.; Morotti, A., et al. Variable but consistent pattern of Meningioma 1 gene (MN1) expression in different genetic subsets of acute myelogenous leukaemia and its potential use as a marker for minimal residual disease detection. *Oncotarget* **2016**, *7*, 74082-74096, doi:10.18632/oncotarget.12269.
155. Valente, A.J.; Maddalena, L.A.; Robb, E.L.; Moradi, F.; Stuart, J.A. A simple ImageJ macro tool for analyzing mitochondrial network morphology in mammalian cell culture. *Acta histochemica* **2017**, *119*, 315-326, doi:10.1016/j.acthis.2017.03.001.
156. Shen, J.; Sheng, X.; Chang, Z.; Wu, Q.; Wang, S.; Xuan, Z.; Li, D.; Wu, Y.; Shang, Y.; Kong, X., et al. Iron metabolism regulates p53 signaling through direct heme-p53 interaction and modulation of p53 localization, stability, and function. *Cell Rep* **2014**, *7*, 180-193, doi:10.1016/j.celrep.2014.02.042.
157. Morotti, A.; Panuzzo, C.; Crivellaro, S.; Carra, G.; Guerrasio, A.; Saglio, G. HAUSP compartmentalization in chronic myeloid leukemia. *European journal of haematology* **2015**, *94*, 318-321, doi:10.1111/ejh.12422.
158. Nigro, J.M.; Baker, S.J.; Preisinger, A.C.; Jessup, J.M.; Hostetter, R.; Cleary, K.; Bigner, S.H.; Davidson, N.; Baylin, S.; Devilee, P., et al. Mutations in the p53 gene occur in diverse human tumour types. *Nature* **1989**, *342*, 705-708, doi:10.1038/342705a0.
159. Hollstein, M.; Sidransky, D.; Vogelstein, B.; Harris, C.C. p53 mutations in human cancers. *Science* **1991**, *253*, 49-53, doi:10.1126/science.1905840.
160. Wu, H.; Leng, R.P. MDM2 mediates p73 ubiquitination: a new molecular mechanism for suppression of p73 function. *Oncotarget* **2015**, *6*, 21479-21492, doi:10.18632/oncotarget.4086.
161. Tomasini, R.; Seux, M.; Nowak, J.; Bontemps, C.; Carrier, A.; Dagorn, J.C.; Pebusque, M.J.; Iovanna, J.L.; Dusetti, N.J. TP53INP1 is a novel p73 target gene that induces cell cycle arrest and cell death by modulating p73 transcriptional activity. *Oncogene* **2005**, *24*, 8093-8104, doi:10.1038/sj.onc.1208951.
162. De la Fuente, I.M.; Cortes, J.M.; Valero, E.; Desroches, M.; Rodrigues, S.; Malaina, I.; Martinez, L. On the dynamics of the adenylate energy system: homeorhesis vs homeostasis. *PloS one* **2014**, *9*, e108676, doi:10.1371/journal.pone.0108676.
163. Toyokuni, S. Role of iron in carcinogenesis: cancer as a ferrotoxic disease. *Cancer science* **2009**, *100*, 9-16, doi:10.1111/j.1349-7006.2008.01001.x.

164. Stanga, S.; Vrancx, C.; Tasiaux, B.; Marinangeli, C.; Karlstrom, H.; Kienlen-Campard, P. Specificity of presenilin-1- and presenilin-2-dependent gamma-secretases towards substrate processing. *Journal of cellular and molecular medicine* **2018**, *22*, 823-833, doi:10.1111/jcmm.13364.
165. Zacharski, L.R.; Chow, B.K.; Howes, P.S.; Shamayeva, G.; Baron, J.A.; Dalman, R.L.; Malenka, D.J.; Ozaki, C.K.; Lavori, P.W. Decreased cancer risk after iron reduction in patients with peripheral arterial disease: results from a randomized trial. *Journal of the National Cancer Institute* **2008**, *100*, 996-1002, doi:10.1093/jnci/djn209.
166. Hilken, A.; Langebrake, C.; Wolschke, C.; Kersten, J.F.; Rohde, H.; Nielsen, P.; Kroger, N. Impact of non-transferrin-bound iron (NTBI) in comparison to serum ferritin on outcome after allogeneic stem cell transplantation (ASCT). *Annals of hematology* **2017**, *96*, 1379-1388, doi:10.1007/s00277-017-3034-6.
167. Smyth, G.K.; Michaud, J.; Scott, H.S. Use of within-array replicate spots for assessing differential expression in microarray experiments. *Bioinformatics* **2005**, *21*, 2067-2075, doi:10.1093/bioinformatics/bti270.
168. Kinsella, R.J.; Kahari, A.; Haider, S.; Zamora, J.; Proctor, G.; Spudich, G.; Almeida-King, J.; Staines, D.; Derwent, P.; Kerhornou, A., et al. Ensembl BioMarts: a hub for data retrieval across taxonomic space. *Database : the journal of biological databases and curation* **2011**, *2011*, bar030, doi:10.1093/database/bar030.
169. Nemajerova, A.; Palacios, G.; Nowak, N.J.; Matsui, S.; Petrenko, O. Targeted deletion of p73 in mice reveals its role in T cell development and lymphomagenesis. *PloS one* **2009**, *4*, e7784, doi:10.1371/journal.pone.0007784.
170. Flores, E.R.; Tsai, K.Y.; Crowley, D.; Sengupta, S.; Yang, A.; McKeon, F.; Jacks, T. p63 and p73 are required for p53-dependent apoptosis in response to DNA damage. *Nature* **2002**, *416*, 560-564, doi:10.1038/416560a.
171. Ashcroft, M.; Taya, Y.; Vousden, K.H. Stress signals utilize multiple pathways to stabilize p53. *Molecular and cellular biology* **2000**, *20*, 3224-3233, doi:10.1128/mcb.20.9.3224-3233.2000.
172. Kuleshov, M.V.; Jones, M.R.; Rouillard, A.D.; Fernandez, N.F.; Duan, Q.; Wang, Z.; Koplev, S.; Jenkins, S.L.; Jagodnik, K.M.; Lachmann, A., et al. Enrichr: a comprehensive gene set enrichment analysis web server 2016 update. *Nucleic acids research* **2016**, *44*, W90-97, doi:10.1093/nar/gkw377.
173. Fernandez, N.F.; Gundersen, G.W.; Rahman, A.; Grimes, M.L.; Rikova, K.; Hornbeck, P.; Ma'ayan, A. Clustergrammer, a web-based heatmap visualization and analysis tool for high-dimensional biological data. *Scientific data* **2017**, *4*, 170151, doi:10.1038/sdata.2017.151.
174. Schaefer, C.F.; Anthony, K.; Krupa, S.; Buchoff, J.; Day, M.; Hannay, T.; Buetow, K.H. PID: the Pathway Interaction Database. *Nucleic acids research* **2009**, *37*, D674-679, doi:10.1093/nar/gkn653.
175. Cilloni, D.; Ravera, S.; Calabrese, C.; Gaidano, V.; Niscola, P.; Balleari, E.; Gallo, D.; Petiti, J.; Signorino, E.; Rosso, V., et al. Iron overload alters the energy metabolism in patients with myelodysplastic syndromes: results from the multicenter FISM BIOFER study. *Scientific reports* **2020**, *10*, 9156, doi:10.1038/s41598-020-66162-y.
176. Zhan, L.; Cao, H.; Wang, G.; Lyu, Y.; Sun, X.; An, J.; Wu, Z.; Huang, Q.; Liu, B.; Xing, J. Drp1-mediated mitochondrial fission promotes cell proliferation through crosstalk of p53 and NF-kappaB pathways in hepatocellular carcinoma. *Oncotarget* **2016**, *7*, 65001-65011, doi:10.18632/oncotarget.11339.
177. Rehman, J.; Zhang, H.J.; Toth, P.T.; Zhang, Y.; Marsboom, G.; Hong, Z.; Salgia, R.; Husain, A.N.; Wietholt, C.; Archer, S.L. Inhibition of mitochondrial fission prevents cell cycle progression in lung cancer. *FASEB journal : official publication of the Federation of American Societies for Experimental Biology* **2012**, *26*, 2175-2186, doi:10.1096/fj.11-196543.
178. Huang, X.T.; Liu, X.; Ye, C.Y.; Tao, L.X.; Zhou, H.; Zhang, H.Y. Iron-induced energy supply deficiency and mitochondrial fragmentation in neurons. *Journal of neurochemistry* **2018**, *147*, 816-830, doi:10.1111/jnc.14621.
179. Lohrum, M.A.; Vousden, K.H. Regulation and activation of p53 and its family members. *Cell death and differentiation* **1999**, *6*, 1162-1168, doi:10.1038/sj.cdd.4400625.

180. Kruse, J.P.; Gu, W. SnapShot: p53 posttranslational modifications. *Cell* **2008**, *133*, 930-930 e931, doi:10.1016/j.cell.2008.05.020.
181. Sermeus, A.; Michiels, C. Reciprocal influence of the p53 and the hypoxic pathways. *Cell death & disease* **2011**, *2*, e164, doi:10.1038/cddis.2011.48.